NIEHS Report on the In Vivo Repeat Dose Biological Potency Study of 6:1 Fluorotelomer Alcohol (CASRN 375-82-6) in Sprague Dawley (Hsd:Sprague Dawley® SD®) Rats (Gavage Studies)

NIEHS 07

March 2023

NIEHS Report on the
In Vivo Repeat Dose Biological Potency Study of
6:1 Fluorotelomer Alcohol
(CASRN 375-82-6) in Sprague Dawley
(Hsd:Sprague Dawley® SD®) Rats
(Gavage Studies)

NIEHS Report 07

March 2023

Foreword

The [National Institute of Environmental Health Sciences (NIEHS)](#) is one of 27 institutes and centers of the National Institutes of Health, which is part of the U.S. Department of Health and Human Services. The NIEHS mission is to discover how the environment affects people in order to promote healthier lives. NIEHS works to accomplish its mission by conducting and funding research on human health effects of environmental exposures; developing the next generation of environmental health scientists; and providing critical research, knowledge, and information to citizens and policymakers who are working to prevent hazardous exposures and reduce the risk of disease and disorders connected to the environment. NIEHS is a foundational leader in environmental health sciences and committed to ensuring that its research is directed toward a healthier environment and healthier lives for all people.

The NIEHS Report series began in 2022. The environmental health sciences research described in this series is conducted primarily by the [Division of Translational Toxicology (DTT)](#) at NIEHS. NIEHS/DTT scientists conduct innovative toxicology research that aligns with real-world public health needs and translates scientific evidence into knowledge that can inform individual and public health decision-making.

NIEHS reports are available free of charge on the [NIEHS/DTT website](#) and cataloged in [PubMed](#), a free resource developed and maintained by the National Library of Medicine (part of the National Institutes of Health).

In Vivo Repeat Dose Biological Potency Study of
6:1 Fluorotelomer Alcohol in Sprague Dawley Rats

Table of Contents

In Vivo Repeat Dose Biological Potency Study of
6:1 Fluorotelomer Alcohol in Sprague Dawley Rats

Tables

In Vivo Repeat Dose Biological Potency Study of
6:1 Fluorotelomer Alcohol in Sprague Dawley Rats

About This Report

Authors

Scott S. Auerbach[1], Kristin L. Aillon[2], Jeff D. Ballin[3], Bradley J. Collins[1], Michelle C. Cora[1], Nathan S. Duncan[2], Jennifer M. Fostel[1], Ying F. Liu[4], Jeanne Luh[5], Nicholas J. Machesky[3], Sarah J. Pickett[2], Georgia K. Roberts[1], Kelly A. Shipkowski[1], Anthony J. Skowronek[3], Lori L. Smith[2], Barney R. Sparrow[3], Heather Toy[6], Suramya Waidyanatha[1], AtLee T.D. Watson[1]

[1]Division of Translational Toxicology, National Institute of Environmental Health Sciences, Research Triangle Park, North Carolina, USA

[2]MRIGlobal, Kansas City, Missouri, USA

[3]Battelle, Columbus, Ohio, USA

[4]ASRC Federal, Research Triangle Park, North Carolina, USA

[5]ICF, Reston, Virginia, USA

[6]AmplifyBio, West Jefferson, Ohio, USA

Division of Translational Toxicology, National Institute of Environmental Health Sciences, Research Triangle Park, North Carolina, USA
Evaluated and interpreted the results and reported findings; developed reporting framework
Scott S. Auerbach, Ph.D., Study Scientist
Michelle C. Cora, D.V.M.
Georgia K. Roberts, Ph.D.
Kelly A. Shipkowski, Ph.D.
AtLee T.D. Watson, Ph.D.

Coordinated data integration
Jennifer M. Fostel, Ph.D.

Analyzed and interpreted analytical chemistry data
Bradley J. Collins, M.S.P.H.
Suramya Waidyanatha, Ph.D.

Battelle, Columbus, Ohio, USA
Provided contract oversight
Barney R. Sparrow, Ph.D.

Conducted in-life studies
Anthony J. Skowronek, D.V.M., Ph.D.

Performed RNA isolation
Nicholas J. Machesky, Ph.D.

Conducted thyroid biomarker analysis
Jeff D. Ballin, Ph.D.

AmplifyBio, West Jefferson, Ohio, USA
Compiled results
Heather Toy, B.S., Study Director

MRIGlobal, Kansas City, Missouri, USA
Conducted prestart chemistry activities, dose formulations, and biological sample chemistry analyses
Kristin L. Aillon, Ph.D., Principal Investigator
Nathan S. Duncan, Ph.D.
Sarah J. Pickett, B.S.
Lori L. Smith, Ph.D.

ICF, Reston, Virginia, USA
Contributed to technical writing and data integration and ensured report quality
Jeanne Luh, Ph.D.

ASRC Federal, Research Triangle Park, North Carolina, USA
Developed data tables and supplemental materials
Ying F. Liu, Ph.D.

Contributors

Division of Translational Toxicology, National Institute of Environmental Health Sciences, Research Triangle Park, North Carolina, USA
Critically reviewed report and results
John R. Bucher, Ph.D.
Fred M. Parham, Ph.D.
Nigel J. Walker, Ph.D.

Contributed to development and review of reporting framework
Michael J. DeVito, Ph.D.
William M. Gwinn, Ph.D.
Alison H. Harrill, Ph.D.
Scott A. Masten, Ph.D.
Matthew D. Stout, Ph.D.
Greg S. Travlos, D.V.M.
Mary S. Wolfe, Ph.D.

Developed and updated BMDS software package
Andrew J. Shapiro, M.S.P.H.

RTI International, Research Triangle Park, North Carolina, USA
Conducted biological sample chemistry analyses of total thyroid hormone levels
Reshan A. Fernando, Ph.D., Principal Investigator
Melanie A.R. Silinski, Ph.D.

ASRC Federal, Research Triangle Park, North Carolina, USA
Developed data tables and supplemental materials
Julie Berke, B.S.
Shihan He, Ph.D.
Christina Myers, M.S.

CSS Corporation, Research Triangle Park, North Carolina, USA
Prepared quality assessment audits
Steven Brecher, Ph.D., Principal Investigator
Sudha Iyer, B.S.
Varghese S. Tharakan, D.V.M.

Sciome LLC, Research Triangle Park, North Carolina, USA
Provided bioinformatics analysis
Michele R. Balik-Meisner, Ph.D.
Dhiral P. Phadke, M.S.
Ruchir R. Shah, Ph.D.

ICF, Reston, Virginia, USA
Provided contract oversight
David F. Burch, M.E.M., Principal Investigator
Cary E. Haver, M.P.H.
Jessica A. Wignall, M.S.P.H.

Prepared and edited report
Lauren M. Browning, M.S.
Katherine S. Duke, Ph.D.
Tara Hamilton, M.S.
Pamela A. Hartman, M.E.M.
Lisa M. Prince, Ph.D.
Samantha J. Snow, Ph.D.
Jonathan R. Thompson, B.S.
James W. Tracy, M.H.S.
Nkoli Ukpabi, M.S.

Peer Review

This report was modeled after the *NTP Research Report on In Vivo Repeat Dose Biological Potency Study of Triphenyl Phosphate (CAS No. 115-86-6) in Male Sprague Dawley (Hsd:Sprague Dawley® SD®) Rats (Gavage Studies)* (https://doi.org/10.22427/NTP-RR-8), which was reviewed internally at the National Institute of Environmental Health Sciences and peer reviewed by external experts. Importantly, these reports employ mathematical model-based approaches to identify and report potency of dose-responsive effects and do not attempt more subjective interpretation (i.e., make calls or reach conclusions on hazard). The peer reviewers of the initial 5-day research report determined that the study design, analysis methods, and results presentation were appropriate. The study design, analysis methods, and results presentation employed for this study are identical to those previously reviewed, approved, and reported; therefore, following internal review, the *NIEHS Report on the In Vivo Repeat Dose Biological Potency Study of 6:1 Fluorotelomer Alcohol (CASRN 375-82-6) in Sprague Dawley (Hsd:Sprague Dawley® SD®) Rats (Gavage Studies)* was not subjected to further external peer review.

Publication Details

Acknowledgments

In Vivo Repeat Dose Biological Potency Study of
6:1 Fluorotelomer Alcohol in Sprague Dawley Rats

Abstract

Background: 6:1 Fluorotelomer alcohol (6:1 FTOH) is a member of the per- and polyfluoroalkyl class of compounds to which humans are widely exposed. Toxicological information on this class of chemicals is sparse. A short-term, in vivo transcriptomic study was used to assess the biological potency of 6:1 FTOH.

Methods: A short-term in vivo biological potency study on 6:1 FTOH in adult male and female Sprague Dawley (Hsd:Sprague Dawley® SD®) rats was conducted. 6:1 FTOH was formulated in corn oil and administered once daily for 5 consecutive days by gavage (study days 0–4). 6:1 FTOH was administered at 10 doses (0, 0.15, 0.5, 1.4, 4, 12, 37, 111, 333, and 1,000 mg/kg body weight [mg/kg]). Blood was collected from animals dedicated for internal dose assessment in the 4 and 37 mg/kg groups. On study day 5, the day after the final dose was administered, animals were euthanized, standard toxicological measures were assessed, and the liver and kidney were assayed in gene expression studies using the TempO-Seq assay. Modeling was conducted to identify the benchmark doses (BMDs) associated with apical toxicological endpoints and transcriptional changes in the liver and kidney. A benchmark response of one standard deviation was used to model all endpoints.

Results: Several clinical pathology and organ weight measurements showed dose-related changes from which BMD values were calculated. In male rats, the effects included significantly decreased total thyroxine concentration, increased relative liver weight, increased albumin concentration, increased relative left kidney weight, increased aspartate aminotransferase activity, increased absolute liver weight, increased alanine aminotransferase activity, increased alkaline phosphatase activity, and increased creatinine concentration. The BMDs and benchmark dose lower confidence limits (BMD$_{LS}$) were 3.19 (1.774), 12.122 (9.527), 13.365 (4.084), 20.907 (4.272), 28.117 (19.352), 28.507 (15.286), 36.116 (21.468), 89.383 (74.114), and 97.38 (32.365) mg/kg, respectively. In female rats, the effects included significantly decreased reticulocyte count, increased large unstained cell count, decreased total triiodothyronine concentration, increased monocyte count, increased thyroid stimulating hormone concentration, and increased aspartate aminotransferase activity. The BMDs (BMD$_{LS}$) were 15.578 (3.622), 54.339 (15.759), 161.48 (122.215), 257.111 (160.613), 356.61 (268.917), and 497.046 (340.458) mg/kg, respectively. Average 6:1 FTOH plasma concentrations at 2 hours postdose were lower in female rats than in male rats. At 24 hours postdose, the concentration fell below the limit of detection of the analytical method in both male and female rats, suggesting short plasma half-lives of 6:1 FTOH in rats.

In the liver of male and female rats, no Gene Ontology biological process or individual genes had BMD median values below the lower limit of extrapolation (<0.050 mg/kg). The most sensitive gene sets in male rats for which a reliable estimate of the BMD could be made were cellular response to epidermal growth factor stimulus and response to epidermal growth factor with median BMDs of 0.368 and 0.690 mg/kg and median BMD$_{LS}$ of 0.103 and 0.456 mg/kg, respectively. The most sensitive gene sets in female rats for which a reliable estimate of the BMD could be made were positive regulation of phagocytosis and regulation of phagocytosis with median BMDs of 44.730 and 48.555 mg/kg and median BMD$_{LS}$ of 22.260 and 27.154 mg/kg, respectively. The most sensitive upregulated genes in male rats with reliable BMD estimates included *Acot2*, *Eci1*, *Loc100911558/Spink1l*, *Spink1*, *Ehhadh*, *Crot*, *Acaa1a*, and *Acaa1b* with BMDs (BMD$_{LS}$) of 1.012 (0.809), 1.013 (0.769), 1.270 (0.542), 1.270 (0.542),

1.280 (1.047), 1.411 (1.092), 1.874 (1.524), and 1.874 (1.524) mg/kg, respectively. The most sensitive downregulated genes in male rats with reliable BMD estimates were *Myc* and *Zfp36* with BMDs (BMD$_L$s) of 0.186 (0.103) and 0.368 (0.097) mg/kg, respectively. In female rats, the top 10 most sensitive individual genes were upregulated. These genes were *Gdf15*, *Igfbp1*, *Eci1*, *Etfdh*, *Cyp2b1*, *Loc108348266/Cyp2b1*, *Dhrs7*, *Dhrs7l1*, *Slc27a2*, and *Vnn1* with BMDs (BMD$_L$s) of 17.724 (8.696), 18.792 (7.230), 32.546 (27.162), 34.846 (26.297), 35.483 (29.479), 35.483 (29.479), 35.986 (10.630), 35.986 (10.630), 36.103 (26.571), and 37.026 (30.688) mg/kg, respectively.

In the kidney of male rats, two Gene Ontology biological processes had BMD median values <0.050 mg/kg, which relate to astrocyte activation and negative regulation of response to biotic stimulus. The most sensitive gene sets in male rats for which a reliable estimate of the BMD could be made were acetyl-CoA metabolic process and acyl-CoA metabolic process with median BMDs of 1.346 and 1.928 mg/kg and median BMD$_L$s of 0.541 and 1.305 mg/kg, respectively. No gene sets in the kidney of female rats had estimated BMD median values <0.050 mg/kg. The most sensitive gene sets in female rats for which a reliable estimate of the BMD could be made were fatty acid beta-oxidation and fatty acid oxidation with median BMDs of 21.079 and 27.058 mg/kg and median BMD$_L$s of 13.312 and 13.877 mg/kg, respectively. No individual kidney genes in male rats had median BMD values <0.050 mg/kg. The most sensitive upregulated genes in male rats with reliable BMD estimates included *Decr1*, *Vnn1*, *Hmgcs2*, *Ehhadh*, *Eci2*, *Acaa2*, *Acot1*, *Cyp4a1*, and *Ech1* with BMDs (BMD$_L$s) of 0.680 (0.505), 0.705 (0.488), 0.804 (0.541), 0.953 (0.671), 0.989 (0.643), 1.346 (0.539), 1.363 (0.938), 1.593 (1.021), and 2.055 (1.124) mg/kg, respectively. One gene, *Acmsd*, was downregulated with a BMD (BMD$_L$) of 0.775 (0.183) mg/kg. In female rats, the top 10 most sensitive individual genes were upregulated. One individual gene, *Plod3*, had a BMD value <0.050 mg/kg. The next most sensitive upregulated genes with reliable BMD estimates included *Eci1*, *Vnn1*, *Hmgcs2*, *Ehhadh*, *Eci2*, *Acaa1a*, *Acaa1b*, *Ech1*, and *Acaa2* with BMDs (BMD$_L$s) of 9.486 (7.353), 10.025 (7.993), 11.644 (9.266), 12.212 (9.437), 12.789 (9.488), 13.850 (11.009), 13.850 (11.009), 19.820 (14.141), and 22.339 (13.614) mg/kg, respectively.

Summary: Taken together, in male rats, the most sensitive gene set BMD (BMD$_L$) median, individual gene BMD (BMD$_L$), and apical endpoint BMD (BMD$_L$) values that could be reliably determined occurred at 0.368 (0.103), 0.186 (0.103), and 3.19 (1.774) mg/kg, respectively. The BMDs (BMD$_L$s) could not be determined for two gene sets and were estimated to be <0.050 mg/kg. In female rats, the most sensitive gene set BMD (BMD$_L$) median, individual gene BMD (BMD$_L$), and apical endpoint BMD (BMD$_L$) values that could be reliably determined occurred at 21.079 (13.312), 9.486 (7.353), and 15.578 (3.622) mg/kg, respectively. The BMD (BMD$_L$) could not be determined for one individual gene and was estimated to be <0.050 mg/kg. Future studies investigating lower doses would be helpful to obtain more accurate estimates of BMD values for the most sensitive gene sets.

Background

6:1 Fluorotelomer alcohol (6:1 FTOH) (CASRN: 375-82-6, U.S. Environmental Protection Agency [EPA] Chemical Dashboard: DTXSID00190950,[1] PubChem CID: 550386,[2] European Committee Number: 206-796-8[3]) is a member of the per- and polyfluoroalkyl class of compounds that are associated with numerous toxicological effects.[4] There is widespread human exposure to this class of compounds.[5; 6] The predicted upper 95th percentile human exposure to 6:1 FTOH is 0.0000806 mg/kg body weight/day.[7] A review of the existing literature failed to identify any in vivo toxicological information on 6:1 FTOH, and according to the EPA Chemical Dashboard, no quantitative risk assessment values or quantitative hazard values exist for this test article.[8] Publicly available information on 6:1 FTOH can be found in PubChem[2] and the EPA Chemical Dashboard.[1]

Recent studies have demonstrated that short-term in vivo gavage studies coupled with transcriptomics on select target organs can be used to estimate a biological potency that provides a reasonable approximation of toxicological potency in long-term guideline toxicological assessments.[9] To estimate biological potency and gain insight into the nature of biological changes elicited by 6:1 FTOH, the National Institute of Environmental Health Sciences performed a short-term in vivo biological potency study of male and female Sprague Dawley (Hsd:Sprague Dawley® SD®) rats. The results of this study are presented in this report.

Materials and Methods

Study Design

Male and female Sprague Dawley (Hsd:Sprague Dawley® SD®) rats were obtained from Envigo (Haslett, MI). On receipt, the rats were 6–7 weeks of age. Animals were quarantined for a minimum of 10 days and then randomly assigned to 1 of 10 dose groups. The rats in each dose group were then administered 6:1 fluorotelomer alcohol (6:1 FTOH) in corn oil by gavage for 5 consecutive days (study days 0–4) at a dose level of 0, 0.15, 0.5, 1.4, 4, 12, 37, 111, 333, or 1,000 mg/kg body weight (mg/kg). There were 5 rats per sex in each dosed group and 10 per sex in the vehicle control group; an additional 3 rats per sex were added to the 4 and 37 mg/kg groups for internal dose assessment. Dosage volume was 5 mL/kg body weight and was based on each animal's most recent body weight. Euthanasia, blood/serum collection, and tissue sample collection were completed on study day 5, the day following the final administration of the test article. Blood was also collected from animals dedicated for internal dose assessment at 2 and 24 hours following the last dose administered on study day 4. Animal identification numbers and FASTQ data file names for each animal are presented in Appendix B.

Dose Selection Rationale

Dose selection was informed by a median lethal dose (LD_{50}) prediction from the OPEn structure-activity/property Relationship App (OPERA),[10; 11] which estimated 460 mg/kg/day with an uncertainty range of 230–918 mg/kg/day. Further, an estimated point of departure of 85 mg/kg/day with an uncertainty range of 0.6–637 mg/kg/day was provided by the U.S. Environmental Protection Agency (EPA).[12] To be certain that a 5-day maximum tolerated dose was achieved, in addition to identifying a minimum biological effect level dose, a top dose of 1,000 mg/kg was chosen, and approximately half-log dose spacing of nine lower dose levels, including a vehicle control, was selected to carry out the study.

Chemistry

6:1 FTOH was obtained in one lot from Apollo Scientific, Ltd. (Stockport, UK; lot AS489852). The identity and purity (>99%) of the chemical were confirmed by gas chromatography-mass spectrometry (GC/MS). Bulk chemical was stored refrigerated under inert headspace. Using the same GC/MS system and authentic standards, perfluorooctanoic acid was not detected, whereas a small percentage (approximately 0.002%) of perfluorooctanesulfonic acid was identified in lot AS489852.

Dose formulations were prepared in corn oil at 0 (vehicle control), 0.03, 0.10, 0.28, 0.80, 2.4, 7.4, 22.2, 66.6, and 200 mg/mL. The preadministration concentration of test article in the vehicle was analyzed using a qualified GC/MS method. The 0.28, 7.4, 22.2, and 66.6 mg/mL concentrations were 22.5%, 10.3%, 11.6%, and 10.2% below their target concentrations, respectively. All other formulations were within 10% of the target concentration. Formulation stability was confirmed in a 0.03 mg/mL formulation for up to 22 days at refrigerated (5ºC) and ambient temperatures while protected from light. All chemistry activities were conducted by MRIGlobal (Kansas City, MO).

Clinical Examinations and Sample Collection

Clinical Observations

All rats were observed twice daily for signs of mortality or moribundity. Formal (out of cage) clinical observations were performed daily.

Body and Organ Weights

Animals were weighed during quarantine for randomization on the first day of dosing (study day 0) and on the day of necropsy (study day 5). A gross necropsy was performed on all rats that died spontaneously or were humanely euthanized due to moribund condition. During necropsy for all animals, the heart, liver, and kidneys were removed, and organ weights were recorded; bilateral organs were weighed separately.

Clinical Pathology

Animals were euthanized in random order by CO_2/O_2 (70%/30%) anesthesia 1 day after the final day of dosing. Blood samples were collected from each sex within a 1-hour window and were taken via vena cava or aorta. Blood was collected into tubes containing K_3 EDTA (tripotassium ethylenediaminetetraacetic acid) for hematology analysis and into tubes void of anticoagulant for serum chemistry and thyroid hormone measurements. The following hematology parameters were measured on an Advia® 120 Hematology Analyzer (Siemens Medical Solutions USA, Inc., Malvern, PA): erythrocyte count, hemoglobin, hematocrit, mean cell volume, mean cell hemoglobin, mean cell hemoglobin concentration, white blood cell count and differential, reticulocyte count, platelet count, and nucleated erythrocyte count. Manual hematocrit was determined using a microcentrifuge and capillary reader. Blood smears were prepared, and qualitative evaluation of cellular morphology was performed per study protocol. The following clinical chemistry parameters were measured on a Roche cobas® c501 Chemistry Analyzer (Roche Diagnostics, Indianapolis, IN): alanine aminotransferase (ALT), albumin, alkaline phosphatase (ALP), aspartate aminotransferase (AST), total bile acids, total bilirubin, direct bilirubin, cholesterol, creatine kinase, creatinine, glucose, sorbitol dehydrogenase (SDH), total protein, triglycerides, and urea nitrogen. Globulin, albumin/globulin (A/G) ratio, and indirect bilirubin were calculated based on direct measurements (e.g., indirect bilirubin = total bilirubin − direct bilirubin). Serum concentrations for thyroid stimulating hormone (TSH) and free thyroxine (fT4) were determined by immunoassay using commercially available immunoassay kits from EMD Millipore Corporation (Billerica, MA) for TSH and Biomatik Corporation (Kitchener, Ontario, Canada) for fT4. Serum concentrations of total thyroxine (total T4) and total triiodothyronine (total T3) were determined using a validated method as described elsewhere.[13] Individual animal and summary clinical chemistry, hematology, and hormonal data are available in Appendix F.

Internal Dose Assessment

A screening level assessment of the internal dose was performed to determine whether the test chemical had bioaccumulative properties (i.e., if the half-life was >24 hours). Blood was collected from animals dedicated for internal dose assessment in the 4 and 37 mg/kg groups at 2 and 24 hours following the last dose administered on study day 4. At 2 hours postdose, blood was collected from the jugular vein of unanesthetized animals. At 24 hours postdose (study

day 5), blood was collected from all study animals and dedicated internal dose assessment animals from the vena cava or abdominal aorta while animals were anesthetized with CO_2/O_2 (70%/30%). Blood was collected into tubes containing K_3 EDTA and kept on wet ice until plasma isolation, within 2 hours of collection. Samples were stored frozen ($-85°C$ to $-60°C$) until analysis as described in Appendix A.

Transcriptomics

Sample Collection for Transcriptomics

Within 5 minutes of euthanasia, samples from the left liver lobe and right kidney were collected from all study animals for transcriptomic analysis. Half of the left liver lobe and half of the right kidney were processed for RNA isolation. Approximately 250 mg of each tissue was cut into small pieces (approximately 5 mm^3) and placed into cryotubes containing RNA*later*™. The tissue samples were stored at 2°C to 8°C overnight. The RNA*later*™ was then removed and the samples were stored in a $-85°C$ to $-60°C$ freezer until processed for RNA isolation.

RNA Isolation, Library Creation, and Sequencing

RNA isolation was performed on tissue samples preserved in RNA*later*™. Tissues were homogenized in QIAzol buffer (Qiagen Inc., Valencia, CA) using the TissueLyser II bead-beating system followed by RNA extraction using the Rneasy 96 QIAcube HT kits (Cat# 74171, Qiagen Inc., Valencia, CA) with a DNA digestion step. The concentration and purity of all isolated samples were determined from absorbency readings taken at 260 and 280 nm using a NanoDrop ND-8000 Spectrophotometer (NanoDrop Technologies, Wilmington, DE). The readings accurately determined the concentration of each sample while ensuring that an acceptable purity (A_{260}/A_{280} ratio) between 1.80 and 2.20 was achieved. After quantification, RNA was stored at $-70°C \pm 10°C$ until further processing.

One microliter of each RNA sample (500–660 ng/µL) was hybridized with the S1500+ beta detector oligo pool mix (2 µL per sample) using the following thermocycler settings: 10 minutes at 70°C, followed by a gradual decrease to 45°C over 49 minutes, and ending with a 45°C hold for 1 minute. Hybridization was followed by nuclease digestion (24 µL nuclease mix addition followed by 90 minutes at 37°C), ligation (24 µL ligation mix addition followed by 60 minutes at 37°C), and heat denaturation (at 80°C for 15 minutes). Ten microliters of each ligation product were then transferred to a 96-well polymerase chain reaction (PCR) amplification microplate with 10 µL of PCR mix per well. Through 25 cycles of amplification, well-specific "barcoded" primer pairs were introduced to templates. Five microliters of the PCR amplification products from each well were then pooled into a single sequencing library. The TempO-Seq library was then processed with a PCR clean-up kit (Machery-Nagel, Mountain View, CA) prior to sequencing. Sequencing was performed using a 50-cycle single-end read flow cell on a HiSeq 2500 Sequencing System (Illumina, San Diego, CA). Processing of sequencing data was conducted using Illumina's BCL2FASTQ software employing default parameter settings.

Sequence Data Processing

FASTQ files of TempO-Seq reads were aligned to the probe sequences from the target platform using Bowtie version 1.2.2[14] with the following parameters: -v 3 -k 1 -m 1 --best --strata. This configuration allows up to three mismatches and reports the single best alignment. After

alignment, the total sequenced reads, the percentage of reads aligning to the platform manifest, the alignment rate, and the percentage of expressed probes (≥5 reads per probe) were calculated for each sample.

Sequencing Quality Checks and Outlier Removal

Samples were flagged for values below the following thresholds: sequencing depth <300 K, total alignment rate <40%, unique alignment rate <30%, number of aligned reads <300 K, or percentage of probes with at least five reads <50%. Filtering on the percentage of expressed probes eliminates biased samples for which the sequenced reads only reflect a small portion of the measured transcriptome. In addition, FastQC was run on all samples to ensure adequate per base quality and per base N content, where N represents bases that could not be identified. This procedure resulted in one kidney 6:1 FTOH sample on one plate being flagged and removed (unique alignment rate of 1.86%).

Principal component (PCA), hierarchical cluster, and inter-replicate correlation analyses were performed. These analyses highlighted three additional outlier liver samples, which were removed before downstream analysis.

The processing of samples from the study of 6:1 FTOH was done in parallel with three other chemicals that were studied under a similar protocol, therefore allowing for a more powerful collective assessment of the data. Specifically, the samples from all four studies were distributed over twelve 96-well plates (i.e., one plate per chemical per tissue and four additional plates with overflow samples for three of the chemicals, with nine doses plus vehicle control). For kidney samples, average read depth per chemical varied across plates. Kidney samples on one of the overflow plates also clustered separately (in the PCA and hierarchical cluster analysis) from the other kidney samples for a given chemical. Therefore, kidney samples on that overflow plate were removed, resulting in one plate of data per chemical for the downstream analysis of kidney samples. The exclusion of these data had limited impact on the analysis as the samples from each dose group were randomly sorted into the overflow plates. The final sample counts that were used for benchmark dose (BMD) analysis of the transcriptomics data are shown in Table 1.

Table 1. Final Sample Counts for Benchmark Dose Analysis of the Transcriptomics Data

	0 mg/kg	0.15 mg/kg	0.5 mg/kg	1.4 mg/kg	4 mg/kg	12 mg/kg	37 mg/kg	111 mg/kg	333 mg/kg	1,000 mg/kg
Male										
Liver	10	5	5	5	5	5	5	5	4	0
Kidney	10	5	5	4	3	5	4	5	4	0
Female										
Liver	10	5	5	5	4	5	5	5	5	5
Kidney	8	4	2	5	5	5	4	4	3	5

Data Normalization

The aligned read counts for attenuated probes were properly readjusted to calculate unattenuated equivalent counts using the attenuation factors provided in the platform manifest. To account for between-sample sequencing depth variation, unattenuated read counts were normalized at the probe level by applying reads per million normalization. A pseudo-read-count of 1.0 was added

to each normalized expression value, and then the values were log2 transformed to complete the normalization. Principal component-based visualizations of the final expression data set used from modeling are available in Appendix C.

Data Analysis

Statistical Analysis of Body Weights, Organ Weights, and Clinical Pathology

Two approaches were employed to assess the significance of pairwise comparisons between dosed and vehicle control groups in the analysis of continuous variables. Organ and body weight data, which have approximately normal distributions, were analyzed using the parametric multiple comparison procedures of Williams[15; 16] and Dunnett.[17] Clinical pathology data, which typically have skewed distributions, were analyzed using the nonparametric multiple comparison methods of Shirley[18] and Dunn.[19] The Jonckheere test[20] was used to assess the significance of dose-response trends and to determine whether a trend-sensitive test (Williams or Shirley test) was more appropriate for pairwise comparisons than a test that assumes no monotonic dose response (Dunnett or Dunn test). Trend-sensitive tests were used when the Jonckheere test was significant at $p \leq 0.01$.

Prior to analysis, values identified by the outlier test of Dixon and Massey[21] were examined by National Institute of Environmental Health Sciences (NIEHS) staff. Values from animals suspected of illness due to causes other than experimental exposure and values that the laboratory indicated as inadequate due to measurement problems were eliminated from the analysis.

A no-observed-effect level (NOEL) was identified as the highest dose not showing a significant ($p \leq 0.05$) pairwise difference relative to the vehicle control group. A lowest-observed-effect level (LOEL) was identified as the lowest dose demonstrating a significant ($p \leq 0.05$) pairwise difference relative to the vehicle control group. Throughout the results section for apical endpoints, interpretation of BMDs is made in relationship to NOEL and LOEL values for specific endpoints, as defined here, and are not meant to reflect an overall study NOEL or LOEL.

Benchmark Dose Analysis of Body Weights, Organ Weights, and Clinical Pathology

Clinical pathology, body weight, and organ weight endpoints that exhibited a significant trend and pairwise test were submitted in batch for automated BMD modeling analysis. For body weight, the BMD and benchmark dose lower confidence limit (BMDL) were presented as not determined when there were no significant results. BMD modeling and analysis was conducted using a modification of Benchmark Dose Modeling Software (BMDS) version 2.7.0. Data sets were executed using the Python BMDS interface (https://pypi.python.org/pypi/bmds; version 0.11), which allows for batch processing of multiple data sets. Data for all endpoints submitted were continuous. A default benchmark response (BMR) of one standard deviation (relative to control) was used for all data sets. The following BMDS 2.7.0 models were used to model the means of the data sets:

- Linear

- Polynomial 2°, 3°, 4°, 5°, 6°, 7°, 8°
- Power
- Hill
- Exponential M2, M3, M4, M5

Multiple versions of the polynomial model were executed, from a polynomial of degree 2 to a polynomial of degree equal to the number of dose groups minus 1 (e.g., if a data set had five dose groups, a 2°, 3°, and 4° polynomial model would be executed). Models were initialized using BMDS 2.7.0 model defaults, including restricting the power parameter of the power model and n-parameter of the Hill model to >1 and the beta parameters of the polynomial model to positive or negative, depending on the mean response direction of the data set. For all models, either a constant or nonconstant variance model was selected as outlined in the EPA BMD technical guidance[22] and was implemented in the BMDS 2.7.0 software.

After model execution, BMDs were selected using the model recommendation procedures generally described in the EPA BMD technical guidance[22] and the automated decision logic described in Wignall et al.[23] and summarized in Appendix D, Table D-1. Models were placed into one of four possible bins, depending on the results and the bin recommendation logic:

(1) **Failure:** model did not successfully complete

(2) **Nonviable model (NVM):** model successfully completed but failed acceptability criteria

(3) **Not reportable (NR):** model is identified and meets all acceptability criteria with the exception of the estimated BMD being below the lower limit of extrapolation (<1/3 the lowest nonzero dose tested); BMD reported as <1/3 the lowest nonzero dose tested and BMD$_L$ is not reportable

(4) **Viable model:** candidate for recommended model without warning

If only one model was in the viable model bin, it was selected as the best-fitting model. If the viable bin had more than one model, consistent with EPA guidance,[22] either the model with the lowest Akaike information criterion (AIC) or lowest BMD$_L$ was selected. If the range of BMD$_L$ values was sufficiently close (less than threefold difference), the AIC value was used; otherwise, the BMD$_L$ value was used. If no model was recommended, no BMD was presented in the results. Details on the analysis criteria and decision tree are provided in Table D-1 and Figure D-1, respectively. To avoid effects of model extrapolation, BMD values derived from viable models that were threefold lower than the lowest nonzero dose tested were reported as <1/3 the lowest nonzero dose tested, and corresponding BMD$_L$ values were not reported. Finally, all modeling results from apical data yielding a BMD were reviewed by a subject matter expert to determine the validity of the modeling results and potency estimates.

Benchmark Dose Analysis of Transcriptomics Data

The BMD analysis of the transcriptomic data was performed in accordance with the National Toxicology Program (NTP) best practices for genomic dose-response modeling as reviewed by an independent panel of experts in October 2017. These recommendations are described in the 2018 publication, *National Toxicology Program Approach to Genomic Dose Response Modeling*.[24]

Dose-response analyses of normalized gene expression data were performed using BMDExpress 2.30.0507 BETA (https://github.com/auerbachs/BMDExpress-2/releases). A trend test (the Williams trend test[15; 16] $p \le 0.05$, 10,000 permutations) and fold change filter (1.5-fold change up or down relative to the vehicle control group for probe sets) were applied to the data set to remove probe sets demonstrating no response to chemical exposure from subsequent analysis. These filter criteria were empirically determined with the goal of balancing false discovery with reproducibility. The criteria are consistent with the MicroArray Quality Control recommendations to combine the nominal p value threshold with a fold change filter to maximize replicability of transcriptomic findings across labs.[25] The following dose-response models were fit to the probe sets that passed the trend test and fold change filter:

- Hill
- Power
- Linear
- Polynomial 2°
- Exponential M2, M3, M4, M5

All gene expression data analyzed in BMDExpress were log2 transformed, and thus nearly all probes (also known as detection oligos or DO) were assumed to exhibit constant variance across the doses. For this reason and for efficiency purposes, each model was run assuming constant variance. Lacking any broadly applicable guidance regarding the level of change in gene expression considered biologically significant, a BMR of one standard deviation (relative to the fit at control) was used in this study. This approach enables standardization of the BMR between apical endpoints and transcriptomic endpoints and provides a standard for use across multiple chemicals tested in this rapid screening paradigm. The expression direction (upregulated or downregulated) for each probe was determined by a trend test intrinsic to the model executables (provided by EPA) contained in BMDExpress.

To identify the best-fit model for each fitted probe, the AIC values for each fitted model were compared and the model with the lowest AIC was selected. The best model for each probe was used to calculate the BMD, BMD_L, and BMD upper confidence limit (BMD_U). The specific parameter settings, selected from the BMDExpress software when performing probe-level BMD analysis, were as follows: maximum iterations – 250, confidence level – 0.95, BMR factor – 1 (the multiplier of the standard deviation that defined the BMD), restrict power – no restriction, and constant variance – selected. The specific model selection setting in the BMDExpress software when performing probe set-level BMD analysis was as follows: best poly model test – lowest AIC, flag Hill model with "k" parameters – <1/3 the lowest nonzero dose tested, and best model selection with flagged Hill model – include flagged Hill model. The inclusion of the flagged models is a deviation from EPA BMD analysis guidance.[22] The justification for this deviation relates to subsequent use of the data in which the probe BMD values are grouped into gene sets from which a median BMD is derived. If the probes were removed from the analysis or forced to another model, the probe might not be counted in the gene set analysis and could lead to loss of "active" gene sets. Importantly, most of the probes that produce flagged Hill models show highly potent responses and should therefore be counted in the analysis.

To perform Gene Ontology (GO; annotation accession date: 07/15/2020) gene set analysis, only GO terms with ≥10 and ≤250 annotated genes measured on the gene expression platform were

considered. Before sorting genes into the GO terms, the best-fit model for each probe was subjected to a filtering process to remove those probes (1) with a BMD greater than the highest dose tested, (2) that mapped to more than one gene, (3) that had a global goodness-of-fit p value ≤ 0.1, and (4) with a BMD_U/BMD_L ratio >40. GO terms that were at least 5% populated and contained three genes that passed the criteria mentioned above were considered "active" (i.e., responsive to chemical exposure). For this report, GO terms populated with identical sets of differentially expressed genes were filtered to limit redundancy in reporting based on the following selection criteria: (1) highest percentage populated and (2) most specific/highest GO level. Redundant GO terms failing to differentiate on the basis of these criteria were retained and reported. A complete list of "active" GO terms can be found in Appendix F. To avoid effects of model extrapolation, GO terms exhibiting BMD values below the lower limit of extrapolation (<1/3 the lowest nonzero dose tested) were reported as <1/3 the lowest nonzero dose tested and corresponding BMD_L and BMD_U values were not reported.

To perform Individual Gene Analysis, the best-fit model for each probe was subjected to a filtering process to remove those probes (1) with a BMD greater than the highest dose tested, (2) that mapped to more than one gene, (3) that had a global goodness-of-fit p value ≤ 0.1, or (4) with a BMD_U/BMD_L ratio >40. For genes that had more than one probe represented on the platform and passed this filtering process, a median BMD was used to estimate the BMD, BMD_L, and BMD_U values. To ensure only genes with a robust response were assessed for potency, genes with probes that had a median fold change <|2| were removed prior to reporting. A complete list of genes and their corresponding metrics can be found in Appendix F. To avoid effects of model extrapolation, genes exhibiting BMD values below the lower limit of extrapolation (<1/3 the lowest nonzero dose tested) were reported as <1/3 the lowest nonzero dose tested and corresponding BMD_L and BMD_U values were not reported.

A summary of the BMDExpress gene expression analysis pipeline used in this study is shown in Figure D-2.

Empirical False Discovery Rate Determination for Genomic Dose-response Modeling

The genomic dose-response analysis pipeline is a complex multistep process with multiple modeling steps and parameter variables. Because of this complexity, traditional statistical models for determining false discovery rates for the genes and pathways are not straightforward to apply. To overcome this issue, an empirical false discovery rate was determined on the basis of the totality of the analysis pipeline. This was done through the evaluation of synthetic null data sets derived from vehicle control data from four short-term repeat dose toxicogenomic studies including 6:1 FTOH (each with 10 vehicle control samples). The other toxicogenomic studies, which are reported in separate NIEHS reports, are of perfluorohexanesulfonamide,[26] 1,1,2,2-tetrahydroperfluoro-1-dodecanol,[27] and 2,3-benzofluorene.[28] Samples from all four studies were processed as a group and subjected to sequencing at the same time and were visually inspected to ensure there was no batch effect between the different studies.

To create synthetic null data for a given group (tissue per sex combination), up to 40 vehicle control samples from the original studies (10 replicates × 4 chemicals) were used to generate the data sets, with outliers excluded from the analysis. Each computationally generated sample was created by mixing two randomly selected vehicle control samples via a weighted average

approach through which weights were obtained from random uniform (0,1) distribution. A total of 55 samples (10 vehicle control samples + 45 dosed samples [9 doses × 5 replicates]) were computationally generated per data set and assigned doses spaced by approximately half-log. A total of 20 data sets were generated per group (i.e., 20 data sets each for female kidney, male kidney, female liver, and male liver) and analyzed using both the individual gene-level and GO biological process (gene set) analysis pipeline employed to analyze the data from each study. The median empirical false discovery rates across the 20 null sets in each group for gene-level analysis across each group were 0.037%, 0.037%, 0%, and 0% (female kidney, male kidney, female liver, and male liver, respectively). The median empirical false discovery rate for each of the 20 null data sets in each group using the GO biological process (gene set) level analysis was 0%. Details of the empirical false discovery rate analysis are available in Appendix C. The associated bm2 analysis file that is the basis of the empirical false discovery rate can be found in Appendix F.

Data Accessibility

Primary and analyzed data used in this study are available to the public at
https://doi.org/10.22427/NIEHS-DATA-NIEHS-07.[29]

Results

Animal Condition, Body Weights, and Organ Weights

Male and female rats administered 333 or 1,000 mg/kg body weight (mg/kg) of
6:1 fluorotelomer alcohol (6:1 FTOH) began exhibiting signs of overt toxicity on study days 1–2, which included red discharge from eyes, slow breathing, ruffled or unkempt coat, cold to touch, soft feces, hunched posture, prone positioning, wet urogenital area, and lethargy (Appendix F). The 1,000 mg/kg male rats exhibited high mortality, with three rats found dead on study day 4 and one male rat moribund on study day 1 and euthanized at that time due to severe toxicity. No significant changes in terminal body weight for male or female rats occurred with exposure to 6:1 FTOH (Table 2).

In male rats at study termination, a significant increase in absolute and relative liver weights occurred in dose groups ≥ 37 mg/kg; both endpoints had positive trends (Table 3). The benchmark doses (benchmark dose lower confidence limits)—BMDs (BMD_{LS})—for increased absolute and relative liver weights were 28.507 (15.286) and 12.122 (9.527) mg/kg, respectively. Relative left kidney weight showed a significant pairwise increase at 333 mg/kg with a positive trend; the BMD (BMD_L) was 20.907 (4.272) mg/kg. Relative right kidney weight had significant trend and pairwise comparisons. Although a BMD was estimated for relative right kidney weight, its value was much lower (approximately 25- to 80-fold) than would be expected given the endpoint-specific no-observed-effect level (NOEL) and lowest-observed-effect level (LOEL) values, suggesting that the BMD estimate did not accurately reflect the true potency of the effect and was likely an anomalous product of the BMD modeling approach. The BMDs for all organ weights were reviewed by a subject matter expert for anomalous modeling results (i.e., when the traditional statistics are notably different from the estimated BMD values). Significant trend and pairwise comparisons were not observed in absolute left or right kidney weights or absolute or relative heart weights (Appendix F).

In female rats at study termination, a significant increase in absolute and relative liver weights occurred in the 333 and 1,000 mg/kg groups and both endpoints had positive trends (Table 3); BMDs (BMD_{LS}) for increased absolute and relative liver weights were not determined because no viable models were available. Significant trend and pairwise comparisons were not observed in absolute or relative heart, right kidney, or left kidney weights (Appendix F).

Table 2. Summary of Body Weights of Male and Female Rats Administered 6:1 Fluorotelomer Alcohol for Five Days

Study Day[a,b]	0 mg/kg	0.15 mg/kg	0.5 mg/kg	1.4 mg/kg	4 mg/kg	12 mg/kg	37 mg/kg	111 mg/kg	333 mg/kg	1,000 mg/kg	BMD_{1Std} (mg/kg)	BMD_{L1Std} (mg/kg)
Male												
n	10	5	5	5	5	5	5	5	5	5	NA	NA
0	299.9 ± 6.3	307.1 ± 5.6	300.7 ± 4.3	307.3 ± 8.3	295.0 ± 10.2	304.3 ± 2.6	300.7 ± 11.9	303.8 ± 9.1	306.4 ± 3.4	298.7 ± 7.3	ND	ND
5	315.0 ± 6.8	320.7 ± 5.3	310.7 ± 5.1	324.0 ± 10.6	310.8 ± 9.7	317.0 ± 2.4	316.2 ± 12.6	319.4 ± 10.3	304.4 ± 4.9	295.8[c]	ND	ND
Female												
n	10	5	5	5	5	5	5	5	5	5	NA	NA
0	213.2 ± 6.4	216.5 ± 4.8	213.1 ± 6.6	215.7 ± 4.6	209.1 ± 6.4	209.8 ± 2.8	218.0 ± 5.3	211.5 ± 4.1	210.5 ± 4.8	215.1 ± 2.8	ND	ND
5	218.8 ± 7.0	224.9 ± 8.6	218.9 ± 6.0	219.1 ± 6.6	213.9 ± 6.1	219.3 ± 2.9	222.0 ± 5.5	216.2 ± 3.9	219.7 ± 5.7	222.8 ± 3.0	ND	ND

BMD_{1Std} = benchmark dose corresponding to a benchmark response set to one standard deviation from the mean; BMD_{L1Std} = benchmark dose lower confidence limit corresponding to a benchmark response set to one standard deviation from the mean; NA = not applicable; ND = not determined.
[a]Data are displayed as mean ± standard error of the mean; body weight data are presented in grams.
[b]Statistical analysis performed by the Jonckheere (trend) and Williams or Dunnett (pairwise) tests.
[c]One male rat was moribund and euthanized on study day 1 and three male rats were found dead on study day 4. Body weight data from the remaining male rat were excluded from statistical analysis and BMD calculations.

Table 3. Summary of Select Organ Weights of Male and Female Rats Administered 6:1 Fluorotelomer Alcohol for Five Days

Endpoint[a,b,c]	0 mg/kg	0.15 mg/kg	0.5 mg/kg	1.4 mg/kg	4 mg/kg	12 mg/kg	37 mg/kg	111 mg/kg	333 mg/kg	1,000 mg/kg	BMD$_{1Std}$ (mg/kg)	BMD$_{L1Std}$ (mg/kg)
Male												
n	10	5	5	5	5	5	5	5	5	1[d]	NA	NA
Terminal Body Wt. (g)	315.0 ± 6.8	320.7 ± 5.3	310.7 ± 5.1	324.0 ± 10.6	310.8 ± 9.7	317.0 ± 2.4	316.2 ± 12.6	319.4 ± 10.3	304.4 ± 4.9	295.8	ND	ND
Right Kidney												
Relative (mg/g)[e]	3.10 ± 0.04**	3.16 ± 0.04	3.16 ± 0.13	3.19 ± 0.12	3.43 ± 0.08	3.20 ± 0.06	3.50 ± 0.04**	3.41 ± 0.10**	3.50 ± 0.15**	3.45	0.464[f]	0.082[f]
Left Kidney												
Relative (mg/g)	3.10 ± 0.06**	3.21 ± 0.03	3.15 ± 0.08	3.11 ± 0.07	3.24 ± 0.07	3.20 ± 0.05	3.37 ± 0.05	3.19 ± 0.09	3.44 ± 0.14**	3.28	20.907	4.272
Liver												
Absolute (g)	11.78 ± 0.39**	12.05 ± 0.23	11.83 ± 0.52	12.37 ± 0.65	12.29 ± 0.59	12.12 ± 0.34	13.47 ± 0.55**	16.63 ± 0.55**	18.04 ± 0.20**	17.87	28.507	15.286
Relative (mg/g)	37.37 ± 0.80**	37.58 ± 0.63	38.03 ± 1.21	38.11 ± 1.05	39.50 ± 1.06	38.26 ± 1.06	42.60 ± 0.63**	52.12 ± 1.06**	59.30 ± 0.73**	60.41	12.122	9.527
Female												
n	10	5	5	5	5	5	5	5	5	5	NA	NA
Terminal Body Wt. (g)	218.8 ± 7.0	224.9 ± 8.6	218.9 ± 6.0	219.1 ± 6.6	213.9 ± 6.1	219.3 ± 2.9	222.0 ± 5.5	216.2 ± 3.9	219.7 ± 5.7	222.8 ± 3.0	ND	ND
Liver												
Absolute (g)	7.92 ± 0.41**	8.47 ± 0.61	8.21 ± 0.22	7.80 ± 0.38	7.87 ± 0.46	8.15 ± 0.21	8.16 ± 0.24	7.87 ± 0.13	9.22 ± 0.18**	12.02 ± 0.17**	NVM	NVM
Relative (mg/g)	36.00 ± 0.72**	37.50 ± 1.29	37.54 ± 0.39	35.52 ± 0.64	36.67 ± 1.13	37.15 ± 0.72	36.76 ± 0.46	36.40 ± 0.34	42.01 ± 0.50**	53.98 ± 0.92**	NVM	NVM

Statistical significance for a dosed group indicates a significant pairwise test compared to the vehicle control group. Statistical significance for the vehicle control group indicates a significant trend test.

**Statistically significant at p ≤ 0.01.

BMD$_{1Std}$ = benchmark dose corresponding to a benchmark response set to one standard deviation from the mean; BMD$_{L1Std}$ = benchmark dose lower confidence limit corresponding to a benchmark response set to one standard deviation from the mean; NA = not applicable; ND = not determined; NVM = nonviable model.

[a]Descriptions of organ weight endpoints and changes are provided in Appendix E.

[b]Data are displayed as mean ± standard error of the mean.

[c]Statistical analysis performed by the Jonckheere (trend) and Williams or Dunnett (pairwise) tests.

[d]One male rat was moribund and euthanized on study day 1 and three male rats were found dead on study day 4. Body weight and organ weight data from the remaining male rat were excluded from statistical analysis and BMD calculations.

[e]Relative organ weights (organ weight-to-body weight ratios) are given as mg organ weight/g body weight.

[f]BMD values are much lower than would be expected given the lowest-observed-effect level and no-observed-effect level values, suggesting that the BMD estimates do not accurately reflect the true potency of the effect of these endpoints and are likely an anomalous product of the BMD modeling approach.

Clinical Pathology

In male rats, triglyceride and cholesterol concentrations were significantly decreased in dose groups ≥12 mg/kg and ≥37 mg/kg, respectively; BMDs (BMD$_L$s) were not determined for these two endpoints because no viable models were available (Table 4). Creatinine concentration was significantly increased in the 333 mg/kg male rats with a BMD (BMD$_L$) of 97.38 (32.365) mg/kg. Albumin concentration was significantly increased in the ≥37 mg/kg male rats with a BMD (BMD$_L$) of 13.365 (4.084) mg/kg. Alanine aminotransferase activity was significantly increased in male rats in the ≥37 mg/kg groups and aspartate aminotransferase (AST) activity was significantly increased in the ≥111 mg/kg groups with BMDs (BMD$_L$s) of 36.116 (21.468) and 28.117 (19.352) mg/kg, respectively. Alkaline phosphatase activity was significantly increased in the 333 mg/kg male rat group with a BMD (BMD$_L$) of 89.383 (74.114) mg/kg. In female rats, AST activity was significantly increased in the 1,000 mg/kg group with a BMD (BMD$_L$) of 497.046 (340.458) mg/kg. Globulin concentration in male rats, albumin/globulin (A/G) ratio in male rats, and cholesterol concentration in female rats had significant trend and pairwise comparisons. Although a BMD was estimated for each of these endpoints, these values were much lower (approximately 10- to 35-fold, 10- to 25-fold, and 70- to 210-fold for globulin concentration in male rats, A/G ratio in male rats, and cholesterol concentration in female rats, respectively) than would be expected given the endpoint-specific NOEL and LOEL values, suggesting that the BMD estimate did not accurately reflect the true potency of the effect and was likely an anomalous product of the BMD modeling approach. The BMDs for all clinical pathology endpoints were reviewed by a subject matter expert for anomalous modeling results (i.e., when the traditional statistics are notably different from the estimated BMD values).

The reticulocyte count was significantly decreased in the ≥37 mg/kg female groups with a BMD (BMD$_L$) of 15.578 (3.622) mg/kg (Table 5). In addition, in female rats, the monocyte and large unstained cell counts were significantly increased in dose groups ≥111 mg/kg and ≥37 mg/kg with BMDs (BMD$_L$s) of 257.111 (160.613) mg/kg and 54.339 (15.759) mg/kg, respectively. The reticulocyte count in male rats had significant trend and pairwise comparisons. Although a BMD was estimated, its value was much lower (approximately 120- to 360-fold) than would be expected given the endpoint-specific NOEL and LOEL values, suggesting that the BMD estimate did not accurately reflect the true potency of the effect and was likely an anomalous product of the BMD modeling approach.

In male rats, total thyroxine (total T4) concentration was significantly decreased in the ≥4 mg/kg groups with a BMD (BMD$_L$) of 3.19 (1.774) mg/kg (Table 6). In addition, free thyroxine (fT4) concentration was significantly decreased in the 333 mg/kg male rats; a BMD (BMD$_L$) was not determined because no viable model was available. In female rats, the total triiodothyronine (total T3) and total T4 concentrations were significantly decreased in the ≥333 mg/kg groups. The BMD (BMD$_L$) for decreased total T3 was 161.48 (122.215) mg/kg. A BMD (BMD$_L$) was not determined for decreased total T4 because no viable model was available. Additionally, thyroid stimulating hormone (TSH) concentration was significantly increased in female rats in the 1,000 mg/kg group with a BMD (BMD$_L$) of 356.61 (268.917) mg/kg. Total T3 concentration in male rats had significant trend and pairwise comparisons. Although a BMD was estimated, its value was much lower (approximately 10- to 25-fold) than would be expected given the endpoint-specific NOEL and LOEL values, suggesting that the BMD estimate did not accurately

14

reflect the true potency of the effect and was likely an anomalous product of the BMD modeling approach.

Table 4. Summary of Select Clinical Chemistry Data for Male and Female Rats Administered 6:1 Fluorotelomer Alcohol for Five Days

Endpoint[a,b]	0 mg/kg	0.15 mg/kg	0.5 mg/kg	1.4 mg/kg	4 mg/kg	12 mg/kg	37 mg/kg	111 mg/kg	333 mg/kg	1,000 mg/kg	BMD$_{1Std}$ (mg/kg)	BMD$_{L1Std}$ (mg/kg)
Male												
n	10	5	5	5	4[c]	5	5	5	5	1[d]	NA	NA
Creatinine (mg/dL)	0.41 ± 0.01**	0.42 ± 0.02	0.42 ± 0.02	0.42 ± 0.02	0.43 ± 0.03	0.38 ± 0.02	0.44 ± 0.02	0.46 ± 0.02	0.50 ± 0.03**	0.50	97.38	32.365
Globulin (g/dL)	1.95 ± 0.03**	1.96 ± 0.05	2.10 ± 0.06	2.28 ± 0.16	2.03 ± 0.09	1.70 ± 0.03*	1.76 ± 0.05*	1.40 ± 0.10**	1.34 ± 0.14**	1.20	0.322[e]	0.188[e]
A/G Ratio	2.29 ± 0.06**	2.28 ± 0.06	2.13 ± 0.04	2.03 ± 0.13	2.27 ± 0.08	2.69 ± 0.07*	2.71 ± 0.06*	3.50 ± 0.31**	3.75 ± 0.31**	3.92	0.456[e]	0.237[e]
Albumin (g/dL)	4.46 ± 0.06**	4.46 ± 0.07	4.46 ± 0.08	4.54 ± 0.06	4.58 ± 0.05	4.56 ± 0.05	4.76 ± 0.07**	4.78 ± 0.07**	4.86 ± 0.11**	4.70	13.365	4.084
Cholesterol (mg/dL)	106.6 ± 3.8**	107.6 ± 1.8	103.2 ± 2.2	114.0 ± 15.8	92.8 ± 5.4	89.6 ± 6.9	84.8 ± 4.2**	75.6 ± 2.8**	69.2 ± 4.9**	50.0	NVM	NVM
Triglycerides (mg/dL)	99.9 ± 9.9**	85.6 ± 9.9	107.4 ± 19.0	118.4 ± 35.2	82.0 ± 3.0	48.8 ± 8.3**	66.8 ± 14.0*	53.0 ± 2.9**	58.6 ± 14.8*	111.0	NVM	NVM
Alanine Aminotransferase (IU/L)	61.2 ± 3.6**	64.0 ± 5.2	55.0 ± 2.6	58.8 ± 3.2	70.5 ± 4.3	57.4 ± 3.7	72.2 ± 3.1*	110.2 ± 19.6*	209.2 ± 67.2**	134.0	36.116	21.468
Alkaline Phosphatase (IU/L)	302.2 ± 19.9**[f]	315.8 ± 18.4[f]	277.2 ± 11.1	322.8 ± 18.7	346.0 ± 15.5	325.0 ± 16.9	335.8 ± 23.5	357.2 ± 18.3	527.8 ± 34.1**	466.0	89.383	74.114
Aspartate Aminotransferase (U/L)	80.10 ± 4.72**	83.40 ± 4.86	72.20 ± 3.09	78.40 ± 3.36	82.50 ± 4.56	74.20 ± 3.73	91.00 ± 4.71	128.40 ± 17.32**	195.00 ± 54.03**	154.00	28.117	19.352
Female												
n	10	5	5	5	5	5	5	5	5	5	NA	NA
Cholesterol (mg/dL)	95.6 ± 4.9**	100.6 ± 7.7	104.8 ± 8.0	93.6 ± 11.9	82.2 ± 3.8	84.8 ± 2.2	90.4 ± 2.7	92.8 ± 3.1	38.0 ± 4.5**	54.0 ± 6.8**	1.591[e]	0.58[e]
Aspartate Aminotransferase (U/L)	72.80 ± 1.78**	73.60 ± 2.44	71.80 ± 2.03	76.40 ± 3.53	77.00 ± 2.59	75.60 ± 2.48	79.20 ± 2.97	74.00 ± 3.70	76.00 ± 2.74	103.60 ± 19.79**	497.046	340.458

Statistical significance for a dosed group indicates a significant pairwise test compared to the vehicle control group. Statistical significance for the vehicle control group indicates a significant trend test.

*Statistically significant at $p \leq 0.05$; **$p \leq 0.01$.

BMD$_{1Std}$ = benchmark dose corresponding to a benchmark response set to one standard deviation from the mean; BMD$_{L1Std}$ = benchmark dose lower confidence limit corresponding to a benchmark response set to one standard deviation from the mean; NA = not applicable; A/G Ratio = ratio of albumin to globulin; NVM = nonviable model.

[a]Data are displayed as mean ± standard error of the mean.

[b]Statistical analysis performed by the Jonckheere (trend) and Shirley or Dunn (pairwise) tests.

[c]One sample in the indicated dose group was not received.

[d]One male rat was moribund and euthanized on study day 1 and three male rats were found dead on study day 4. Clinical chemistry data from the remaining male rat were excluded from statistical analysis and BMD calculations.

[e]BMD values are much lower than would be expected given the lowest-observed-effect level and no-observed-effect level values, suggesting that the BMD estimates do not accurately reflect the true potency of the effect of these endpoints and are likely an anomalous product of the BMD modeling approach.

[f]One value for alkaline phosphatase in the vehicle control group and the 0.15 mg/kg group were excluded due to sample and/or analysis concerns.

In Vivo Repeat Dose Biological Potency Study of
6:1 Fluorotelomer Alcohol in Sprague Dawley Rats

Table 5. Summary of Select Hematology Data for Male and Female Rats Administered 6:1 Fluorotelomer Alcohol for Five Days

Endpoint[a,b]	0 mg/kg	0.15 mg/kg	0.5 mg/kg	1.4 mg/kg	4 mg/kg	12 mg/kg	37 mg/kg	111 mg/kg	333 mg/kg	1,000 mg/kg	BMD$_{1Std}$ (mg/kg)	BMD$_{L1Std}$ (mg/kg)
Male												
n	9[c]	4[c]	5	4[c]	4[c]	5	5	4[c]	4[c]	1[d]	NA	NA
Reticulocytes (10^3/μL)	240.2 ± 8.5**	237.2 ± 4.3	207.4 ± 13.6	228.4 ± 14.9	222.2 ± 6.6	211.9 ± 8.6	235.4 ± 9.9	194.9 ± 12.1*	89.9 ± 9.8**	88.4	0.308[e]	0.112[e]
Female												
n	9[c]	5	5	4[c]	5	5	5	5	5	5	NA	NA
Reticulocytes (10^3/μL)	224.6 ± 11.5**	235.1 ± 17.6	205.3 ± 17.2	206.6 ± 7.6	210.7 ± 11.9	200.6 ± 14.0	161.9 ± 6.5**	199.4 ± 20.2*	126.4 ± 9.4**	112.3 ± 12.7**	15.578	3.622
Monocytes (10^3/μL)	0.19 ± 0.04**	0.31 ± 0.08	0.28 ± 0.03	0.29 ± 0.04	0.28 ± 0.05	0.22 ± 0.04	0.28 ± 0.03	0.37 ± 0.05*	0.40 ± 0.06**	0.66 ± 0.18**	257.111	160.613
Large Unstained Cells (10^3/μL)	0.04 ± 0.01**	0.06 ± 0.01	0.05 ± 0.01	0.05 ± 0.01	0.05 ± 0.01	0.04 ± 0.01	0.06 ± 0.00**	0.07 ± 0.01**	0.07 ± 0.01**	0.07 ± 0.02*	54.339	15.759

Statistical significance for a dosed group indicates a significant pairwise test compared to the vehicle control group. Statistical significance for the vehicle control group indicates a significant trend test.

*Statistically significant at $p \leq 0.05$; **$p \leq 0.01$.

BMD$_{1Std}$ = benchmark dose corresponding to a benchmark response set to one standard deviation from the mean; BMD$_{L1Std}$ = benchmark dose lower confidence limit corresponding to a benchmark response set to one standard deviation from the mean; NA = not applicable.

[a]Data are displayed as mean ± standard error of the mean.

[b]Statistical analysis performed by the Jonckheere (trend) and Shirley or Dunn (pairwise) tests.

[c]One sample from each of the indicated dose groups had a clot present and was not analyzed.

[d]One male rat was moribund and euthanized on study day 1 and three male rats were found dead on study day 4. Hematology data from the remaining male rat were excluded from statistical analysis and BMD calculations.

[e]BMD values are much lower than would be expected given the lowest-observed-effect level and no-observed-effect level values, suggesting that the BMD estimates do not accurately reflect the true potency of the effect of these endpoints and are likely an anomalous product of the BMD modeling approach.

Table 6. Summary of Select Hormone Data for Male and Female Rats Administered 6:1 Fluorotelomer Alcohol for Five Days

Endpoint[a,b]	0 mg/kg	0.15 mg/kg	0.5 mg/kg	1.4 mg/kg	4 mg/kg	12 mg/kg	37 mg/kg	111 mg/kg	333 mg/kg	1,000 mg/kg	BMD$_{1Std}$ (mg/kg)	BMD$_{L1Std}$ (mg/kg)
Male												
n	9[c]	5	5	4[c]	4[c]	5	5	4[c]	4[c]	1[d]	NA	NA
Total T3 (ng/dL)	49.244 ± 2.130**	51.720 ± 1.832	56.580 ± 4.871	47.650 ± 0.999	44.975 ± 1.527	34.920 ± 2.801**	31.960 ± 2.646**	33.025 ± 0.999**	33.150 ± 4.547**	27.600	0.462[e]	0.245[e]
fT4 (ng/dL)	6.761 ± 0.817**	5.864 ± 0.686	6.680 ± 0.316	5.755 ± 0.496	6.410 ± 0.393	4.982 ± 0.435	5.726 ± 0.661	5.115 ± 0.301	4.363 ± 0.424**	3.780	NVM	NVM
Total T4 (µg/dL)	2.71 ± 0.16**	2.47 ± 0.26	2.57 ± 0.30	2.52 ± 0.14	1.58 ± 0.16**	1.01 ± 0.07**	0.93 ± 0.10**	0.66 ± 0.04**	0.50 ± 0.02**	0.66	3.19	1.774
Female												
n	9[c]	4[c]	3[f]	4[c]	5	4[c]	5	5	4[c]	5	NA	NA
TSH (ng/mL)	3.122 ± 0.371**	3.400 ± 1.013	2.800 ± 0.551	2.425 ± 0.375	3.020 ± 0.475	3.400 ± 0.826	2.540 ± 0.367	4.480 ± 0.388	3.775 ± 1.150	6.900 ± 0.933**	356.61	268.917
Total T3 (ng/dL)	66.000 ± 3.455**	58.825 ± 1.727	66.900 ± 4.891	59.825 ± 4.950	61.540 ± 4.315	62.700 ± 4.457	63.740 ± 2.761	59.040 ± 2.090	42.425 ± 2.062**	31.060 ± 1.857**	161.48	122.215
Total T4 (µg/dL)	3.12 ± 0.29**	2.83 ± 0.43	2.31 ± 0.08	2.64 ± 0.43	2.76 ± 0.11	2.79 ± 0.16	2.31 ± 0.22	2.64 ± 0.26	1.20 ± 0.18**	0.86 ± 0.14**	NVM	NVM

Statistical significance for a dosed group indicates a significant pairwise test compared to the vehicle control group. Statistical significance for the vehicle control group indicates a significant trend test.

**Statistically significant at $p \leq 0.01$.

BMD$_{1Std}$ = benchmark dose corresponding to a benchmark response set to one standard deviation from the mean; BMD$_{L1Std}$ = benchmark dose lower confidence limit corresponding to a benchmark response set to one standard deviation from the mean; NA = not applicable; total T3 = total triiodothyronine; fT4 = free thyroxine; NVM = nonviable model; total T4 = total thyroxine; TSH = thyroid stimulating hormone.

[a]Data are displayed as mean ± standard error of the mean.

[b]Statistical analysis performed by the Jonckheere (trend) and Shirley or Dunn (pairwise) tests.

[c]One sample in the indicated dose groups did not have sufficient specimen volume available for analysis.

[d]One male rat was moribund and euthanized on study day 1 and three male rats were found dead on study day 4. Hormone data from the remaining male rat were excluded from statistical analysis and BMD calculations.

[e]BMD values are much lower than would be expected given the lowest-observed-effect level and no-observed-effect level values, suggesting that the BMD estimates do not accurately reflect the true potency of the effect of these endpoints and are likely an anomalous product of the BMD modeling approach.

[f]Two samples in the indicated dose group did not have sufficient specimen volume available for analysis.

Internal Dose Assessment

For the 4 and 37 mg/kg groups, 6:1 FTOH plasma concentrations were determined at 2 and 24 hours following the last dose administered on study day 4 to male and female rats. Average 6:1 FTOH concentrations are given in Table 7. In the 4 mg/kg male rats at 2 hours following administration, the average concentration was slightly above the limit of detection (LOD = 2.9 ng/mL) of the analytical method. As the administered dose increased from 4 to 37 mg/kg (a ninefold increase), there was a more-than-proportional increase (38-fold) in the average 6:1 FTOH plasma concentration, suggesting changes in the absorption, distribution, metabolism, and excretion processes (e.g., saturation of clearance pathways) as the dose increased. In female rats at 2 hours postdose, the 6:1 FTOH plasma concentration was below the LOD of the analytical method in the 4 mg/kg group, and at 37 mg/kg, the average group concentration was lower than that observed in male rats (female, 115 ng/mL; male, 148 ng/mL), demonstrating some sex differences. At 24 hours postdose, the concentration fell below the LOD for both male and female rats suggesting short plasma half-lives of 6:1 FTOH in rats.

Table 7. Summary of Plasma Concentration Data for Male and Female Rats Administered 6:1 Fluorotelomer Alcohol for Five Days[a]

	4 mg/kg	37 mg/kg
n	3	3
Male		
2 Hours Postdose (ng/mL)	3.86 ± 0.164	148 ± 29.0
24 Hours Postdose (ng/mL)	BD	BD
Female		
2 Hours Postdose (ng/mL)	BD[b]	115 ± 44.9
24 Hours Postdose (ng/mL)	BD	BD

If over 20% of the animals in a group are above the limit of detection, then half the limit of detection value is substituted for values that are below it.
BD = below detection; group did not have over 20% of its values above the limit of detection so mean and standard error were not calculated.
[a]Data are displayed as mean ± standard error of the mean.
[b]Only two samples were received for the 4 mg/kg female rats at 2 hours postdose.

Apical Endpoint Benchmark Dose Summary

A summary of the calculated BMDs for each toxicological endpoint is provided in Table 8. The endpoint-specific LOEL and NOEL are included and could be informative for endpoints that lack a calculated BMD either because no viable model was available or because the estimated BMD was below the lower limit of extrapolation (<0.050 mg/kg).

Table 8. BMD, BMD$_L$, LOEL, and NOEL Summary for Apical Endpoints, Sorted by BMD or LOEL from Low to High

Endpoint	BMD$_{1Std}$ (mg/kg)	BMD$_{L1Std}$ (mg/kg)	LOEL (mg/kg)[a]	NOEL (mg/kg)	Direction of Change
Male					
Total Thyroxine	3.19	1.774	4	1.4	DOWN
Relative Liver Weight	12.122	9.527	37	12	UP
Albumin	13.365	4.084	37	12	UP
Relative Left Kidney Weight	20.907	4.272	333	111	UP
Aspartate Aminotransferase	28.117	19.352	111	37	UP
Absolute Liver Weight	28.507	15.286	37	12	UP
Alanine Aminotransferase	36.116	21.468	37	12	UP
Alkaline Phosphatase	89.383	74.114	333	111	UP
Creatinine	97.38	32.365	333	111	UP
A/G Ratio	UREP[b]	UREP[b]	**12**	4	–[b]
Globulin	UREP	UREP	**12**	4	–
Total Triiodothyronine	UREP	UREP	**12**	4	–
Triglycerides	NVM	NVM	**12**	4	DOWN
Cholesterol	NVM	NVM	**37**	12	DOWN
Relative Right Kidney Weight	UREP	UREP	**37**	12	–
Reticulocytes	UREP	UREP	**111**	37	–
Free Thyroxine	NVM	NVM	**333**	111	DOWN
Female					
Reticulocytes	15.578	3.622	37	12	DOWN
Large Unstained Cells	54.339	15.759	37	12	UP
Total Triiodothyronine	161.48	122.215	333	111	DOWN
Monocytes	257.111	160.613	111	37	UP
Thyroid Stimulating Hormone	356.61	268.917	1,000	333	UP
Aspartate Aminotransferase	497.046	340.458	1,000	333	UP
Absolute Liver Weight	NVM	NVM	**333**	111	UP
Cholesterol	UREP	UREP	**333**	111	–
Relative Liver Weight	NVM	NVM	**333**	111	UP
Total Thyroxine	NVM	NVM	**333**	111	DOWN

BMD$_{1Std}$ = benchmark dose corresponding to a benchmark response set to one standard deviation from the mean; BMD$_{L1Std}$ = benchmark dose lower confidence limit corresponding to a benchmark response set to one standard deviation from the mean; LOEL = lowest-observed-effect level; NOEL = no-observed-effect level; A/G Ratio = ratio of albumin to globulin; UREP = unreliable estimate of potency is a label based on review by a subject matter expert and rejection of BMD modeling results; NVM = nonviable model, defined as a modeling result that does not meet prespecified fit criteria and hence is deemed unreliable.
[a]Values in bold text indicate the LOEL of endpoints for which a BMD could not be calculated.
[b]BMD values are much lower than would be expected given the end-point specific LOEL and NOEL values, suggesting that the BMD estimates do not accurately reflect the true potency of the effect of these endpoints and are likely an anomalous product of the BMD modeling approach.

Gene Set Benchmark Dose Analysis

Chemical-induced alterations in liver and kidney gene transcript expression were examined to determine those gene sets most sensitive to 6:1 FTOH exposure. To that end, BMD analysis of transcripts and gene sets (Gene Ontology [GO] biological process) was conducted to determine the potency of the chemical to elicit gene expression changes in the liver and kidney. This analysis used transcript-level BMD data to assess an aggregate score of gene set potency (median transcript BMD) and enrichment.

The "active" gene sets in the liver and kidney with the lowest BMD median values are shown in Table 9 and Table 10, respectively. The gene sets in Table 9 and Table 10 should be interpreted with caution from the standpoint of the underlying biological mechanism and any relationship to toxicity or toxic agents referenced in the GO term definitions. The data primarily should be considered a metric of potency for chemical-induced transcriptional changes (i.e., a concerted biological change) that could serve as a surrogate of estimated biological potency and, by extension, toxicological potency when more definitive toxicological data are unavailable.

No gene sets in the liver of male or female rats had estimated BMD median values <0.050 mg/kg. In male rats, the most sensitive GO biological processes for which a BMD value could be reliably calculated were cellular response to epidermal growth factor stimulus (GO:0071364) and response to epidermal growth factor (GO:0070849) with median BMDs (BMD$_{LS}$) of 0.368 (0.103) and 0.690 (0.456) mg/kg, respectively. In female rats, the most sensitive GO biological processes for which a BMD value could be reliably calculated were positive regulation of phagocytosis (GO:0050766) and regulation of phagocytosis (GO:0050764) with median BMDs (BMD$_{LS}$) of 44.730 (22.260) and 48.555 (27.154) mg/kg, respectively.

Two gene sets in the kidney of male rats had estimated BMD median values <0.050 mg/kg, which were related to astrocyte activation (GO:0048143) and negative regulation of response to biotic stimulus (GO:0002832). The most sensitive GO biological processes for which a BMD value could be reliably calculated were acetyl-CoA metabolic process (GO:0006084) and acyl-CoA metabolic process (GO:0006637) with median BMDs (BMD$_{LS}$) of 1.346 (0.541) and 1.928 (1.305) mg/kg, respectively. No gene sets in the kidney of female rats had estimated BMD median values <0.050 mg/kg. The most sensitive GO biological processes for which a BMD value could be reliably calculated were fatty acid beta-oxidation (GO:0006635) and fatty acid oxidation (GO:0019395) with median BMDs (BMD$_{LS}$) of 21.079 (13.312) and 27.058 (13.877) mg/kg, respectively. The full list of affected gene sets in the liver and kidney of male and female rats can be found in Appendix F.

Table 9. Top 10 Liver Gene Ontology Biological Process Gene Sets Ranked by Potency of Perturbation, Sorted by Benchmark Dose Median[a]

Category Name	No. of Active Genes/ Platform Genes in Gene Set	% Gene Set Coverage	Active Genes	BMD$_{1std}$ Median of Gene Set Transcripts (mg/kg)	Median BMD$_{L1Std}$– BMD$_{U1Std}$ (mg/kg)	Genes with Changed Direction Up	Genes with Changed Direction Down
Male							
GO:0071364 cellular response to epidermal growth factor stimulus	3/20	15%	*Zfp36*; *Ncl*; *Myc*	0.368	0.103– 1.817	1	2
GO:0070849 response to epidermal growth factor	4/26	15%	*Zfp36*; *Ncl*; *Myc*; *Acot2*	0.690	0.456– 1.597	2	2
GO:0006635 fatty acid beta-oxidation	10/33	30%	*Slc27a2*; *Gcdh*; *Etfdh*; *Ehhadh*; *Eci1*; *Ech1*; *Crot*; *Cpt1b*; *Acox1*; *Acadsb*	2.017	1.401– 3.184	9	1
GO:0009062 fatty acid catabolic process	12/42	29%	*Slc27a2*; *Hacl1*; *Gcdh*; *Etfdh*; *Ehhadh*; *Eci1*; *Ech1*; *Crot*; *Cpt1b*; *Acox1*; *Acot2*; *Acadsb*	2.017	1.288– 3.184	11	1
GO:0072329 monocarboxylic acid catabolic process	15/48	31%	*Slc27a2*; *Hacl1*; *Gcdh*; *Etfdh*; *Ehhadh*; *Eci1*; *Ech1*; *Cyp26b1*; *Crot*; *Cpt1b*; *Agxt2*; *Acox1*; *Acot2*; *Acadsb*; *Abat*	2.238	1.439– 3.909	12	3
GO:0070371 ERK1 and ERK2 cascade	3/14	21%	*Tf*; *Myc*; *Apoa1*	2.377	1.208– 5.187	0	3

In Vivo Repeat Dose Biological Potency Study of
6:1 Fluorotelomer Alcohol in Sprague Dawley Rats

Category Name	No. of Active Genes/ Platform Genes in Gene Set	% Gene Set Coverage	Active Genes	BMD$_{1std}$ Median of Gene Set Transcripts (mg/kg)	Median BMD$_{L1Std}$– BMD$_{U1Std}$ (mg/kg)	Genes with Changed Direction Up	Genes with Changed Direction Down
GO:0000038 very long-chain fatty acid metabolic process	5/12	42%	*Slc27a2*; *Acox1*; *Acot4*; *Acot2*; *Acot1*	2.721	1.888– 4.505	5	0
GO:0046395 carboxylic acid catabolic process	21/87	24%	*Cemip2*; *Slc27a2*; *Kynu*; *Kmo*; *Hacl1*; *Gcdh*; *Etfdh*; *Ehhadh*; *Eci1*; *Ech1*; *Cyp26b1*; *Crot*; *Cpt1b*; *Cdo1*; *Blmh*; *Agxt2*; *Acox1*; *Acot4*; *Acot2*; *Acadsb*; *Abat*	3.806	1.610– 6.038	15	6
GO:0006637 acyl-CoA metabolic process	9/31	29%	*Mpc2*; *Kynu*; *Gcdh*; *Acss2*; *Acot4*; *Acot2*; *Acot12*; *Acot1*; *Acadsb*	4.030	2.953– 10.491	7	2
GO:0044282 small molecule catabolic process	23/120	19%	*Cemip2*; *Sult1e1*; *Slc27a2*; *Kynu*; *Kmo*; *Inpp1*; *Hacl1*; *Gcdh*; *Etfdh*; *Ehhadh*; *Eci1*; *Ech1*; *Cyp26b1*; *Crot*; *Cpt1b*; *Cdo1*; *Blmh*; *Agxt2*; *Acox1*; *Acot4*; *Acot2*; *Acadsb*; *Abat*	4.136	1.888– 10.491	17	6
Female							
GO:0050766 positive regulation of phagocytosis	4/35	11%	*Cd36*; *C3*; *Apoa2*; *Ahsg*	44.730	22.260– 122.653	2	2

In Vivo Repeat Dose Biological Potency Study of
6:1 Fluorotelomer Alcohol in Sprague Dawley Rats

Category Name	No. of Active Genes/ Platform Genes in Gene Set	% Gene Set Coverage	Active Genes	BMD$_{1std}$ Median of Gene Set Transcripts (mg/kg)	Median BMD$_{L1Std}$– BMD$_{U1Std}$ (mg/kg)	Genes with Changed Direction Up	Genes with Changed Direction Down
GO:0050764 regulation of phagocytosis	5/51	10%	*Cd36*; *C3*; *Apoa2*; *Alox15*; *Ahsg*	48.555	27.154– 159.716	2	3
GO:0002718 regulation of cytokine production involved in immune response	3/36	8%	*Ticam1*; *Cd36*; *Apoa2*	48.555	17.366– 159.716	3	0
GO:0034381 plasma lipoprotein particle clearance	3/11	27%	*Cd36*; *Apoc3*; *Apoa2*	48.555	17.366– 159.716	2	1
GO:0016051 carbohydrate biosynthetic process	3/32	9%	*Gpd1*; *G6pd*; *Acadm*	48.822	39.627– 63.173	3	0
GO:0006399 tRNA metabolic process	3/20	15%	*Tsen2*; *Iars2*; *Hsd17b10*	57.734	46.011– 76.940	3	0
GO:0051181 cofactor transport	3/10	30%	*Slc27a1*; *Slc22a8*; *Abcg2*	60.649	31.055– 121.705	1	2
GO:0044262 cellular carbohydrate metabolic process	3/40	8%	*Inpp1*; *Acadm*; *Abcg2*	60.649	39.560– 121.705	2	1
GO:0045926 negative regulation of growth	4/72	6%	*Gdf15*; *G6pd*; *Cdkn1a*; *Ahsg*	61.369	35.006– 115.629	2	2

In Vivo Repeat Dose Biological Potency Study of
6:1 Fluorotelomer Alcohol in Sprague Dawley Rats

Category Name	No. of Active Genes/ Platform Genes in Gene Set	% Gene Set Coverage	Active Genes	BMD$_{1std}$ Median of Gene Set Transcripts (mg/kg)	Median BMD$_{L1Std}$– BMD$_{U1Std}$ (mg/kg)	Genes with Changed Direction Up	Genes with Changed Direction Down
GO:0006635 fatty acid beta-oxidation	18/33	55%	*Slc27a2*; *Hadhb*; *Hadh*; *Gcdh*; *Etfdh*; *Ehhadh*; *Eci1*; *Ech1*; *Decr1*; *Crot*; *Crat*; *Cpt2*; *Cpt1b*; *Acox1*; *Acadsb*; *Acadm*; *Acadl*; *Acaa2*	64.027	46.553– 95.058	17	1

BMD$_{1Std}$ = benchmark dose corresponding to a benchmark response set to one standard deviation from the mean; BMD$_{L1Std}$ = benchmark dose lower confidence limit corresponding to a benchmark response set to one standard deviation from the mean; BMD$_{U1Std}$ = benchmark dose upper confidence limit corresponding to a benchmark response set to one standard deviation from the mean; GO = Gene Ontology.

[a]Definitions of GO terms were adapted from the Gene Ontology Resource.[30] Official gene symbols from the Rat Genome Database[31] are shown in the "Active Genes" column.

GO process description version: https://doi.org/10.22427/NTP-DATA-002-00600-0002-000-0.

GO:0071364 cellular response to epidermal growth factor stimulus: Any process that results in a change in state or activity of a cell (in terms of movement, secretion, enzyme production, gene expression, etc.) as a result of an epidermal growth factor stimulus.

GO:0070849 response to epidermal growth factor: Any process that results in a change in state or activity of a cell or an organism (in terms of movement, secretion, enzyme production, gene expression, etc.) as a result of an epidermal growth factor stimulus.

GO:0006635 fatty acid beta-oxidation: A fatty acid oxidation process that results in the complete oxidation of a long-chain fatty acid. Fatty acid beta-oxidation begins with the addition of coenzyme A to a fatty acid and occurs by successive cycles of reactions during each of which the fatty acid is shortened by a two-carbon fragment removed as acetyl-coenzyme A; the cycle continues until only two or three carbons remain (as acetyl-CoA or propionyl-CoA, respectively).

GO:0009062 fatty acid catabolic process: The chemical reactions and pathways resulting in the breakdown of a fatty acid, any of the aliphatic monocarboxylic acids that can be liberated by hydrolysis from naturally occurring fats and oils. Fatty acids are predominantly straight-chain acids of 4 to 24 carbon atoms, which may be saturated or unsaturated; branched fatty acids and hydroxy fatty acids also occur, and very long-chain acids of over 30 carbons are found in waxes.

GO:0072329 monocarboxylic acid catabolic process: The chemical reactions and pathways resulting in the breakdown of monocarboxylic acids, any organic acid containing one carboxyl (-COOH) group.

GO:0070371 ERK1 and ERK2 cascade: An intracellular protein kinase cascade containing at least ERK1 or ERK2 (MAPKs), a MEK (a MAPKK) and a MAP3K. The cascade may involve four different kinases, as it can also contain an additional tier: the upstream MAP4K. The kinases in each tier phosphorylate and activate the kinase in the downstream tier to transmit a signal within a cell.

GO:0000038 very long-chain fatty acid metabolic process: The chemical reactions and pathways involving a fatty acid with a chain length greater than C22.

GO:0046395 carboxylic acid catabolic process: The chemical reactions and pathways resulting in the breakdown of carboxylic acids, which are any organic acid containing one or more carboxyl (-COOH) groups.

GO:0006637 acyl-CoA metabolic process: The chemical reactions and pathways involving acyl-CoA, which is any derivative of coenzyme A in which the sulfhydryl group is in thiolester linkage with an acyl group.

GO:0044282 small molecule catabolic process: The chemical reactions and pathways resulting in the breakdown of small molecules, which are any low molecular weight, monomeric, nonencoded molecule.

GO:0050766 positive regulation of phagocytosis: Any process that activates or increases the frequency, rate, or extent of phagocytosis.

GO:0050764 regulation of phagocytosis: Any process that modulates the frequency, rate, or extent of phagocytosis, the process in which phagocytes engulf external particulate material.

GO:0002718 regulation of cytokine production involved in immune response: Any process that modulates the frequency, rate, or extent of cytokine production that contributes to an immune response.

GO:0034381 plasma lipoprotein particle clearance: The process in which a lipoprotein particle is removed from the blood via receptor-mediated endocytosis and its constituent parts degraded.

GO:0016051 carbohydrate biosynthetic process: The chemical reactions and pathways resulting in the formation of carbohydrates, which are any of a group of organic compounds based on the general formula $C_x(H_2O)_y$.

GO:0006399 tRNA metabolic process: The chemical reactions and pathways involving tRNA (transfer RNA), which is a class of relatively small RNA molecules responsible for mediating the insertion of amino acids into the sequence of nascent polypeptide chains during protein synthesis. Transfer RNA is characterized by the presence of many unusual minor bases, the function of which has not been completely established.

GO:0051181 cofactor transport: The directed movement of a cofactor into, out of, or within a cell, or between cells, by means of some agent such as a transporter or pore. A cofactor is a substance that is required for the activity of an enzyme or other protein.

GO:0044262 cellular carbohydrate metabolic process: The chemical reactions and pathways involving carbohydrates, which are any of a group of organic compounds based on the general formula $C_x(H_2O)_y$, as carried out by individual cells.

GO:0045926 negative regulation of growth: Any process that stops, prevents, or reduces the rate or extent of growth (the increase in size or mass of all or part of an organism).

Table 10. Top 10 Kidney Gene Ontology Biological Process Gene Sets Ranked by Potency of Perturbation, Sorted by Benchmark Dose Median[a]

Category Name	No. of Active Genes/ Platform Genes in Gene Set	% Gene Set Coverage	Active Genes	BMD$_{1std}$ Median of Gene Set Transcripts (mg/kg)	Median BMD$_{L1Std}$– BMD$_{U1Std}$ (mg/kg)	Genes with Changed Direction Up	Genes with Changed Direction Down
Male							
GO:0048143 astrocyte activation	3/11	27%	*Il1b*; *Grn*; *C1qa*	<0.050[b]	NR	1	2
GO:0002832 negative regulation of response to biotic stimulus	3/27	11%	*Parp14*; *Grn*; *Tkfc*	<0.050	NR	0	3
GO:0006084 acetyl-CoA metabolic process	3/16	19%	*Hmgcs2*; *Acot12*; *Acaa2*	1.346	0.541–4.058	2	1
GO:0006637 acyl-CoA metabolic process	6/31	19%	*Hmgcs2*; *Acot4*; *Acot2*; *Acot12*; *Acot1*; *Acaa2*	1.928	1.305–4.031	5	1
GO:0010883 regulation of lipid storage	3/22	14%	*Srebf1*; *Nfkbia*; *C3*	2.189	0.888–5.495	2	1
GO:0030522 intracellular receptor signaling pathway	3/42	7%	*Srebf1*; *Nr1d2*; *Nfkbia*	2.189	0.888–5.495	2	1
GO:0006721 terpenoid metabolic process	3/34	9%	*Pecr*; *Hmgcs2*; *Cyp2e1*	2.994	0.682–13.980	2	1

Category Name	No. of Active Genes/ Platform Genes in Gene Set	% Gene Set Coverage	Active Genes	BMD_{1std} Median of Gene Set Transcripts (mg/kg)	Median BMD_{L1Std}– BMD_{U1Std} (mg/kg)	Genes with Changed Direction Up	Genes with Changed Direction Down
GO:0002698 negative regulation of immune effector process	4/43	9%	*Lgals3*; *Grn*; *Enpp3*; *Tkfc*	3.710	1.436– 9.709	1	3
GO:0009062 fatty acid catabolic process	12/42	29%	*Hadh*; *Etfdh*; *Ehhadh*; *Eci2*; *Ech1*; *Decr1*; *Cpt2*; *Adipoq*; *Acox1*; *Acot2*; *Acadm*; *Acaa2*	3.895	1.678– 6.474	12	0
GO:0000038 very long-chain fatty acid metabolic process	4/12	33%	*Acox1*; *Acot4*; *Acot2*; *Acot1*	4.235	2.759– 6.872	4	0
Female							
GO:0006635 fatty acid beta-oxidation	8/33	24%	*Ppard*; *Ehhadh*; *Eci2*; *Eci1*; *Ech1*; *Acadm*; *Acadl*; *Acaa2*	21.079	13.312– 34.031	7	1
GO:0019395 fatty acid oxidation	10/43	23%	*Ppard*; *Hao2*; *Ehhadh*; *Eci2*; *Eci1*; *Ech1*; *Cd36*; *Acadm*; *Acadl*; *Acaa2*	27.058	13.877– 61.247	8	2
GO:0009062 fatty acid catabolic process	12/42	29%	*Ppard*; *Pck2*; *Pck1*; *Ehhadh*; *Eci2*; *Eci1*; *Ech1*; *Ces1d*; *Acot2*; *Acadm*; *Acadl*; *Acaa2*	27.540	15.179– 63.270	10	2

In Vivo Repeat Dose Biological Potency Study of
6:1 Fluorotelomer Alcohol in Sprague Dawley Rats

Category Name	No. of Active Genes/ Platform Genes in Gene Set	% Gene Set Coverage	Active Genes	BMD₁std Median of Gene Set Transcripts (mg/kg)	Median BMD_L1Std– BMD_U1Std (mg/kg)	Genes with Changed Direction Up	Genes with Changed Direction Down
GO:0006637 acyl-CoA metabolic process	7/31	23%	*Hmgcs2*; *Acss2*; *Acot4*; *Acot2*; *Acot12*; *Acot1*; *Acaa2*	38.393	23.116– 70.139	5	2
GO:0000038 very long-chain fatty acid metabolic process	3/12	25%	*Acot4*; *Acot2*; *Acot1*	38.393	23.116– 70.139	3	0
GO:0033875 ribonucleoside bisphosphate metabolic process	8/41	20%	*Pank1*; *Hmgcs2*; *Acss2*; *Acot4*; *Acot2*; *Acot12*; *Acot1*; *Acaa2*	44.906	31.624– 70.563	6	2
GO:0030258 lipid modification	13/70	19%	*Ppard*; *Hao2*; *Ephx2*; *Ehhadh*; *Eci2*; *Eci1*; *Ech1*; *Cyp2e1*; *Cyp1a1*; *Cd36*; *Acadm*; *Acadl*; *Acaa2*	49.703	38.943– 83.829	10	3
GO:0009409 response to cold	3/27	11%	*Cxcl10*; *Acadm*; *Acadl*	61.062	46.535– 88.000	2	1
GO:0009150 purine ribonucleotide metabolic process	10/80	13%	*Pank1*; *Pde4c*; *Hmgcs2*; *Aldoc*; *Acss2*; *Acot4*; *Acot2*; *Acot12*; *Acot1*; *Acaa2*	67.924	50.324– 104.308	7	3
GO:0006732 coenzyme metabolic process	12/67	18%	*Vnn1*; *Rgn*; *Pank1*; *Mthfd2*; *Hmgcs2*; *Gclc*; *Acss2*; *Acot4*; *Acot2*; *Acot12*; *Acot1*; *Acaa2*	67.924	50.324– 104.308	8	4

BMD₁Std = benchmark dose corresponding to a benchmark response set to one standard deviation from the mean; BMD_L1Std = benchmark dose lower confidence limit corresponding to a benchmark response set to one standard deviation from the mean; BMD_U1Std = benchmark dose upper confidence limit corresponding to a benchmark response set to one standard

deviation from the mean; GO = Gene Ontology; NR = the BMD_{L1Std}–BMD_{U1Std} range is not reportable because the BMD_{1Std} median is below the lower limit of extrapolation (<1/3 of the lowest nonzero dose tested).

[a]Definitions of GO terms were adapted from the Gene Ontology Resource.[30] Official gene symbols from the Rat Genome Database[31] are shown in the "Active Genes" column.

[b]<0.050 = a best-fit model was identified and a BMD_{1Std} was estimated that was <1/3 of the lowest nonzero dose tested.

GO process description version: https://doi.org/10.22427/NTP-DATA-002-00600-0002-000-0.

GO:0048143 astrocyte activation: A change in morphology and behavior of an astrocyte resulting from exposure to a cytokine, chemokine, cellular ligand, or soluble factor.

GO:0002832 negative regulation of response to biotic stimulus: Any process that stops, prevents, or reduces the frequency, rate, or extent of a response to biotic stimulus.

GO:0006084 acetyl-CoA metabolic process: The chemical reactions and pathways involving acetyl-CoA, a derivative of coenzyme A in which the sulfhydryl group is acetylated. Acetyl-CoA is a metabolite derived from several pathways (e.g., glycolysis, fatty acid oxidation, amino-acid catabolism) and is further metabolized by the tricarboxylic acid cycle. It is a key intermediate in lipid and terpenoid biosynthesis.

GO:0006637 acyl-CoA metabolic process: The chemical reactions and pathways involving acyl-CoA, any derivative of coenzyme A in which the sulfhydryl group is in thiolester linkage with an acyl group.

GO:0010883 regulation of lipid storage: Any process that modulates the rate, frequency, or extent of lipid storage. Lipid storage is the accumulation and maintenance in cells or tissues of lipids, which are compounds soluble in organic solvents but insoluble or sparingly soluble in aqueous solvents. Lipid reserves can be accumulated during early developmental stages for mobilization and utilization at later stages of development.

GO:0030522 intracellular receptor signaling pathway: Any series of molecular signals initiated by a ligand binding to a receptor located within a cell.

GO:0006721 terpenoid metabolic process: The chemical reactions and pathways involving terpenoids, which are any member of a class of compounds characterized by an isoprenoid chemical structure and including derivatives with various functional groups.

GO:0002698 negative regulation of immune effector process: Any process that stops, prevents, or reduces the frequency, rate, or extent of an immune effector process.

GO:0009062 fatty acid catabolic process: The chemical reactions and pathways resulting in the breakdown of fatty acids, which are any of the aliphatic monocarboxylic acids that can be liberated by hydrolysis from naturally occurring fats and oils. Fatty acids are predominantly straight-chain acids of 4 to 24 carbon atoms, which may be saturated or unsaturated; branched fatty acids and hydroxy fatty acids also occur, and very long-chain acids of over 30 carbons are found in waxes.

GO:0000038 very long-chain fatty acid metabolic process: The chemical reactions and pathways involving a fatty acid with a chain length greater than C22.

GO:0006635 fatty acid beta-oxidation: A fatty acid oxidation process that results in the complete oxidation of a long-chain fatty acid. Fatty acid beta-oxidation begins with the addition of coenzyme A to a fatty acid and occurs by successive cycles of reactions during each of which the fatty acid is shortened by a two-carbon fragment removed as acetyl-coenzyme A; the cycle continues until only two or three carbons remain (as acetyl-CoA or propionyl-CoA, respectively).

GO:0019395 fatty acid oxidation: The removal of one or more electrons from a fatty acid, with or without the concomitant removal of a proton or protons, by reaction with an electron-accepting substance, by addition of oxygen, or by removal of hydrogen.

GO:0033875 ribonucleoside bisphosphate metabolic process: The chemical reactions and pathways involving a ribonucleoside bisphosphate, which is a compound consisting of a nucleobase linked to a ribose sugar esterified with one phosphate group attached to each of two different hydroxyl groups on the sugar.

GO:0030258 lipid modification: The covalent alteration of one or more fatty acids in a lipid, resulting in a change in the properties of the lipid.

GO:0009409 response to cold: Any process that results in a change in state or activity of a cell or an organism (in terms of movement, secretion, enzyme production, gene expression, etc.) as a result of a cold stimulus (a temperature stimulus below the optimal temperature for that organism).

GO:0009150 purine ribonucleotide metabolic process: The chemical reactions and pathways involving a purine ribonucleotide, which is a compound consisting of ribonucleoside (a purine base linked to a ribose sugar) esterified with a phosphate group at either the 3' or 5'-hydroxyl group of the sugar.

GO:0006732 coenzyme metabolic process: The chemical reactions and pathways involving coenzymes, which are any of various nonprotein organic cofactors that are required, in addition to an enzyme and a substrate, for an enzymatic reaction to proceed.

Gene Benchmark Dose Analysis

The top 10 genes based on BMD potency in the liver and kidney (fold change >|2|, significant Williams trend test, global goodness-of-fit p value >0.1, and BMD_U/BMD_L ≤40) are shown in Table 11 and Table 12. As with the GO analysis, the biological or toxicological significance of

the changes in gene expression shown in Table 11 and Table 12 should be interpreted with caution. The data primarily should be considered a metric of potency for chemical-induced transcriptional changes that could serve as a conservative surrogate of estimated biological potency, and by extension toxicological potency, when more definitive toxicological data are unavailable.

No liver genes in male or female rats had estimated BMD median values <0.050 mg/kg. In male rats, the most sensitive upregulated genes with a calculated BMD were *Acot2* (acyl-CoA thioesterase 2), *Eci1* (enoyl-CoA delta isomerase 1), *Loc100911558*/*Spink1l* (serine peptidase inhibitor, Kazal type 1-like), *Spink1* (serine peptidase inhibitor, Kazal type 1), *Ehhadh* (enoyl-CoA hydratase and 3-hydroxyacyl CoA dehydrogenase), *Crot* (carnitine O-octanoyltransferase), *Acaa1a* (acetyl-CoA acyltransferase 1A), and *Acaa1b* (acetyl-Coenzyme A acyltransferase 1B) with BMDs (BMD$_L$s) of 1.012 (0.809), 1.013 (0.769), 1.270 (0.542), 1.270 (0.542), 1.280 (1.047), 1.411 (1.092), 1.874 (1.524), and 1.874 (1.524) mg/kg, respectively. The most sensitive genes exhibiting a decrease in expression were *Myc* (MYC proto-oncogene, bHLH transcription factor) and *Zfp36* (zinc-finger protein 36) with BMDs (BMD$_L$s) of 0.186 (0.103) and 0.368 (0.097) mg/kg, respectively.

In female rats, all 10 of the most sensitive liver genes were upregulated. These genes were *Gdf15* (growth differentiation factor 15), *Igfbp1* (insulin-like growth factor-binding protein 1), *Eci1* (enoyl-CoA delta isomerase 1), *Etfdh* (electron transfer flavoprotein dehydrogenase), *Cyp2b1* (cytochrome P450, family 2, subfamily b, polypeptide 1), *Loc108348266*/*Cyp2b1* (cytochrome P450 2B1), *Dhrs7* (dehydrogenase/reductase 7), *Dhrs7l1* (dehydrogenase/reductase [SDR family] member 7-like 1), *Slc27a2* (solute carrier family 27 member 2), and *Vnn1* (vanin 1) with BMDs (BMD$_L$s) of 17.724 (8.696), 18.792 (7.230), 32.546 (27.162), 34.846 (26.297), 35.483 (29.479), 35.483 (29.479), 35.986 (10.630), 35.986 (10.630), 36.103 (26.571), and 37.026 (30.688) mg/kg, respectively.

None of the top 10 most sensitive kidney genes in male rats had estimated BMD median values <0.050 mg/kg. The most sensitive upregulated genes with a calculated BMD were *Decr1* (2,4-dienoyl-CoA reductase 1), *Vnn1* (vanin 1)*, Hmgcs2* (3-hydroxy-3-methylglutaryl-CoA synthase 2), *Ehhadh* (enoyl-CoA hydratase and 3-hydroxyacyl CoA dehydrogenase), *Eci2* (enoyl-CoA delta isomerase 2), *Acaa2* (acetyl-CoA acyltransferase 2), *Acot1* (acyl-CoA thioesterase 1), *Cyp4a1* (cytochrome P450, family 4, subfamily a, polypeptide 1), and *Ech1* (enoyl-CoA hydratase 1) with BMDs (BMD$_L$s) of 0.680 (0.505), 0.705 (0.488), 0.804 (0.541), 0.953 (0.671), 0.989 (0.643), 1.346 (0.539), 1.363 (0.938), 1.593 (1.021), and 2.055 (1.124) mg/kg, respectively. One gene, *Acmsd* (aminocarboxymuconate semialdehyde decarboxylase), was downregulated with a BMD (BMD$_L$) of 0.775 (0.183) mg/kg.

The most sensitive kidney gene in female rats, exhibiting an increase in expression, was *Plod3* (procollagen-lysine, 2-oxoglutarate 5-dioxygenase 3) with an estimated BMD median value <0.050 mg/kg. The most sensitive upregulated genes with a calculated BMD were *Eci1* (enoyl-CoA delta isomerase 1), *Vnn1* (vanin 1), *Hmgcs2* (3-hydroxy-3-methylglutaryl-CoA synthase 2), *Ehhadh* (enoyl-CoA hydratase and 3-hydroxyacyl CoA dehydrogenase), *Eci2* (enoyl-CoA delta isomerase 2), *Acaa1a* (acetyl-CoA acyltransferase 1A), *Acaa1b* (acetyl-Coenzyme A acyltransferase 1B), *Ech1* (enoyl-CoA hydratase 1), and *Acaa2* (acetyl-CoA acyltransferase 2) with BMDs (BMD$_L$s) of 9.486 (7.353), 10.025 (7.993), 11.644 (9.266), 12.212 (9.437), 12.789

(9.488), 13.850 (11.009), 13.850 (11.009), 19.820 (14.141), and 22.339 (13.614) mg/kg, respectively. None of the top 10 most sensitive kidney genes in female rats were downregulated.

Table 11. Top 10 Liver Genes Ranked by Potency of Perturbation, Sorted by Benchmark Dose Median[a]

Gene Symbol	Entrez Gene IDs	Probe IDs[b]	BMD_{1Std} (BMD_{L1std}–BMD_{U1std}) in mg/kg	Maximum Fold Change	Direction of Expression Change
Male					
Myc	24577	MYC_9271	0.186 (0.103–0.478)	3.3	DOWN
Zfp36	79426	ZFP36_10204	0.368 (0.097–1.817)	2.1	DOWN
Acot2	192272	ACOT2_7969	1.012 (0.809–1.377)	19.9	UP
Eci1	29740	ECI1_8520	1.013 (0.769–1.465)	23.5	UP
Loc100911558/Spink1l	100911558	SPINK1_32461	1.270 (0.542–3.173)	2.0	UP
Spink1	266602	SPINK1_32461	1.270 (0.542–3.173)	2.0	UP
Ehhadh	171142	EHHADH_8534	1.280 (1.047–1.879)	95.2	UP
Crot	83842	CROT_8384	1.411 (1.092–1.919)	7.5	UP
Acaa1a	24157	ACAA1A_7954	1.874 (1.524–2.760)	39.0	UP
Acaa1b	501072	ACAA1A_7954	1.874 (1.524–2.760)	39.0	UP
Female					
Gdf15	29455	GDF15_33113	17.724 (8.696–37.098)	5.8	UP
Igfbp1	25685	IGFBP1_32306	18.792 (7.230–51.558)	4.3	UP
Eci1	29740	ECI1_8520	32.546 (27.162–40.287)	9.6	UP
Etfdh	295143	ETFDH_8575	34.846 (26.297–48.311)	2.0	UP
Cyp2b1	24300	CYP2B1_32451	35.483 (29.479–44.233)	196.8	UP
Loc108348266/Cyp2b1	108348266	CYP2B1_32451	35.483 (29.479–44.233)	196.8	UP
Dhrs7	299135	DHRS7_8469	35.986 (10.630–156.958)	4.4	UP
Dhrs7l1	299131	DHRS7_8469	35.986 (10.630–156.958)	4.4	UP
Slc27a2	65192	SLC27A2_9860	36.103 (26.571–51.373)	2.3	UP
Vnn1	29142	VNN1_10157	37.026 (30.688–46.324)	15.8	UP

BMD_{1Std} = benchmark dose corresponding to a benchmark response set to one standard deviation from the mean; BMD_{L1Std} = benchmark dose lower confidence limit corresponding to a benchmark response set to one standard deviation from the mean; BMD_{U1Std} = benchmark dose upper confidence limit corresponding to a benchmark response set to one standard deviation from the mean.
[a]Descriptions of orthologous human genes are shown due to the increased detail available in public resources such as UniprotKB[32] and Entrez Gene.[33] Gene definitions adapted from Human UniprotKB were used as the primary resource due to the greater breadth of annotation and depth of functional detail provided. Gene definitions adapted from Rat UniprotKB were used as the secondary resource if the primary source did not provide a detailed description of function. Human Entrez Gene was used as the third resource. Rat Entrez Gene was used as the fourth resource.
[b]In some cases, a probe may map to more than one gene, resulting in duplicate reporting of that probe mapped to different genes.
Gene definition version: https://doi.org/10.22427/NTP-DATA-002-00600-0002-000-0.
Myc: Human Uniprot function (Human *MYC*): Transcription factor that binds DNA in a nonspecific manner, yet also specifically recognizes the core sequence 5'-CAC[GA]TG-3'. Activates the transcription of growth-related genes. Binds to the VEGFA promoter, promoting VEGFA production and subsequent sprouting angiogenesis (PubMed24940000). Regulator of somatic reprogramming; controls self-renewal of embryonic stem cells. Functions with TAF6L to activate target gene expression through

RNA polymerase II pause release (by similarity).{ECO0000250|UniProtKBP01108, ECO0000269|PubMed24940000, ECO0000269|PubMed25956029}.

Zfp36: Human Uniprot function (Human *ZFP36*): Zinc-finger RNA-binding protein that destabilizes several cytoplasmic AU-rich element (ARE)-containing mRNA transcripts by promoting their poly(A) tail removal or deadenylation, and hence provide a mechanism for attenuating protein synthesis (PubMed9703499, PubMed10330172, PubMed10751406, PubMed11279239, PubMed12115244, PubMed12748283, PubMed15187101, PubMed15634918, PubMed17030620, PubMed16702957, PubMed20702587, PubMed20221403, PubMed21775632, PubMed27193233, PubMed23644599, PubMed25815583). Acts as an 3'-untranslated region (UTR) ARE mRNA-binding adapter protein to communicate signaling events to the mRNA decay machinery (PubMed15687258, PubMed23644599). Recruits deadenylase CNOT7 (and probably the CCR4-NOT complex) via association with CNOT1, and hence promotes ARE-mediated mRNA deadenylation (PubMed23644599). Functions also by recruiting components of the cytoplasmic RNA decay machinery to the bound ARE-containing mRNAs (PubMed11719186, PubMed12748283, PubMed15687258, PubMed16364915). Self regulates by destabilizing its own mRNA (PubMed15187101). Binds to 3'-UTR ARE of numerous mRNAs and of its own mRNA (PubMed10330172, PubMed10751406, PubMed12115244, PubMed15187101, PubMed15634918, PubMed17030620, PubMed16702957, PubMed19188452, PubMed20702587, PubMed20221403, PubMed21775632, PubMed25815583). Plays a role in anti-inflammatory responses; suppresses tumor necrosis factor (TNF)-alpha production by stimulating ARE-mediated TNF-alpha mRNA decay and several other inflammatory ARE-containing mRNAs in interferon (IFN)- and/or lipopolysaccharide (LPS)-induced macrophages (by similarity). Also plays a role in the regulation of dendritic cell maturation at the post-transcriptional level, and hence operates as part of a negative feedback loop to limit the inflammatory response (PubMed18367721). Promotes ARE-mediated mRNA decay of hypoxia-inducible factor HIF1A mRNA during the response of endothelial cells to hypoxia (PubMed21775632). Positively regulates early adipogenesis of preadipocytes by promoting ARE-mediated mRNA decay of immediate early genes (IEGs) (by similarity). Negatively regulates hematopoietic/erythroid cell differentiation by promoting ARE-mediated mRNA decay of the transcription factor STAT5B mRNA (PubMed20702587). Plays a role in maintaining skeletal muscle satellite cell quiescence by promoting ARE-mediated mRNA decay of the myogenic determination factor MYOD1 mRNA (by similarity). Associates also with and regulates the expression of non-ARE-containing target mRNAs at the post-transcriptional level, such as MHC class I mRNAs (PubMed18367721). Participates in association with argonaute RISC catalytic components in the ARE-mediated mRNA decay mechanism; assists microRNA (miRNA) targeting ARE-containing mRNAs (PubMed15766526). May also play a role in the regulation of cytoplasmic mRNA decapping; enhances decapping of ARE-containing RNAs, in vitro (PubMed16364915). Involved in the delivery of target ARE-mRNAs to processing bodies (PBs) (PubMed17369404). In addition to its cytosolic mRNA decay function, affects nuclear pre-mRNA processing (by similarity). Negatively regulates nuclear poly(A)-binding protein PABPN1-stimulated polyadenylation activity on ARE-containing pre-mRNA during LPS-stimulated macrophages (by similarity). Also involved in the regulation of stress granule (SG) and P-body formation and fusion (by similarity). Plays a role in the regulation of keratinocyte proliferation, differentiation, and apoptosis (PubMed27182009). Plays a role as a tumor suppressor by inhibiting cell proliferation in breast cancer cells (PubMed26926077).{ECO0000250|UniProtKBP22893, ECO0000269|PubMed10330172, ECO0000269|PubMed10751406, ECO0000269|PubMed11279239, ECO0000269|PubMed11719186, ECO0000269|PubMed12115244, ECO0000269|PubMed12748283, ECO0000269|PubMed15187101, ECO0000269|PubMed15634918, ECO0000269|PubMed15687258, ECO0000269|PubMed15766526, ECO0000269|PubMed16364915, ECO0000269|PubMed16702957, ECO0000269|PubMed17030620, ECO0000269|PubMed17369404, ECO0000269|PubMed18367721, ECO0000269|PubMed19188452, ECO0000269|PubMed20221403, ECO0000269|PubMed20702587, ECO0000269|PubMed21775632, ECO0000269|PubMed23644599, ECO0000269|PubMed25815583, ECO0000269|PubMed26926077, ECO0000269|PubMed27182009, ECO0000269|PubMed27193233, ECO0000269|PubMed9703499}. FUNCTION (Microbial infection) Negatively regulates HTLV-1 TAX-dependent transactivation of viral long terminal repeat (LTR) promoter.{ECO0000269|PubMed14679154}.

Acot2: Human Uniprot function (Human *ACOT2*): Acyl-CoA thioesterases are a group of enzymes that catalyze the hydrolysis of acyl-CoAs to the free fatty acid and coenzyme A (CoASH), providing the potential to regulate intracellular levels of acyl-CoAs, free fatty acids and CoASH (PubMed16940157). Acyl-coenzyme A thioesterase 2/ACOT2 displays higher activity toward long-chain acyl-CoAs (C14-C20) (PubMed16940157, PubMed10944470). The enzyme is involved in enhancing the hepatic fatty acid oxidation in mitochondria (by similarity).{ECO0000250|UniProtKBQ9QYR9, ECO0000269|PubMed10944470, ECO0000269|PubMed16940157, ECO0000303|PubMed16940157}.

Eci1: Human Uniprot function (Human *ECI1*): Able to isomerize both 3-*cis* and 3-*trans* double bonds into the 2-*trans* form in a range of enoyl-CoA species.{ECO0000269|PubMed7818490}.

LOC100911558/*Spink1l*: Human Uniprot function (Human *SPINK1*): Serine protease inhibitor that exhibits anti-trypsin activity (PubMed7142173). In the pancreas, protects against trypsin-catalyzed premature activation of zymogens (by similarity).{ECO0000250|UniProtKBP09036, ECO0000269|PubMed7142173}. FUNCTION: In the male reproductive tract, binds to sperm heads where it modulates sperm capacitance by inhibiting calcium uptake and nitrogen oxide (NO) production.{ECO0000250|UniProtKBP09036}.

Spink1: Human Uniprot function (Human *SPINK1*): Serine protease inhibitor which exhibits anti-trypsin activity (PubMed7142173). In the pancreas, protects against trypsin-catalyzed premature activation of zymogens (by similarity).{ECO:0000250|UniProtKB:P09036, ECO:0000269|PubMed7142173}. FUNCTION: In the male reproductive tract, binds to sperm heads where it modulates sperm capacitance by inhibiting calcium uptake and NO production.{ECO:0000250|UniProtKB:P09036}.

Ehhadh: Human Uniprot function (Human *EHHADH*): Peroxisomal trifunctional enzyme possessing 2-enoyl-CoA hydratase, 3-hydroxyacyl-CoA dehydrogenase, and delta 3, delta 2-enoyl-CoA isomerase activities. Catalyzes two of the four reactions of the long straight-chain fatty acids peroxisomal beta-oxidation pathway. Optimal isomerase for 2,5 double bonds into 3,5 form isomerization in a range of enoyl-CoA species (probable). Also able to isomerize both 3-*cis* and 3-*trans* double bonds into the 2-*trans* form in a range of enoyl-CoA species (by similarity). With HSD17B4, catalyzes the hydration of trans-2-enoyl-CoA and the dehydrogenation of 3-hydroxyacyl-CoA, but with opposite chiral specificity (PubMed15060085). Regulates the amount of medium-chain dicarboxylic fatty acids, which are essential regulators of all fatty acid oxidation pathways (by similarity). Also involved in the degradation of long-chain dicarboxylic acids through peroxisomal beta-oxidation (PubMed15060085). {ECO0000250|UniProtKBP07896, ECO0000250|UniProtKBQ9DBM2, ECO0000269|PubMed15060085, ECO0000305|PubMed15060085}.

Crot: Human Uniprot function (Human *CROT*): Beta-oxidation of fatty acids. The highest activity concerns the C6 to C10 chain length substrate. Converts the end product of pristanic acid beta-oxidation, 4,8-dimethylnonanoyl-CoA, to its corresponding carnitine ester.{ECO0000269|PubMed10486279}.

Acaa1a: Human Entrez Gene Summary (Human *ACAA1*): This gene encodes an enzyme operative in the beta-oxidation system of the peroxisomes. Deficiency of this enzyme leads to pseudo-Zellweger syndrome. Alternative splicing results in multiple transcript variants. (provided by RefSeq, Jul 2008)

Acaa1b: Human Entrez Gene Summary (Human *ACAA1*): This gene encodes an enzyme operative in the beta-oxidation system of the peroxisomes. Deficiency of this enzyme leads to pseudo-Zellweger syndrome. Alternative splicing results in multiple transcript variants. (provided by RefSeq, Jul 2008)

Gdf15: Human Uniprot function (Human *GDF15*): Regulates food intake, energy expenditure and body weight in response to metabolic and toxin-induced stresses (PubMed28953886, PubMed28846097, PubMed28846098, PubMed28846099, PubMed23468844, PubMed29046435). Binds to its receptor, GFRAL, and activates GFRAL-expressing neurons localized in the area postrema and nucleus tractus solitarius of the brainstem (PubMed28953886, PubMed28846097, PubMed28846098, PubMed28846099). It then triggers the activation of neurons localized within the parabrachial nucleus and central amygdala, which constitutes part of the "emergency circuit" that shapes feeding responses to stressful conditions (PubMed28953886). On hepatocytes, inhibits growth hormone signaling (by similarity).{ECO0000250|UniProtKBQ9Z0J7, ECO0000269|PubMed23468844, ECO0000269|PubMed28846097, ECO0000269|PubMed28846098, ECO0000269|PubMed28846099, ECO0000269|PubMed28953886, ECO0000269|PubMed29046435}.

Igfbp1: Human Uniprot function (Human *IGFBP1*): IGF-binding proteins prolong the half-life of the IGFs and have been shown to either inhibit or stimulate the growth-promoting effects of the IGFs on cell culture. They alter the interaction of IGFs with their cell surface receptors. Promotes cell migration.{ECO0000269|PubMed15972819}.

Etfdh: Human Uniprot function (Human *ETFDH*): Accepts electrons from ETF and reduces ubiquinone.

Cyp2b1: Human Uniprot function (Human *CYP2B6*): A cytochrome P450 monooxygenase involved in the metabolism of endocannabinoids and steroids (PubMed21289075, PubMed12865317). Mechanistically, uses molecular oxygen inserting one oxygen atom into a substrate, and reducing the second into a water molecule, with two electrons provided by NADPH via cytochrome P450 reductase (NADPH–hemoprotein reductase). Catalyzes the epoxidation of double bonds of arachidonoylethanolamide (anandamide) to 8,9-, 11,12-, and 14,15-epoxyeicosatrienoic acid ethanolamides (EpETrE-Eas), potentially modulating endocannabinoid system signaling (PubMed21289075). Hydroxylates steroid hormones, including testosterone at C-16 and estrogens at C-2 (PubMed21289075, PubMed12865317). Plays a role in the oxidative metabolism of xenobiotics, including plant lipids and drugs (PubMed11695850, PubMed22909231). Acts as a 1,4-cineole 2-exo-monooxygenase (PubMed11695850).{ECO0000269|PubMed11695850, ECO0000269|PubMed12865317, ECO0000269|PubMed21289075, ECO0000269|PubMed22909231}. FUNCTION Allele 2B6*9: Has low affinity for anandamide and can only produce 11,12 EpETrE-Eas.{ECO0000269|PubMed21289075}.

LOC108348266/Cyp2b1: Human Uniprot function (Human *CYP2B6*): A cytochrome P450 monooxygenase involved in the metabolism of endocannabinoids and steroids (PubMed21289075, PubMed12865317). Mechanistically, uses molecular oxygen inserting one oxygen atom into a substrate, and reducing the second into a water molecule, with two electrons provided by NADPH via cytochrome P450 reductase (NADPH–hemoprotein reductase). Catalyzes the epoxidation of double bonds of arachidonoylethanolamide (anandamide) to 8,9-, 11,12-, and 14,15-epoxyeicosatrienoic acid ethanolamides (EpETrE-Eas), potentially modulating endocannabinoid system signaling (PubMed21289075). Hydroxylates steroid hormones, including testosterone at C-16 and estrogens at C-2 (PubMed21289075, PubMed12865317). Plays a role in the oxidative metabolism of xenobiotics, including plant lipids and drugs (PubMed11695850, PubMed22909231). Acts as a 1,4-cineole 2-exo-monooxygenase (PubMed11695850) {ECO0000269|PubMed11695850, ECO0000269|PubMed12865317, ECO0000269|PubMed21289075, ECO0000269|PubMed22909231}. FUNCTION Allele 2B6*9: Has low affinity for anandamide and can only produce 11,12 EpETrE-Eas.{ECO0000269|PubMed21289075}.

Dhrs7: Human Entrez Gene Summary (Human *DHRS7*): This gene encodes a member of the short-chain dehydrogenases/reductases (SDR) family, which has over 46,000 members. Members in this family are enzymes that metabolize many different compounds, such as steroid hormones, prostaglandins, retinoids, lipids, and xenobiotics. (provided by RefSeq, Apr 2016)

Dhrs7l1: Human Entrez Gene Summary (Human *DHRS7*): This gene encodes a member of the SDR family, which has over 46,000 members. Members in this family are enzymes that metabolize many different compounds, such as steroid hormones, prostaglandins, retinoids, lipids, and xenobiotics. (provided by RefSeq, Apr 2016)

Slc27a2: Human Uniprot function (Human *SLC27A2*): Acyl-CoA synthetase that activates long-chain and very long-chain fatty acids (VLCFAs) by catalyzing the formation of fatty acyl-CoA (PubMed10198260, PubMed10749848, PubMed11980911). Can also activate branched-chain fatty acids such as phytanic acid and pristanic acid (PubMed10198260). Does not activate C24 bile acids, cholate, and chenodeoxycholate (PubMed11980911). In vitro, activates 3-alpha,7-alpha,12-alpha-trihydroxy-5-beta-cholestanate (THCA), the C27 precursor of cholic acid deriving from the de novo synthesis from cholesterol (PubMed11980911). Exhibits long-chain fatty acids (LCFAs) transport activity and plays an important role in hepatic fatty acid uptake (PubMed20530735).{ECO0000269|PubMed10198260, ECO0000269|PubMed10749848, ECO0000269|PubMed11980911, ECO0000269|PubMed20530735}. FUNCTION [Isoform 1]: Exhibits both LCFAs transport activity and acyl-CoA synthetase toward VLCFAs (PubMed21768100). Shows a preference for generating CoA derivatives of n-3 fatty acids, which are preferentially trafficked into phosphatidylinositol (PubMed21768100).{ECO0000269|PubMed21768100}. FUNCTION [Isoform 2]: Exhibits LCFAs transport activity but lacks acyl-CoA synthetase toward VLCFAs.{ECO0000269|PubMed21768100}.
Vnn1: Human Uniprot function (Human *VNN1*): Amidohydrolase that hydrolyzes one of the carboamide linkages specifically in D-pantetheine thus recycling pantothenic acid (vitamin B5) and releasing cysteamine.{ECO0000269|PubMed10567687, ECO0000269|PubMed11491533, ECO0000269|PubMed25478849}.

Table 12. Top 10 Kidney Genes Ranked by Potency of Perturbation, Sorted by Benchmark Dose Median[a]

Gene Symbol	Entrez Gene IDs	Probe IDs[b]	BMD$_{1Std}$ (BMD$_{L1std}$–BMD$_{U1std}$) in mg/kg	Maximum Fold Change	Direction of Expression Change
Male					
Decr1	117543	DECR1_8458	0.680 (0.505–1.264)	3.1	UP
Vnn1	29142	VNN1_10157	0.705 (0.488–1.353)	6.0	UP
Acmsd	171385	ACMSD_32377	0.775 (0.183–4.177)	2.3	DOWN
Hmgcs2	24450	HMGCS2_8812	0.804 (0.541–1.442)	11.8	UP
Ehhadh	171142	EHHADH_8534	0.953 (0.671–1.585)	8.7	UP
Eci2	291075	ECI2_8521	0.989 (0.643–1.915)	2.1	UP
Acaa2	170465	ACAA2_7955	1.346 (0.539–4.058)	2.8	UP
Acot1	50559	ACOT1_7968	1.363 (0.938–2.405)	2.2	UP
Cyp4a1	50549	CYP4A1_33111	1.593 (1.021–3.028)	4.5	UP
Ech1	64526	ECH1_8516	2.055 (1.124–4.620)	2.2	UP
Female					
Plod3	288583	PLOD3_9507	<0.050[c] (NR)	2.1	UP
Eci1	29740	ECI1_8520	9.486 (7.353–12.810)	4.4	UP
Vnn1	29142	VNN1_10157	10.025 (7.993–13.110)	7.8	UP
Hmgcs2	24450	HMGCS2_8812	11.644 (9.266–15.267)	37.7	UP
Ehhadh	171142	EHHADH_8534	12.212 (9.437–16.563)	6.7	UP
Eci2	291075	ECI2_8521	12.789 (9.488–18.156)	2.0	UP
Acaa1a	24157	ACAA1A_7954	13.850 (11.009–18.172)	5.2	UP
Acaa1b	501072	ACAA1A_7954	13.850 (11.009–18.172)	5.2	UP
Ech1	64526	ECH1_8516	19.820 (14.141–29.396)	2.1	UP
Acaa2	170465	ACAA2_7955	22.339 (13.614–38.665)	2.3	UP

BMD$_{1Std}$ = benchmark dose corresponding to a benchmark response set to one standard deviation from the mean; BMD$_{L1Std}$ = benchmark dose lower confidence limit corresponding to a benchmark response set to one standard deviation from the mean; BMD$_{U1Std}$ = benchmark dose upper confidence limit corresponding to a benchmark response set to one standard

deviation from the mean; NR = the BMD_{L1Std}–BMD_{U1Std} range is not reportable because the BMD_{1Std} median is below the lower limit of extrapolation (<1/3 of the lowest nonzero dose tested).

[a]Descriptions of orthologous human genes are shown due to the increased detail available in public resources such as UniprotKB[32] and Entrez Gene.[33] Gene definitions adapted from Human UniprotKB were used as the primary resource due to the greater breadth of annotation and depth of functional detail provided. Gene definitions adapted from Rat UniprotKB were used as the secondary resource if the primary source did not provide a detailed description of function. Human Entrez Gene was used as the third resource. Rat Entrez Gene was used as the fourth resource.

[b]In some cases, a probe may map to more than one gene, resulting in duplicate reporting of that probe mapped to different genes.

[c]<0.050 = a best-fit model was identified and a BMD_{1Std} was estimated that was <1/3 of the lowest nonzero dose tested.

Gene definition version: https://doi.org/10.22427/NTP-DATA-002-00600-0002-000-0.

Decr1: Human Uniprot function (Human *DECR1*): Auxiliary enzyme of beta-oxidation. It participates in the metabolism of unsaturated fatty enoyl-CoA esters having double bonds in both even- and odd-numbered positions in mitochondria. Catalyzes the NADP-dependent reduction of 2,4-dienoyl-CoA to yield trans-3-enoyl-CoA.{ECO0000269|PubMed15531764}.

Vnn1: Human Uniprot function (Human *VNN1*): Amidohydrolase that hydrolyzes one of the carboamide linkages specifically in D-pantetheine thus recycling pantothenic acid (vitamin B5) and releasing cysteamine.{ECO0000269|PubMed10567687, ECO0000269|PubMed11491533, ECO0000269|PubMed25478849}.

Acmsd: Human Uniprot function (Human *ACMSD*): Converts alpha-amino-beta-carboxymuconate-epsilon-semialdehyde (ACMS) to alpha-aminomuconate semialdehyde (AMS). ACMS can be converted nonenzymatically to quinolate, a key precursor of NAD, and a potent endogenous excitotoxin of neuronal cells, which is implicated in the pathogenesis of various neurodegenerative disorders. In the presence of ACMSD, ACMS is converted to AMS, a benign catabolite. ACMSD ultimately controls the metabolic fate of tryptophan catabolism along the kynurenine pathway.{ECO0000269|PubMed19843166}.

Hmgcs2: Human Uniprot function (Human *HMGCS2*): Catalyzes the first irreversible step in ketogenesis, condensing acetyl-CoA to acetoacetyl-CoA to form HMG-CoA, which is converted by HMG-CoA reductase (HMGCR) into mevalonate.{ECO0000269|PubMed11228257, ECO0000269|PubMed23751782, ECO0000269|PubMed29597274}.

Ehhadh: Human Uniprot function (Human *EHHADH*): Peroxisomal trifunctional enzyme possessing 2-enoyl-CoA hydratase, 3-hydroxyacyl-CoA dehydrogenase, and delta 3, delta 2-enoyl-CoA isomerase activities. Catalyzes two of the four reactions of the long straight-chain fatty acids peroxisomal beta-oxidation pathway. Optimal isomerase for 2,5 double bonds into 3,5 form isomerization in a range of enoyl-CoA species (probable). Also able to isomerize both 3-*cis* and 3-*trans* double bonds into the 2-*trans* form in a range of enoyl-CoA species (by similarity). With HSD17B4, catalyzes the hydration of trans-2-enoyl-CoA and the dehydrogenation of 3-hydroxyacyl-CoA, but with opposite chiral specificity (PubMed15060085). Regulates the amount of medium-chain dicarboxylic fatty acids, which are essential regulators of all fatty acid oxidation pathways (by similarity). Also involved in the degradation of long-chain dicarboxylic acids through peroxisomal beta-oxidation (PubMed15060085). {ECO0000250|UniProtKBP07896, ECO0000250|UniProtKBQ9DBM2, ECO0000269|PubMed15060085, ECO0000305|PubMed15060085}.

Eci2: Human Uniprot function (Human *ECI2*): Able to isomerize both 3-*cis* and 3-*trans* double bonds into the 2-*trans* form in a range of enoyl-CoA species. Has a preference for 3-*trans* substrates.{ECO0000269|PubMed10419495}.

Acaa2: Human Uniprot function (Human *ACAA2*): In the production of energy from fats, this is one of the enzymes that catalyzes the last step of the mitochondrial beta-oxidation pathway, an aerobic process breaking down fatty acids into acetyl-CoA (probable). Using free coenzyme A/CoA, catalyzes the thiolytic cleavage of medium- to long-chain unbranched 3-oxoacyl-CoAs into acetyl-CoA and a fatty acyl-CoA shortened by two carbon atoms (probable). Also catalyzes the condensation of two acetyl-CoA molecules into acetoacetyl-CoA and could be involved in the production of ketone bodies (probable). Also displays hydrolase activity on various fatty acyl-CoAs (PubMed25478839); therefore, could be responsible for the production of acetate in a side reaction to beta-oxidation (probable). Abolishes BNIP3-mediated apoptosis and mitochondrial damage (PubMed18371312).{ECO0000269|PubMed18371312, ECO0000269|PubMed25478839, ECO0000305|PubMed25478839}.

Acot1: Human Uniprot function (Human *ACOT1*): Acyl-CoA thioesterases are a group of enzymes that catalyze the hydrolysis of acyl-CoAs into free fatty acids and coenzyme A (CoASH), regulating intracellular levels of acyl-CoAs, free fatty acids, and CoASH. More active toward saturated and unsaturated long-chain fatty acyl-CoAs (C12-C20) {ECO0000269|PubMed16940157}.

Cyp4a1: Human Uniprot function (Human *CYP4A22*): Catalyzes the omega- and (omega-1)-hydroxylation of various fatty acids such as laurate and palmitate. Shows no activity toward arachidonic acid and prostaglandin A1. Lacks functional activity in the kidney and does not contribute to renal 20-hydroxyeicosatetraenoic acid (20-HETE) biosynthesis {ECO0000269|PubMed10860550, ECO0000269|PubMed15611369}.

Ech1: Human Uniprot function (Human *ECH1*): Isomerization of 3-*trans*,5-*cis*-dienoyl-CoA to 2-*trans*,4-*trans*-dienoyl-CoA.{ECO0000250|UniProtKBQ62651}.

Plod3: Human Uniprot function (Human *PLOD3*): Multifunctional enzyme that catalyzes a series of essential post-translational modifications on Lys residues in procollagen (PubMed11956192, PubMed12475640, PubMed18298658, PubMed30089812, PubMed18834968). Plays a redundant role in catalyzing the formation of hydroxylysine residues in -Xaa-Lys-Gly- sequences in collagens (PubMed9582318, PubMed9724729, PubMed11956192, PubMed12475640, PubMed18298658, PubMed30089812, PubMed18834968). Plays a redundant role in catalyzing the transfer of galactose onto hydroxylysine groups, giving rise to galactosyl 5-hydroxylysine (PubMed12475640, PubMed18298658, PubMed30089812, PubMed18834968). Has an essential role by catalyzing the subsequent transfer of glucose moieties, giving rise to 1,2-glucosylgalactosyl-5-hydroxylysine residues (PubMed10934207, PubMed11896059, PubMed11956192, PubMed12475640, PubMed18298658, PubMed30089812,

PubMed18834968). Catalyzes hydroxylation and glycosylation of Lys residues in the MBL1 collagen-like domain, giving rise to hydroxylysine and 1,2-glucosylgalactosyl-5-hydroxylysine residues (PubMed25419660). Essential for normal biosynthesis and secretion of type IV collagens (PubMed18834968) (probable). Essential for normal formation of basement membranes (by similarity).{ECO0000250|UniProtKBQ9R0E1, ECO0000269|PubMed10934207, ECO0000269|PubMed11896059, ECO0000269|PubMed11956192, ECO0000269|PubMed12475640, ECO0000269|PubMed18298658, ECO0000269|PubMed18834968, ECO0000269|PubMed25419660, ECO0000269|PubMed30089812, ECO0000269|PubMed9582318, ECO0000269|PubMed9724729}.

Eci1: Human Uniprot function (Human *ECI1*): Able to isomerize both 3-*cis* and 3-*trans* double bonds into the 2-*trans* form in a range of enoyl-CoA species.{ECO0000269|PubMed7818490}.

Acaa1a: Human Entrez Gene Summary (Human *ACAA1*): This gene encodes an enzyme operative in the beta-oxidation system of the peroxisomes. Deficiency of this enzyme leads to pseudo-Zellweger syndrome. Alternative splicing results in multiple transcript variants. (provided by RefSeq, Jul 2008)

Acaa1b: Human Entrez Gene Summary (Human *ACAA1*): This gene encodes an enzyme operative in the beta-oxidation system of the peroxisomes. Deficiency of this enzyme leads to pseudo-Zellweger syndrome. Alternative splicing results in multiple transcript variants. (provided by RefSeq, Jul 2008)

Summary

6:1 Fluorotelomer alcohol (6:1 FTOH) is a member of the per- and polyfluoroalkyl class of compounds to which humans are widely exposed. A review of the literature did not identify toxicological data for estimating the potential adverse health effects of 6:1 FTOH. This study used a transcriptomic approach and standard toxicological endpoints to estimate the in vivo biological potency of 6:1 FTOH.

A subset of standard toxicological endpoints (albumin/globulin ratio, globulin concentration, total triiodothyronine concentration, relative right kidney weight, and reticulocyte count in male rats; cholesterol concentration in female rats) exhibited benchmark dose (BMD) values much lower than would be expected given the endpoint-specific no-observed-effect level and lowest-observed-effect level values. Expert review of the data suggests that the BMD estimates do not accurately reflect the true potency of the effect of these endpoints and were likely an anomalous product of the BMD modeling approach.

Taking this into account, the most sensitive apical endpoint in male rats was a decrease in total thyroxine concentration with an estimated BMD and benchmark dose lower confidence limit (BMD$_L$) of 3.19 (1.774) mg/kg. Increases in relative liver weight and albumin concentration were the next most sensitive apical endpoint changes observed in male rats with BMDs (BMD$_{LS}$) of 12.122 (9.527) and 13.365 (4.084) mg/kg, respectively. In female rats, the most sensitive apical endpoint was a decrease in reticulocyte count with a BMD (BMD$_L$) of 15.578 (3.622) mg/kg. The next most sensitive apical endpoints observed were an increase in large unstained cell count and a decrease in total triiodothyronine concentration with BMDs (BMD$_{LS}$) of 54.339 (15.759) and 161.48 (122.215) mg/kg, respectively.

Gene set-level transcriptional changes in the liver following 6:1 FTOH exposure were estimated to occur at a BMD (BMD$_L$) as low as 0.368 (0.103) mg/kg in male rats, corresponding to cellular response to epidermal growth factor stimulus (GO:0071364), and as low as 44.730 (22.260) mg/kg in female rats, corresponding to positive regulation of phagocytosis (GO:0050766). The most sensitive liver gene for which a reliable BMD could be determined was *Myc*, with a BMD (BMD$_L$) of 0.186 (0.103) mg/kg, in male rats and *Gdf15*, with a BMD (BMD$_L$) of 17.724 (8.696) mg/kg, in female rats.

Gene set-level transcriptional changes in the kidney were estimated to occur at a BMD (BMD$_L$) as low as 1.346 (0.541) mg/kg in male rats, corresponding to acetyl-CoA metabolic process (GO:0006084), and as low as 21.079 (13.312) mg/kg in female rats, corresponding to fatty acid beta-oxidation (GO:0006635). Two kidney gene sets in male rats had BMD estimates below the lower limit of extrapolation (<0.050 mg/kg). The most sensitive kidney gene in male rats for which a reliable BMD could be determined was *Decr1* with a BMD (BMD$_L$) of 0.680 (0.505) mg/kg. In female rats, one kidney gene exhibited changes in expression at dose levels below which a reliable estimate of potency could be achieved (<0.050 mg/kg). The most sensitive gene in female rats for which a reliable BMD could be determined was *Eci1* with a BMD (BMD$_L$) of 9.486 (7.353) mg/kg.

Under the conditions of this short-duration transcriptomic study in Sprague Dawley (Hsd:Sprague Dawley® SD®) rats, the most sensitive point of departure with a reliable estimate in male rats was a transcriptional change in a gene, *Myc*, with a BMD (BMD$_L$) of 0.186

(0.103) mg/kg. Gene set transcriptional changes provided potency estimates slightly higher than *Myc*, while apical endpoints provided potency estimates higher than *Myc*. In female rats, the most sensitive point of departure with a reliable estimate was a transcriptional change in a gene, *Eci1*, with a BMD (BMD$_L$) of 9.486 (7.353) mg/kg. Gene set transcriptional changes and apical endpoints provided potency estimates slightly higher than *Eci1*. Follow-up studies that investigate transcriptional changes at lower doses will be a useful future direction to determine the biological potency of 6:1 FTOH more accurately.

References

1. U.S. Environmental Protection Agency (USEPA). CompTox Chemicals Dashboard: 6:1 Fluorotelomer alcohol 375-82-6 | DTXSID00190950. 2021. https://comptox.epa.gov/dashboard/chemical/details/DTXSID00190950

2. National Center for Biotechnology Information (NCBI). PubChem Compound Summary for CID 550386, 1H,1H-Perfluoro-1-heptanol. 2021. https://pubchem.ncbi.nlm.nih.gov/compound/1H_1H-Perfluoro-1-heptanol

3. European Chemicals Agency (ECHA). Substance Infocard: 2,2,3,3,4,4,5,5,6,6,7,7,7-Tridecafluoroheptan-1-ol. 2021. https://echa.europa.eu/substance-information/-/substanceinfo/100.006.179

4. Fenton SE, Ducatman A, Boobis A, DeWitt JC, Lau C, Ng C, Smith JS, Roberts SM. Per- and polyfluoroalkyl substance toxicity and human health review: Current state of knowledge and strategies for informing future research. Environ Toxicol Chem. 2021; 40(3):606-630. https://doi.org/10.1002/etc.4890

5. Domingo JL, Nadal M. Human exposure to per- and polyfluoroalkyl substances (PFAS) through drinking water: A review of the recent scientific literature. Environ Res. 2019; 177:108648. https://doi.org/10.1016/j.envres.2019.108648

6. Domingo JL, Nadal M. Per- and polyfluoroalkyl substances (PFASs) in food and human dietary intake: A review of the recent scientific literature. J Agric Food Chem. 2017; 65(3):533-543. https://doi.org/10.1021/acs.jafc.6b04683

7. U.S. Environmental Protection Agency (USEPA). CompTox Chemicals Dashboard: 6:1 Fluorotelomer alcohol 375-82-6 | DTXSID00190950: Exposure predictions. 2021. https://comptox.epa.gov/dashboard/chemical/exposure-predictions/DTXSID00190950

8. U.S. Environmental Protection Agency (USEPA). CompTox Chemicals Dashboard: 6:1 Fluorotelomer alcohol 375-82-6 | DTXSID00190950: Executive summary. 2021. https://comptox.epa.gov/dashboard/chemical/executive-summary/DTXSID00190950

9. Gwinn WM, Auerbach SS, Parham F, Stout MD, Waidyanatha S, Mutlu E, Collins B, Paules RS, Merrick BA, Ferguson S et al. Evaluation of 5-day in vivo rat liver and kidney with high-throughput transcriptomics for estimating benchmark doses of apical outcomes. Toxicol Sci. 2020; 176(2):343-354. https://doi.org/10.1093/toxsci/kfaa081

10. Mansouri K, Karmaus AL, Fitzpatrick J, Patlewicz G, Pradeep P, Alberga D, Alepee N, Allen TEH, Allen D, Alves VM et al. CATMoS: Collaborative Acute Toxicity Modeling Suite. Environ Health Perspect. 2021; 129(4):47013. https://doi.org/10.1289/EHP8495

11. Mansouri K, Grulke CM, Judson RS, Williams AJ. OPERA models for predicting physicochemical properties and environmental fate endpoints. J Cheminform. 2018; 10(1):10. https://doi.org/10.1186/s13321-018-0263-1

12. Patlewitz G. Personal Communication: EPA Point of Departure Estimate. 2021.

13. Waidyanatha S, Fletcher BL, Fernando RA, Cora MC, Silinski MAR. Development and validation of an ultraperformance liquid chromatography-tandem mass spectrometry method for quantitation of total 3,3',5-triiodo-L-thyronine and 3,3',5,5'-tetraiodo-L-thyronine in rodent serum. Anal Lett. 2021; 55(5):796-811. https://doi.org/10.1080/00032719.2021.1967969

14. Langmead B, Trapnell C, Pop M, Salzberg SL. Ultrafast and memory-efficient alignment of short DNA sequences to the human genome. Genome Biol. 2009; 10(3):R25. https://doi.org/10.1186/gb-2009-10-3-r25

15. Williams DA. A test for differences between treatment means when several dose levels are compared with a zero dose control. Biometrics. 1971; 27(1):103-117. http://dx.doi.org/10.2307/2528930

16. Williams DA. The comparison of several dose levels with a zero dose control. Biometrics. 1972; 28(2):519-531. http://dx.doi.org/10.2307/2556164

17. Dunnett CW. A multiple comparison procedure for comparing several treatments with a control. J Am Stat Assoc. 1955; 50(272):1096-1121. http://dx.doi.org/10.1080/01621459.1955.10501294

18. Shirley E. A non-parametric equivalent of Williams' test for contrasting increasing dose levels of a treatment. Biometrics. 1977; 33(2):386-389. http://dx.doi.org/10.2307/2529789

19. Dunn OJ. Multiple comparisons using rank sums. Technometrics. 1964; 6(3):241-252. http://dx.doi.org/10.1080/00401706.1964.10490181

20. Jonckheere AR. A distribution-free k-sample test against ordered alternatives. Biometrika. 1954; 41(1/2):133-145. http://dx.doi.org/10.2307/2333011

21. Dixon WJ, Massey FJ. Introduction to Statistical Analysis. New York,: McGraw-Hill; 1951.

22. U.S. Environmental Protection Agency (USEPA). Benchmark dose technical guidance. Washington, DC: U.S. Environmental Protection Agency, Risk Assessment Forum; 2012. https://www.epa.gov/sites/production/files/2015-01/documents/benchmark_dose_guidance.pdf

23. Wignall JA, Shapiro AJ, Wright FA, Woodruff TJ, Chiu WA, Guyton KZ, Rusyn I. Standardizing benchmark dose calculations to improve science-based decisions in human health assessments. Environ Health Perspect. 2014; 122(5):499-505. http://dx.doi.org/10.1289/ehp.1307539

24. National Toxicology Program (NTP). NTP research report on National Toxicology Program approach to genomic dose-response modeling. Research Triangle Park, NC: U.S. Department of Health and Human Services, National Institute of Environmental Health Sciences, National Toxicology Program; 2018. NTP Research Report No. 5.

25. Shi L, Jones WD, Jensen RV, Harris SC, Perkins RG, Goodsaid FM, Guo L, Croner LJ, Boysen C, Fang H et al. The balance of reproducibility, sensitivity, and specificity of lists of differentially expressed genes in microarray studies. BMC Bioinformatics. 2008; 9:S10. https://doi.org/10.1186/1471-2105-9-s9-s10

26. Auerbach SS, Ballin JD, Blake JC, Browning DB, Collins BJ, Cora MC, Fernando RA, Fostel JM, Liu YF, Luh J et al. NIEHS report on the in vivo repeat dose biological potency study of perfluorohexanesulfonamide (CASRN 41997-13-1) in Sprague Dawley (Hsd:Sprague Dawley® SD®) rats (gavage studies). Research Triangle Park, NC: U.S. Department of Health and Human Services, Public Health Service, National Institute of Environmental Health Sciences; 2023. NIEHS Report 10. https://doi.org/10.22427/NIEHS-10

27. Auerbach SS, Ballin JD, Blake JC, Browning DB, Collins BJ, Cora MC, Fernando RA, Fostel JM, Liu YF, Luh J et al. NIEHS report on the in vivo repeat dose biological potency study of 1,1,2,2-tetrahydroperfluoro-1-dodecanol (CASRN 865-86-1) in Sprague Dawley (Hsd:Sprague Dawley® SD®) rats (gavage studies). Research Triangle Park, NC: U.S. Department of Health and Human Services, Public Health Service, National Institute of Environmental Health Sciences; 2023. NIEHS Report 08. https://doi.org/10.22427/NIEHS-08

28. Auerbach SS, Aillon KL, Ballin JD, Collins BJ, Cora MC, Duncan NS, Fostel JM, Kerns SP, Liu YF, Luh J et al. NIEHS report on the in vivo repeat dose biological potency study of 2,3-benzofluorene (CASRN 243-17-4) in Sprague Dawley (Hsd:Sprague Dawley® SD®) rats (gavage studies). Research Triangle Park, NC: U.S. Department of Health and Human Services, Public Health Service, National Institute of Environmental Health Sciences; 2023. NIEHS Report 09. https://doi.org/10.22427/NIEHS-09

29. National Toxicology Program (NTP). NIEHS 07: Chemical Effects in Biological Systems (CEBS) data repository. Research Triangle Park, NC: U.S. Department of Health and Human Services, National Institute of Environmental Health Sciences, National Toxicology Program; 2023. https://doi.org/10.22427/NIEHS-DATA-NIEHS-07

30. Geneontology. The gene ontology resource. 2021. http://geneontology.org/

31. Medical College of Wisconsin. Rat Genome Database. 2021. https://rgd.mcw.edu/

32. UniProt. UniProtKB results. 2021. https://www.uniprot.org/uniprot/

33. Entrez Gene. Gene. 2021. https://www.ncbi.nlm.nih.gov/gene/

34. Thomas RS, Allen BC, Nong A, Yang L, Bermudez E, Clewell HJ, III, Andersen ME. A method to integrate benchmark dose estimates with genomic data to assess the functional effects of chemical exposure. Toxicol Sci. 2007; 98(1):240-248.
http://dx.doi.org/10.1093/toxsci/kfm092

Appendix A. Internal Dose Assessment

Table of Contents

A.1. Quantitation of 6:1 Fluorotelomer Alcohol in Plasma

Quantification of 6:1 fluorotelomer alcohol (6:1 FTOH) in plasma samples was completed by MRIGlobal (Kansas City, MO). A high-performance liquid chromatography-tandem mass spectrometry (LC-MS/MS) method was developed to determine 6:1 FTOH concentrations in rat plasma. A six-point matrix calibration curve, in the range of 10–160 ng/mL, was prepared by adding 10 µL of an appropriate spiking solution of 6:1 FTOH in methanol to 50 µL of control matrix (adult male Sprague Dawley rat plasma). Quality control (QC) samples were prepared similarly at a target concentration of 50 ng/mL in plasma. Blanks and study samples were prepared like standards, except 10 µL of methanol was used in place of spiking solution. To each sample, 100 µL of prechilled solution containing 250 ng 2-perfluorohexyl-[1,1-2H2]-[1,2-13C2]-ethanol/mL (internal standard) in methanol was added, mixed for 1 minute, and allowed to stand at 4°C for 10 minutes. All samples were centrifuged at approximately $18,000 \times g$ for 10 minutes and supernatants were collected for analysis.

All samples were analyzed using a Sciex Exion AC LC coupled to an API 4000 MS/MS (Framingham, MA). An Agilent Zorbax Eclipse Plus C18 column (2.1 × 150 mm, 5 µm) was used with mobile phases A (water) and B (methanol). A flow rate of 0.3 mL/min was run with a linear gradient of 80%–100% B in 4 minutes and held for 4 minutes. The electrospray ion source was operated in negative ion mode with a source temperature of 400°C and an ion spray voltage of −4,500 V. Transition ranges monitored were m/z 349 to 169 (quantitation ion) and 349 to 309 (confirmation ion) for 6:1 FTOH, and m/z 367 to 306 for the internal standard.

A linear regression with 1/X weighting was used to relate peak area ratio of analyte to internal standard and analyte concentration. Calibration curves were linear (r > 0.99). The limit of detection (LOD; 2.9 ng/mL) was estimated as three times the standard deviation of the lower limit of quantitation (LOQ; 10.0 ng/mL), expressed as concentration. For QC samples, the accuracy measured as percent relative error was within ±27.8% of the nominal concentration with relative standard deviations ≤4.7%. The concentrations (ng/mL) of 6:1 FTOH in study samples were calculated using peak area ratios and the regression equation. All values above LOD were reported.

Appendix B. Animal Identifiers

Tables

In Vivo Repeat Dose Biological Potency Study of
6:1 Fluorotelomer Alcohol in Sprague Dawley Rats

Table B-1. Animal Numbers and FASTQ Data File Names

Animal Number	Sex	Group	Dose (mg/kg)	Survived to Study Termination	Tissue	FASTQ File ID
321	Male	Vehicle control	0	Yes	Kidney	Plate6-321
321	Male	Vehicle control	0	Yes	Liver	Plate2-321
322	Male	Vehicle control	0	Yes	Kidney	Plate6-322
322	Male	Vehicle control	0	Yes	Liver	Plate2-322
323	Male	Vehicle control	0	Yes	Kidney	Plate6-323
323	Male	Vehicle control	0	Yes	Liver	Plate2-323
324	Male	Vehicle control	0	Yes	Kidney	Plate6-324
324	Male	Vehicle control	0	Yes	Liver	Plate2-324
325	Male	Vehicle control	0	Yes	Kidney	Plate6-325
325	Male	Vehicle control	0	Yes	Liver	Plate2-325
326	Male	Vehicle control	0	Yes	Kidney	Plate6-326
326	Male	Vehicle control	0	Yes	Liver	Plate2-326
327	Male	Vehicle control	0	Yes	Kidney	Plate6-327
327	Male	Vehicle control	0	Yes	Liver	Plate4-327
328	Male	Vehicle control	0	Yes	Kidney	Plate6-328
328	Male	Vehicle control	0	Yes	Liver	Plate2-328
329	Male	Vehicle control	0	Yes	Kidney	Plate6-329
329	Male	Vehicle control	0	Yes	Liver	Plate2-329
330	Male	Vehicle control	0	Yes	Kidney	Plate6-330
330	Male	Vehicle control	0	Yes	Liver	Plate2-330
331	Female	Vehicle control	0	Yes	Kidney	Plate6-331
331	Female	Vehicle control	0	Yes	Liver	Plate2-331
332	Female	Vehicle control	0	Yes	Kidney	Plate6-332
332	Female	Vehicle control	0	Yes	Liver	Plate2-332
333	Female	Vehicle control	0	Yes	Kidney	Plate6-333
333	Female	Vehicle control	0	Yes	Liver	Plate2-333
334	Female	Vehicle control	0	Yes	Kidney	Plate8-334[a]
334	Female	Vehicle control	0	Yes	Liver	Plate4-334
335	Female	Vehicle control	0	Yes	Kidney	Plate8-335[a]
335	Female	Vehicle control	0	Yes	Liver	Plate4-335
336	Female	Vehicle control	0	Yes	Kidney	Plate6-336
336	Female	Vehicle control	0	Yes	Liver	Plate2-336
337	Female	Vehicle control	0	Yes	Kidney	Plate6-337
337	Female	Vehicle control	0	Yes	Liver	Plate2-337
338	Female	Vehicle control	0	Yes	Kidney	Plate6-338
338	Female	Vehicle control	0	Yes	Liver	Plate2-338
339	Female	Vehicle control	0	Yes	Kidney	Plate6-339

In Vivo Repeat Dose Biological Potency Study of 6:1 Fluorotelomer Alcohol in Sprague Dawley Rats

Animal Number	Sex	Group	Dose (mg/kg)	Survived to Study Termination	Tissue	FASTQ File ID
339	Female	Vehicle control	0	Yes	Liver	Plate4-339
340	Female	Vehicle control	0	Yes	Kidney	Plate6-340
340	Female	Vehicle control	0	Yes	Liver	Plate2-340
341	Male	6:1 Fluorotelomer alcohol	0.15	Yes	Kidney	Plate6-341
341	Male	6:1 Fluorotelomer alcohol	0.15	Yes	Liver	Plate2-341
342	Male	6:1 Fluorotelomer alcohol	0.15	Yes	Kidney	Plate6-342
342	Male	6:1 Fluorotelomer alcohol	0.15	Yes	Liver	Plate2-342
343	Male	6:1 Fluorotelomer alcohol	0.15	Yes	Kidney	Plate6-343
343	Male	6:1 Fluorotelomer alcohol	0.15	Yes	Liver	Plate2-343
344	Male	6:1 Fluorotelomer alcohol	0.15	Yes	Kidney	Plate6-344
344	Male	6:1 Fluorotelomer alcohol	0.15	Yes	Liver	Plate2-344
345	Male	6:1 Fluorotelomer alcohol	0.15	Yes	Kidney	Plate6-345
345	Male	6:1 Fluorotelomer alcohol	0.15	Yes	Liver	Plate2-345
346	Female	6:1 Fluorotelomer alcohol	0.15	Yes	Kidney	Plate6-346
346	Female	6:1 Fluorotelomer alcohol	0.15	Yes	Liver	Plate2-346
347	Female	6:1 Fluorotelomer alcohol	0.15	Yes	Kidney	Plate6-347
347	Female	6:1 Fluorotelomer alcohol	0.15	Yes	Liver	Plate2-347
348	Female	6:1 Fluorotelomer alcohol	0.15	Yes	Kidney	Plate8-348[a]
348	Female	6:1 Fluorotelomer alcohol	0.15	Yes	Liver	Plate2-348
349	Female	6:1 Fluorotelomer alcohol	0.15	Yes	Kidney	Plate6-349
349	Female	6:1 Fluorotelomer alcohol	0.15	Yes	Liver	Plate2-349
350	Female	6:1 Fluorotelomer alcohol	0.15	Yes	Kidney	Plate6-350
350	Female	6:1 Fluorotelomer alcohol	0.15	Yes	Liver	Plate4-350
351	Male	6:1 Fluorotelomer alcohol	0.5	Yes	Kidney	Plate6-351
351	Male	6:1 Fluorotelomer alcohol	0.5	Yes	Liver	Plate2-351
352	Male	6:1 Fluorotelomer alcohol	0.5	Yes	Kidney	Plate6-352
352	Male	6:1 Fluorotelomer alcohol	0.5	Yes	Liver	Plate2-352
353	Male	6:1 Fluorotelomer alcohol	0.5	Yes	Kidney	Plate6-353
353	Male	6:1 Fluorotelomer alcohol	0.5	Yes	Liver	Plate2-353
354	Male	6:1 Fluorotelomer alcohol	0.5	Yes	Kidney	Plate6-354
354	Male	6:1 Fluorotelomer alcohol	0.5	Yes	Liver	Plate2-354
355	Male	6:1 Fluorotelomer alcohol	0.5	Yes	Kidney	Plate6-355
355	Male	6:1 Fluorotelomer alcohol	0.5	Yes	Liver	Plate2-355
356	Female	6:1 Fluorotelomer alcohol	0.5	Yes	Kidney	Plate8-356[a]
356	Female	6:1 Fluorotelomer alcohol	0.5	Yes	Liver	Plate2-356
357	Female	6:1 Fluorotelomer alcohol	0.5	Yes	Kidney	Plate8-357[a]
357	Female	6:1 Fluorotelomer alcohol	0.5	Yes	Liver	Plate2-357
358	Female	6:1 Fluorotelomer alcohol	0.5	Yes	Kidney	Plate6-358

In Vivo Repeat Dose Biological Potency Study of
6:1 Fluorotelomer Alcohol in Sprague Dawley Rats

Animal Number	Sex	Group	Dose (mg/kg)	Survived to Study Termination	Tissue	FASTQ File ID
358	Female	6:1 Fluorotelomer alcohol	0.5	Yes	Liver	Plate2-358
359	Female	6:1 Fluorotelomer alcohol	0.5	Yes	Kidney	Plate8-359[a]
359	Female	6:1 Fluorotelomer alcohol	0.5	Yes	Liver	Plate4-359
360	Female	6:1 Fluorotelomer alcohol	0.5	Yes	Kidney	Plate6-360
360	Female	6:1 Fluorotelomer alcohol	0.5	Yes	Liver	Plate2-360
361	Male	6:1 Fluorotelomer alcohol	1.4	Yes	Kidney	Plate6-361
361	Male	6:1 Fluorotelomer alcohol	1.4	Yes	Liver	Plate2-361
362	Male	6:1 Fluorotelomer alcohol	1.4	Yes	Kidney	Plate6-362
362	Male	6:1 Fluorotelomer alcohol	1.4	Yes	Liver	Plate2-362
363	Male	6:1 Fluorotelomer alcohol	1.4	Yes	Kidney	Plate8-363[a]
363	Male	6:1 Fluorotelomer alcohol	1.4	Yes	Liver	Plate2-363
364	Male	6:1 Fluorotelomer alcohol	1.4	Yes	Kidney	Plate6-364
364	Male	6:1 Fluorotelomer alcohol	1.4	Yes	Liver	Plate2-364
365	Male	6:1 Fluorotelomer alcohol	1.4	Yes	Kidney	Plate6-365
365	Male	6:1 Fluorotelomer alcohol	1.4	Yes	Liver	Plate2-365
366	Female	6:1 Fluorotelomer alcohol	1.4	Yes	Kidney	Plate6-366
366	Female	6:1 Fluorotelomer alcohol	1.4	Yes	Liver	Plate2-366
367	Female	6:1 Fluorotelomer alcohol	1.4	Yes	Kidney	Plate6-367
367	Female	6:1 Fluorotelomer alcohol	1.4	Yes	Liver	Plate2-367
368	Female	6:1 Fluorotelomer alcohol	1.4	Yes	Kidney	Plate6-368
368	Female	6:1 Fluorotelomer alcohol	1.4	Yes	Liver	Plate2-368
369	Female	6:1 Fluorotelomer alcohol	1.4	Yes	Kidney	Plate6-369
369	Female	6:1 Fluorotelomer alcohol	1.4	Yes	Liver	Plate2-369
370	Female	6:1 Fluorotelomer alcohol	1.4	Yes	Kidney	Plate6-370
370	Female	6:1 Fluorotelomer alcohol	1.4	Yes	Liver	Plate4-370
371	Male	6:1 Fluorotelomer alcohol	4.0	Yes	Kidney	Plate8-371[a]
371	Male	6:1 Fluorotelomer alcohol	4.0	Yes	Liver	Plate2-371
372	Male	6:1 Fluorotelomer alcohol	4.0	Yes	Kidney	Plate6-372
372	Male	6:1 Fluorotelomer alcohol	4.0	Yes	Liver	Plate2-372
373	Male	6:1 Fluorotelomer alcohol	4.0	Yes	Kidney	Plate6-373
373	Male	6:1 Fluorotelomer alcohol	4.0	Yes	Liver	Plate2-373
374	Male	6:1 Fluorotelomer alcohol	4.0	Yes	Kidney	Plate6-374
374	Male	6:1 Fluorotelomer alcohol	4.0	Yes	Liver	Plate2-374
375	Male	6:1 Fluorotelomer alcohol	4.0	Yes	Kidney	Plate8-375[a]
375	Male	6:1 Fluorotelomer alcohol	4.0	Yes	Liver	Plate2-375
376	Female	6:1 Fluorotelomer alcohol	4.0	Yes	Kidney	Plate6-376
376	Female	6:1 Fluorotelomer alcohol	4.0	Yes	Liver	Plate2-376
377	Female	6:1 Fluorotelomer alcohol	4.0	Yes	Kidney	Plate6-377

In Vivo Repeat Dose Biological Potency Study of
6:1 Fluorotelomer Alcohol in Sprague Dawley Rats

Animal Number	Sex	Group	Dose (mg/kg)	Survived to Study Termination	Tissue	FASTQ File ID
377	Female	6:1 Fluorotelomer alcohol	4.0	Yes	Liver	Plate4-377
378	Female	6:1 Fluorotelomer alcohol	4.0	Yes	Kidney	Plate6-378
378	Female	6:1 Fluorotelomer alcohol	4.0	Yes	Liver	Plate2-378[b]
379	Female	6:1 Fluorotelomer alcohol	4.0	Yes	Kidney	Plate6-379
379	Female	6:1 Fluorotelomer alcohol	4.0	Yes	Liver	Plate2-379
380	Female	6:1 Fluorotelomer alcohol	4.0	Yes	Kidney	Plate6-380
380	Female	6:1 Fluorotelomer alcohol	4.0	Yes	Liver	Plate2-380
381	Male	6:1 Fluorotelomer alcohol	12.0	Yes	Kidney	Plate6-381
381	Male	6:1 Fluorotelomer alcohol	12.0	Yes	Liver	Plate2-381[a]
382	Male	6:1 Fluorotelomer alcohol	12.0	Yes	Kidney	Plate6-382
382	Male	6:1 Fluorotelomer alcohol	12.0	Yes	Liver	Plate2-382[c]
383	Male	6:1 Fluorotelomer alcohol	12.0	Yes	Kidney	Plate6-383
383	Male	6:1 Fluorotelomer alcohol	12.0	Yes	Liver	Plate4-383
384	Male	6:1 Fluorotelomer alcohol	12.0	Yes	Kidney	Plate6-384
384	Male	6:1 Fluorotelomer alcohol	12.0	Yes	Liver	Plate2-384
385	Male	6:1 Fluorotelomer alcohol	12.0	Yes	Kidney	Plate6-385
385	Male	6:1 Fluorotelomer alcohol	12.0	Yes	Liver	Plate2-385
386	Female	6:1 Fluorotelomer alcohol	12.0	Yes	Kidney	Plate6-386
386	Female	6:1 Fluorotelomer alcohol	12.0	Yes	Liver	Plate2-386
387	Female	6:1 Fluorotelomer alcohol	12.0	Yes	Kidney	Plate6-387
387	Female	6:1 Fluorotelomer alcohol	12.0	Yes	Liver	Plate2-387
388	Female	6:1 Fluorotelomer alcohol	12.0	Yes	Kidney	Plate6-388
388	Female	6:1 Fluorotelomer alcohol	12.0	Yes	Liver	Plate2-388
389	Female	6:1 Fluorotelomer alcohol	12.0	Yes	Kidney	Plate6-389
389	Female	6:1 Fluorotelomer alcohol	12.0	Yes	Liver	Plate2-389
390	Female	6:1 Fluorotelomer alcohol	12.0	Yes	Kidney	Plate6-390
390	Female	6:1 Fluorotelomer alcohol	12.0	Yes	Liver	Plate4-390
391	Male	6:1 Fluorotelomer alcohol	37.0	Yes	Kidney	Plate6-391
391	Male	6:1 Fluorotelomer alcohol	37.0	Yes	Liver	Plate2-391
392	Male	6:1 Fluorotelomer alcohol	37.0	Yes	Kidney	Plate6-392
392	Male	6:1 Fluorotelomer alcohol	37.0	Yes	Liver	Plate2-392
393	Male	6:1 Fluorotelomer alcohol	37.0	Yes	Kidney	Plate6-393
393	Male	6:1 Fluorotelomer alcohol	37.0	Yes	Liver	Plate2-393
394	Male	6:1 Fluorotelomer alcohol	37.0	Yes	Kidney	Plate6-394
394	Male	6:1 Fluorotelomer alcohol	37.0	Yes	Liver	Plate2-394
395	Male	6:1 Fluorotelomer alcohol	37.0	Yes	Kidney	Plate8-395[a]
395	Male	6:1 Fluorotelomer alcohol	37.0	Yes	Liver	Plate4-395
396	Female	6:1 Fluorotelomer alcohol	37.0	Yes	Kidney	Plate8-396[c]

In Vivo Repeat Dose Biological Potency Study of
6:1 Fluorotelomer Alcohol in Sprague Dawley Rats

Animal Number	Sex	Group	Dose (mg/kg)	Survived to Study Termination	Tissue	FASTQ File ID
396	Female	6:1 Fluorotelomer alcohol	37.0	Yes	Liver	Plate2-396
397	Female	6:1 Fluorotelomer alcohol	37.0	Yes	Kidney	Plate6-397
397	Female	6:1 Fluorotelomer alcohol	37.0	Yes	Liver	Plate2-397
398	Female	6:1 Fluorotelomer alcohol	37.0	Yes	Kidney	Plate6-398
398	Female	6:1 Fluorotelomer alcohol	37.0	Yes	Liver	Plate2-398[a]
399	Female	6:1 Fluorotelomer alcohol	37.0	Yes	Kidney	Plate6-399
399	Female	6:1 Fluorotelomer alcohol	37.0	Yes	Liver	Plate4-399
400	Female	6:1 Fluorotelomer alcohol	37.0	Yes	Kidney	Plate6-400[b]
400	Female	6:1 Fluorotelomer alcohol	37.0	Yes	Liver	Plate2-400
401	Male	6:1 Fluorotelomer alcohol	111.0	Yes	Kidney	Plate6-401
401	Male	6:1 Fluorotelomer alcohol	111.0	Yes	Liver	Plate4-401
402	Male	6:1 Fluorotelomer alcohol	111.0	Yes	Kidney	Plate6-402
402	Male	6:1 Fluorotelomer alcohol	111.0	Yes	Liver	Plate2-402
403	Male	6:1 Fluorotelomer alcohol	111.0	Yes	Kidney	Plate6-403
403	Male	6:1 Fluorotelomer alcohol	111.0	Yes	Liver	Plate2-403
404	Male	6:1 Fluorotelomer alcohol	111.0	Yes	Kidney	Plate6-404
404	Male	6:1 Fluorotelomer alcohol	111.0	Yes	Liver	Plate2-404
405	Male	6:1 Fluorotelomer alcohol	111.0	Yes	Kidney	Plate6-405
405	Male	6:1 Fluorotelomer alcohol	111.0	Yes	Liver	Plate2-405
406	Female	6:1 Fluorotelomer alcohol	111.0	Yes	Kidney	Plate6-406
406	Female	6:1 Fluorotelomer alcohol	111.0	Yes	Liver	Plate2-406
407	Female	6:1 Fluorotelomer alcohol	111.0	Yes	Kidney	Plate6-407
407	Female	6:1 Fluorotelomer alcohol	111.0	Yes	Liver	Plate2-407
408	Female	6:1 Fluorotelomer alcohol	111.0	Yes	Kidney	Plate6-408
408	Female	6:1 Fluorotelomer alcohol	111.0	Yes	Liver	Plate2-408
409	Female	6:1 Fluorotelomer alcohol	111.0	Yes	Kidney	Plate8-409[a]
409	Female	6:1 Fluorotelomer alcohol	111.0	Yes	Liver	Plate2-409
410	Female	6:1 Fluorotelomer alcohol	111.0	Yes	Kidney	Plate6-410
410	Female	6:1 Fluorotelomer alcohol	111.0	Yes	Liver	Plate2-410
411	Male	6:1 Fluorotelomer alcohol	333.0	Yes	Kidney	Plate6-411
411	Male	6:1 Fluorotelomer alcohol	333.0	Yes	Liver	Plate2-411
412	Male	6:1 Fluorotelomer alcohol	333.0	Yes	Kidney	Plate8-412[a]
412	Male	6:1 Fluorotelomer alcohol	333.0	Yes	Liver	Plate2-412
413	Male	6:1 Fluorotelomer alcohol	333.0	Yes	Kidney	Plate6-413
413	Male	6:1 Fluorotelomer alcohol	333.0	Yes	Liver	Plate2-413[b]
414	Male	6:1 Fluorotelomer alcohol	333.0	Yes	Kidney	Plate6-414
414	Male	6:1 Fluorotelomer alcohol	333.0	Yes	Liver	Plate4-414
415	Male	6:1 Fluorotelomer alcohol	333.0	Yes	Kidney	Plate6-415

In Vivo Repeat Dose Biological Potency Study of
6:1 Fluorotelomer Alcohol in Sprague Dawley Rats

Animal Number	Sex	Group	Dose (mg/kg)	Survived to Study Termination	Tissue	FASTQ File ID
415	Male	6:1 Fluorotelomer alcohol	333.0	Yes	Liver	Plate4-415
416	Female	6:1 Fluorotelomer alcohol	333.0	Yes	Kidney	Plate6-416
416	Female	6:1 Fluorotelomer alcohol	333.0	Yes	Liver	Plate2-416
417	Female	6:1 Fluorotelomer alcohol	333.0	Yes	Kidney	Plate6-417
417	Female	6:1 Fluorotelomer alcohol	333.0	Yes	Liver	Plate2-417
418	Female	6:1 Fluorotelomer alcohol	333.0	Yes	Kidney	Plate8-418[a]
418	Female	6:1 Fluorotelomer alcohol	333.0	Yes	Liver	Plate2-418
419	Female	6:1 Fluorotelomer alcohol	333.0	Yes	Kidney	Plate8-419[a]
419	Female	6:1 Fluorotelomer alcohol	333.0	Yes	Liver	Plate2-419
420	Female	6:1 Fluorotelomer alcohol	333.0	Yes	Kidney	Plate6-420
420	Female	6:1 Fluorotelomer alcohol	333.0	Yes	Liver	Plate2-420
421	Male	6:1 Fluorotelomer alcohol	1,000.0	Yes	Kidney	Plate8-421[a]
421	Male	6:1 Fluorotelomer alcohol	1,000.0	Yes	Liver	Plate2-421[b]
422	Male	6:1 Fluorotelomer alcohol	1,000.0	No	None	NA
423	Male	6:1 Fluorotelomer alcohol	1,000.0	No	None	NA
424	Male	6:1 Fluorotelomer alcohol	1,000.0	No	None	NA
425	Male	6:1 Fluorotelomer alcohol	1,000.0	No	None	NA
426	Female	6:1 Fluorotelomer alcohol	1,000.0	Yes	Kidney	Plate6-426
426	Female	6:1 Fluorotelomer alcohol	1,000.0	Yes	Liver	Plate2-426
427	Female	6:1 Fluorotelomer alcohol	1,000.0	Yes	Kidney	Plate6-427
427	Female	6:1 Fluorotelomer alcohol	1,000.0	Yes	Liver	Plate2-427
428	Female	6:1 Fluorotelomer alcohol	1,000.0	Yes	Kidney	Plate6-428
428	Female	6:1 Fluorotelomer alcohol	1,000.0	Yes	Liver	Plate2-428
429	Female	6:1 Fluorotelomer alcohol	1,000.0	Yes	Kidney	Plate6-429
429	Female	6:1 Fluorotelomer alcohol	1,000.0	Yes	Liver	Plate4-429
430	Female	6:1 Fluorotelomer alcohol	1,000.0	Yes	Kidney	Plate6-430
430	Female	6:1 Fluorotelomer alcohol	1,000.0	Yes	Liver	Plate2-430

NA = no transcriptomics data collected for selected animal.
[a]Removed due to plate/batch effect.
[b]Removed due to principal component analysis/hierarchical cluster analysis outlier.
[c]Removed due to quality control fail.

Appendix C. Transcriptomic Quality Control and Empirical False Discovery Rate

Table of Contents

Tables

Figures

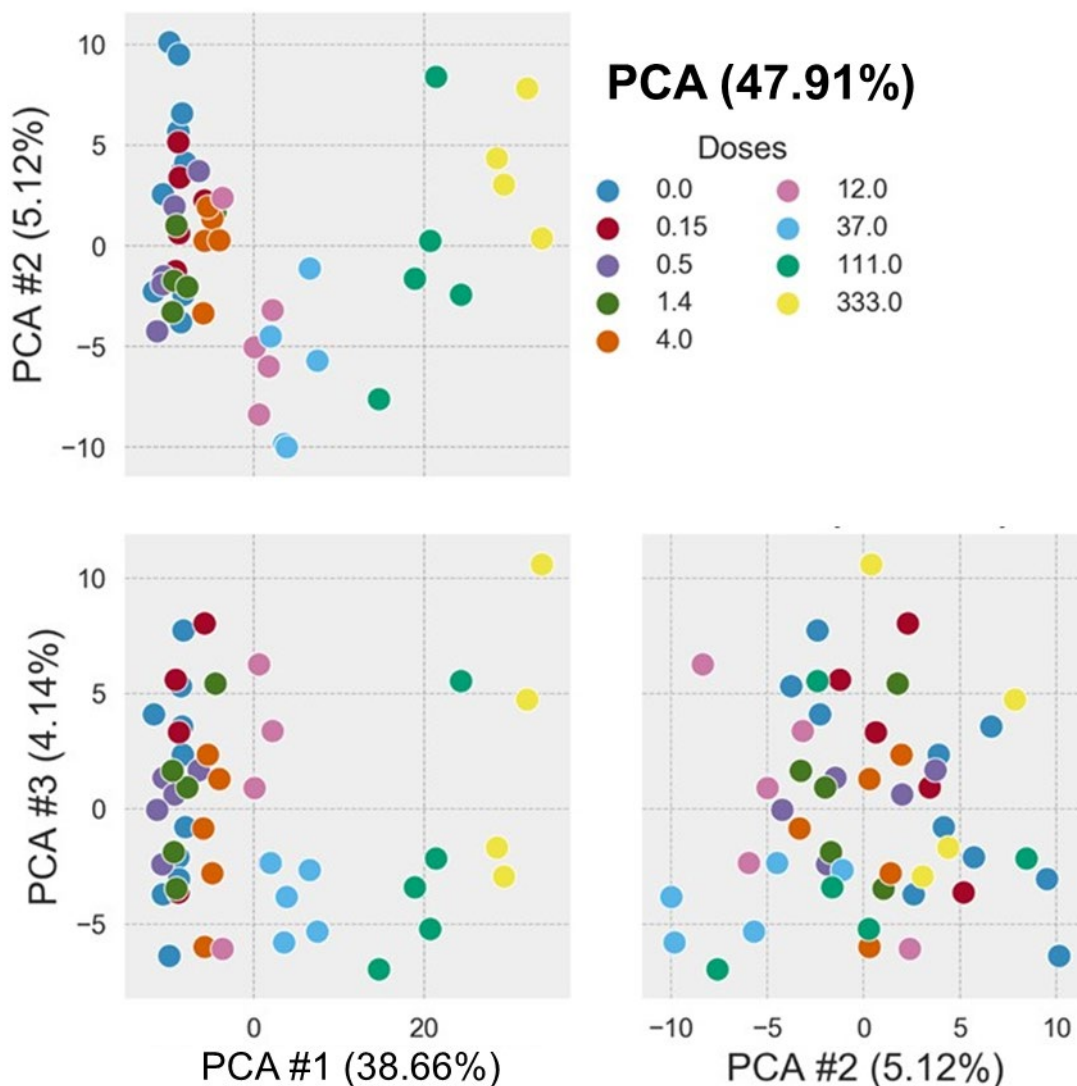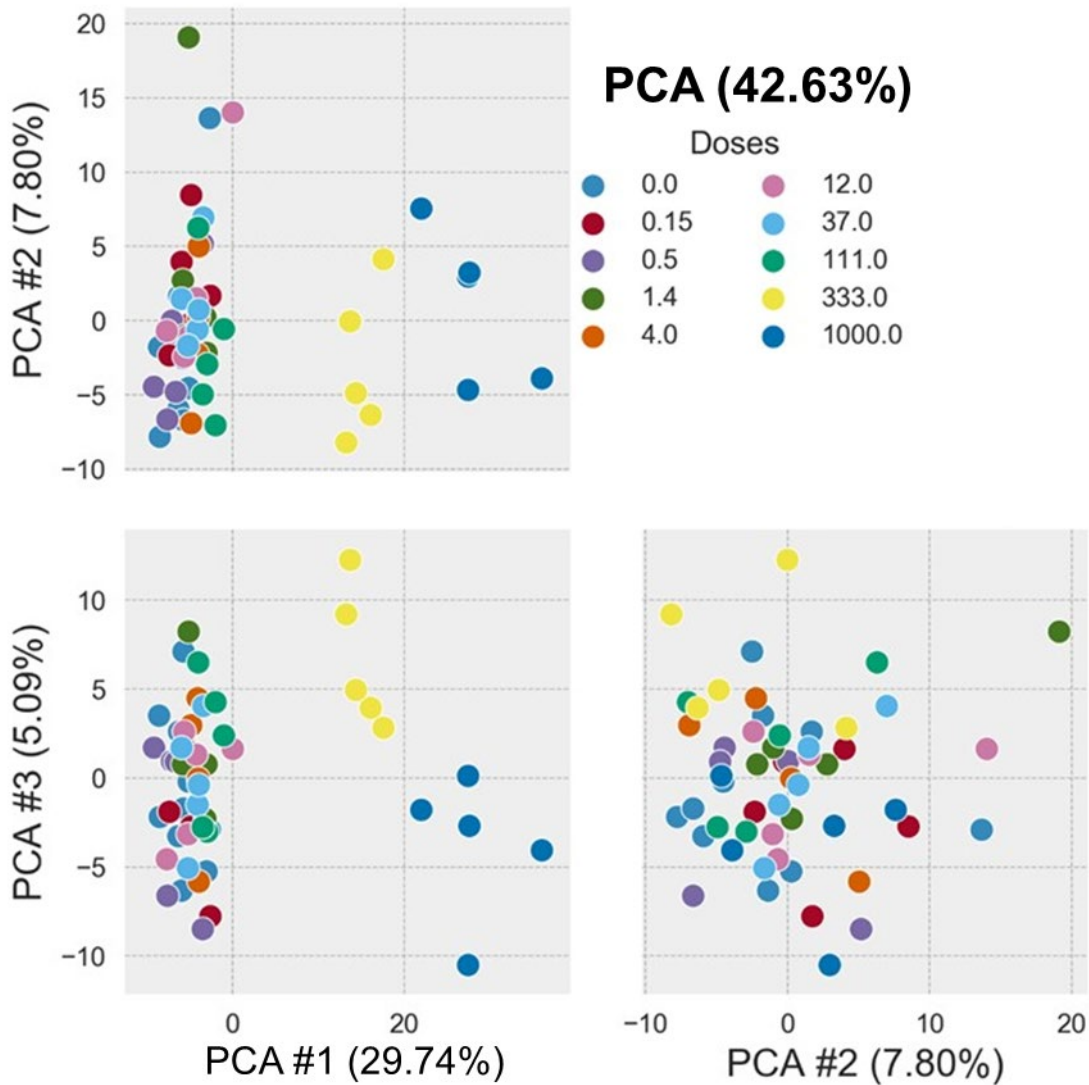## C.1. Gene Expression Quality Control

Figure C-1. A Principal Component Analysis of the Normalized Data from the Liver of Male Rats

A principal component analysis (PCA) plot enables visualization of global transcriptional changes in two dimensions, with each plot showing a different angle on the basis of the principal components plotted. Global transcript data are shown for individual animals (dots) within each dose group (designated by color). Dots that are spatially closer to each other indicate more similarity in global expression profiles; dots that are farther apart indicate dissimilarity in global expression profiles for those animals. The data represented in the plot are those employed in dose response modeling (i.e., if outliers were identified in the quality control process, they were removed from the data set and are not present in the plot). Visual inspection does not suggest subgrouping of the data other than dose-related changes, which indicates any technical batch-related effects are minimal.
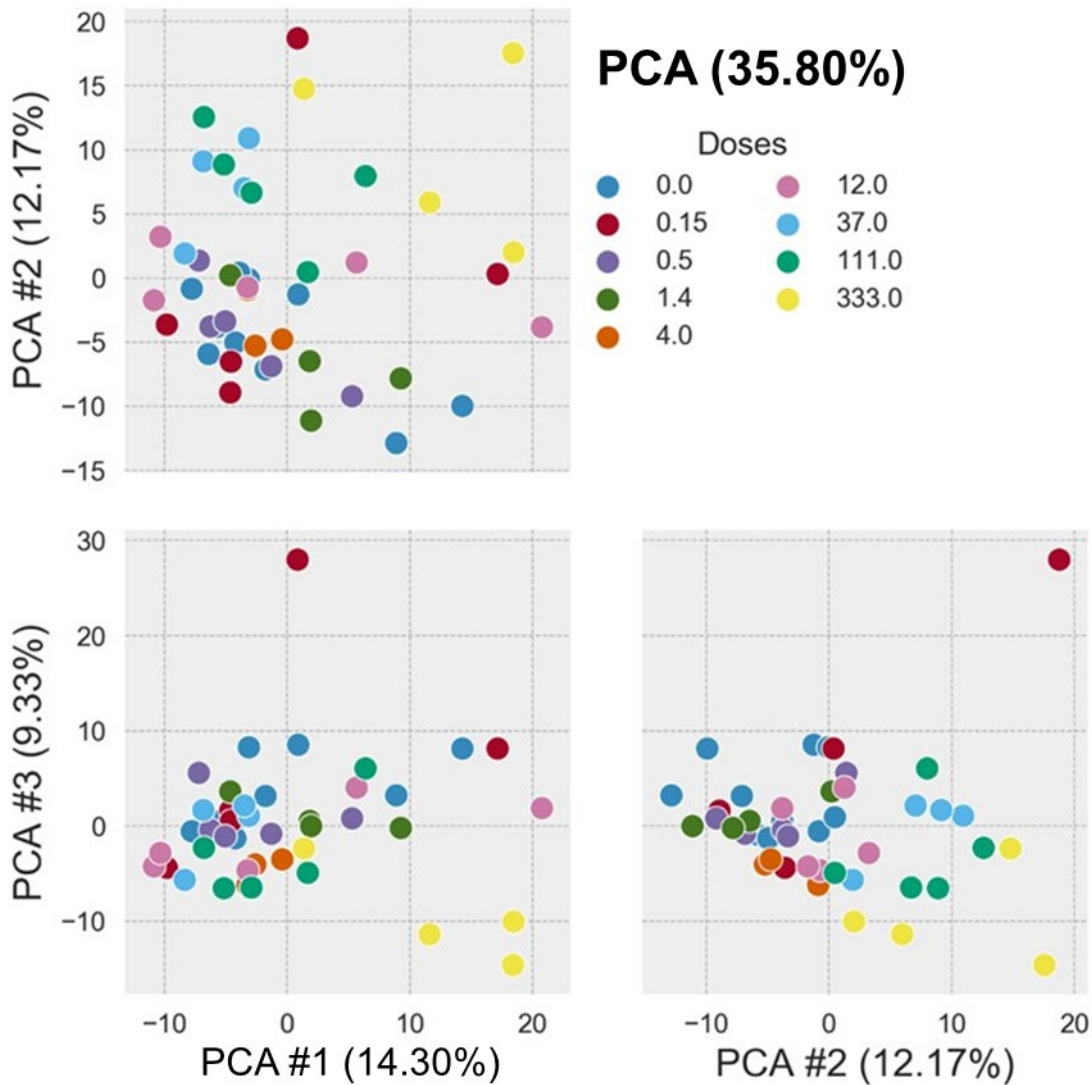
Figure C-2. A Principal Component Analysis of the Normalized Data from the Liver of Female Rats

A principal component analysis (PCA) plot enables visualization of global transcriptional changes in two dimensions, with each plot showing a different angle on the basis of the principal components plotted. Global transcript data are shown for individual animals (dots) within each dose group (designated by color). Dots that are spatially closer to each other indicate more similarity in global expression profiles; dots that are farther apart indicate dissimilarity in global expression profiles for those animals. The data represented in the plot are those employed in dose response modeling (i.e., if outliers were identified in the quality control process, they were removed from the data set and are not present in the plot). Visual inspection does not suggest subgrouping of the data other than dose-related changes, which indicates any technical batch-related effects are minimal.
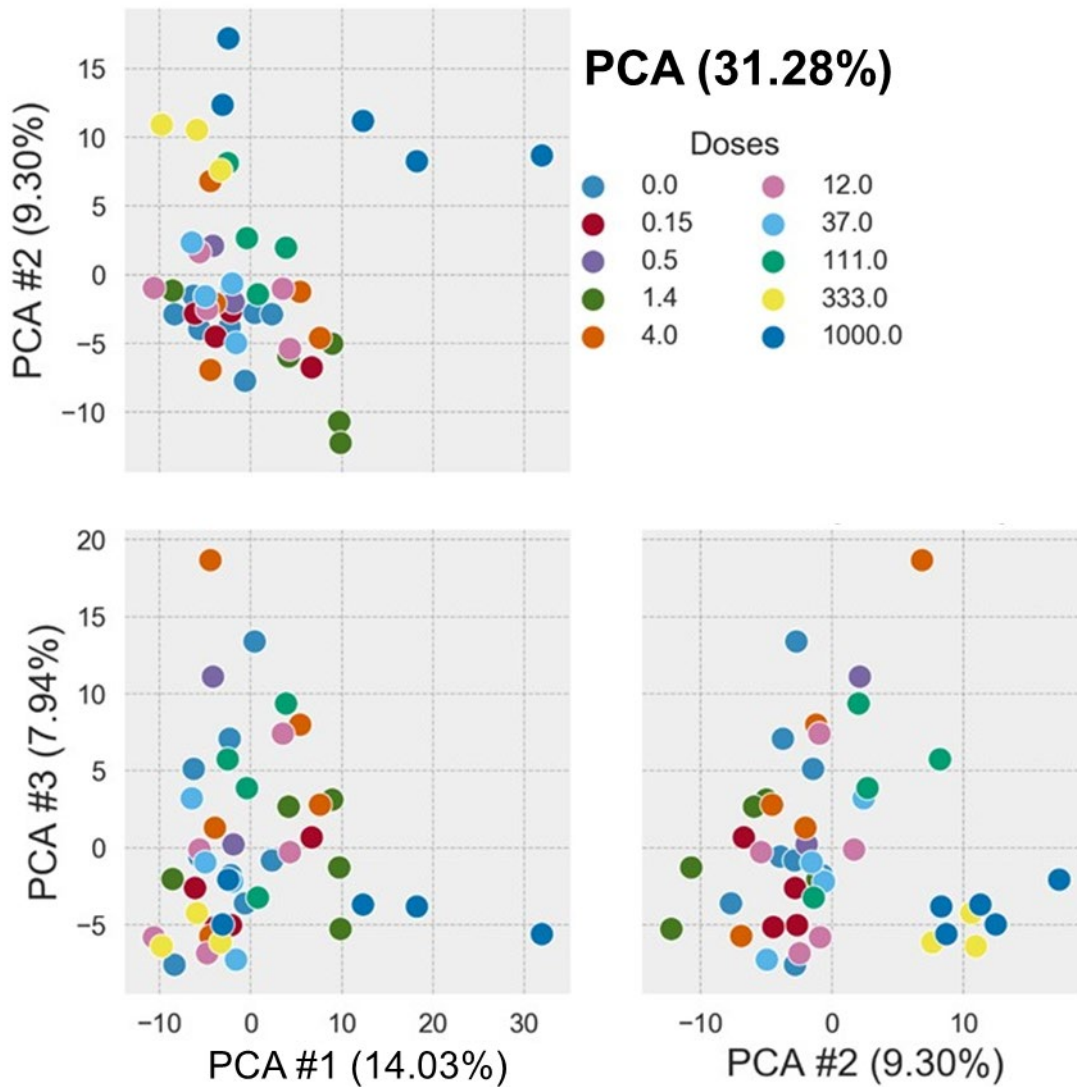
Figure C-3. A Principal Component Analysis of the Normalized Data from the Kidney of Male Rats

A principal component analysis (PCA) plot enables visualization of global transcriptional changes in two dimensions, with each plot showing a different angle on the basis of the principal components plotted. Global transcript data are shown for individual animals (dots) within each dose group (designated by color). Dots that are spatially closer to each other indicate more similarity in global expression profiles; dots that are farther apart indicate dissimilarity in global expression profiles for those animals. The data represented in the plot are those employed in dose response modeling (i.e., if outliers were identified in the quality control process, they were removed from the data set and are not present in the plot). Visual inspection does not suggest subgrouping of the data other than dose-related changes, which indicates any technical batch-related effects are minimal.

Figure C-4. A Principal Component Analysis of the Normalized Data from the Kidney of Female Rats

A principal component analysis (PCA) plot enables visualization of global transcriptional changes in two dimensions, with each plot showing a different angle on the basis of the principal components plotted. Global transcript data are shown for individual animals (dots) within each dose group (designated by color). Dots that are spatially closer to each other indicate more similarity in global expression profiles; dots that are farther apart indicate dissimilarity in global expression profiles for those animals. The data represented in the plot are those employed in dose response modeling (i.e., if outliers were identified in the quality control process, they were removed from the data set and are not present in the plot). Visual inspection does not suggest subgrouping of the data other than dose-related changes, which indicates any technical batch-related effects are minimal.

C.2. Empirical False Discovery Rate

C.2.1. Methods

Empirical false discovery assessment was performed to evaluate the performance of the benchmark dose (BMD) analysis technique and underlining probe/pathway filtering criteria. Toward this goal, 20 computationally generated data sets were used with this study design (each data set containing 10 vehicle control replicates and 5 replicates per dose), and equivalent BMD analysis was performed using the same parameter configurations. The 20 data sets were generated from the original 6:1 fluorotelomer alcohol (6:1 FTOH) study data, along with data from three other chemicals that were studied in parallel under a similar protocol.[26-28]

For a given group (tissue per sex combination), up to 40 vehicle control samples from the original studies (10 replicates × 4 chemicals) were used for this analysis. The previously identified outlier vehicle control samples and overflow plate control samples exhibiting a batch effect were excluded from this analysis.

Each computationally generated sample was created by randomly mixing the normalized expression signal from two randomly selected vehicle control samples using a weighted average approach. The weights utilized during per-probe mixing were randomly simulated from uniform (0,1) distribution. A total of 55 samples (10 vehicle control samples + 45 dosed samples [9 doses × 5 replicates]) were computationally generated per data set and assigned to either vehicle control or 1 of the 9 dosed groups that were separated by approximately half-log spacing, consistent with the dose spacing used in the original studies. For each group, 20 such data sets were generated. Because each of the 20 generated data sets used in the empirical false discovery analysis was derived from actual vehicle control samples, none of the data sets should have any true dose-responsive genes.

Each data set was then analyzed using the same parameter settings and significance criteria that were implemented in the original study. At the gene level, genes that passed the following criteria were considered false positive discoveries: fold change ≥|2|, Williams's trend p value ≤0.05, global goodness-of-fit p value >0.1, BMD upper confidence limit/BMD lower confidence limit (BMD_U/BMD_L) ≤40, and BMD <highest dose tested. Categorical analysis on Gene Ontology (GO) gene sets was performed using the genes that passed the gene-level criteria with maximum absolute fold change ≥1.5. At the gene set GO level, GO biological processes that passed the following criteria were considered false positive discoveries: ≥3 genes that pass all filters, totaling at least 5% of the genes in a gene set.

False positive discovery rates were assessed for each computationally generated data set using the following equations:

$$\text{False Positive Gene Rate} = \frac{\text{\# False Positive Entrez Gene IDs}}{2,680} \times 100 \qquad (1)$$

$$\text{False Positive GO Biological Process Rate} = \frac{\text{\# False Positive GO Biological Processes}}{5,667} \times 100 \qquad (2)$$

where 2,680 is the number of unique Entrez Gene IDs on the rat S1500+ platform and 5,667 is the number of GO biological processes that have at least three genes in rat S1500+.

Mean and median false discovery rates across all 20 computationally generated data sets were calculated for each tissue per sex in the study.

C.2.2. Results

The number of false positives for genes and GO biological processes are given in Table C-1. Mean and median false positive rates were <0.1% for genes and <0.5% for GO biological processes for all tissue per sex group (Figure C-5 and Figure C-6). The maximum false positive rates for any of the 80 computationally generated control data sets were 0.3% (gene) and 4.4% (GO biological process).
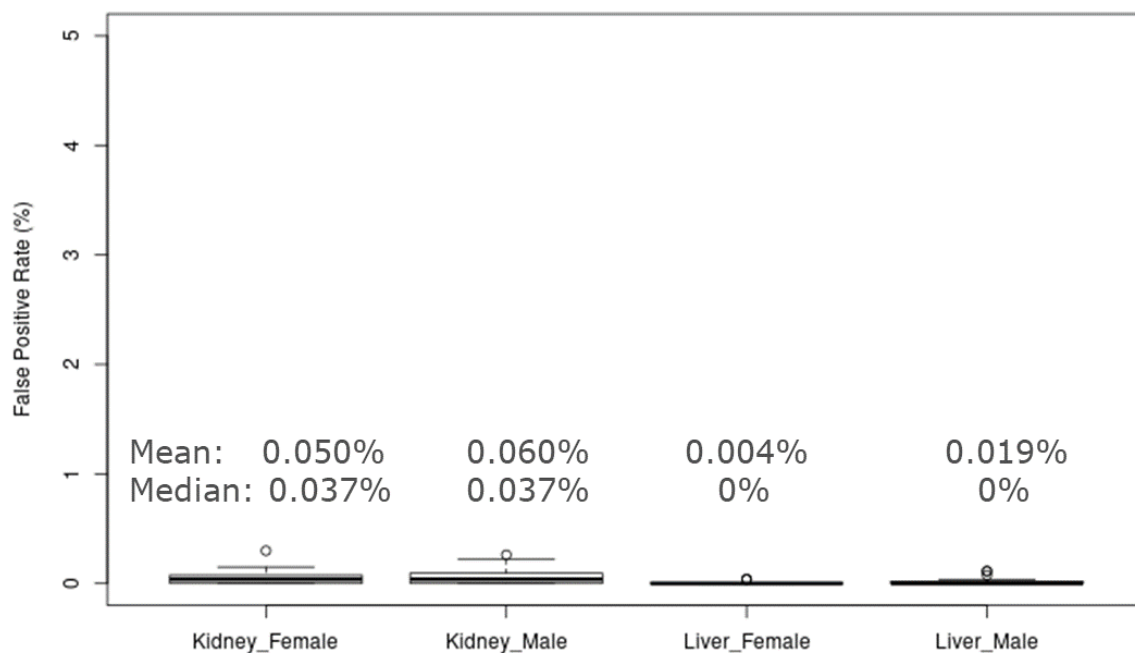
Figure C-5. Boxplots of the False Positive Gene Rate for Each Tissue per Sex Combination

Each boxplot displays the distribution of the false positive rates for 20 computationally generated data sets.

In Vivo Repeat Dose Biological Potency Study of
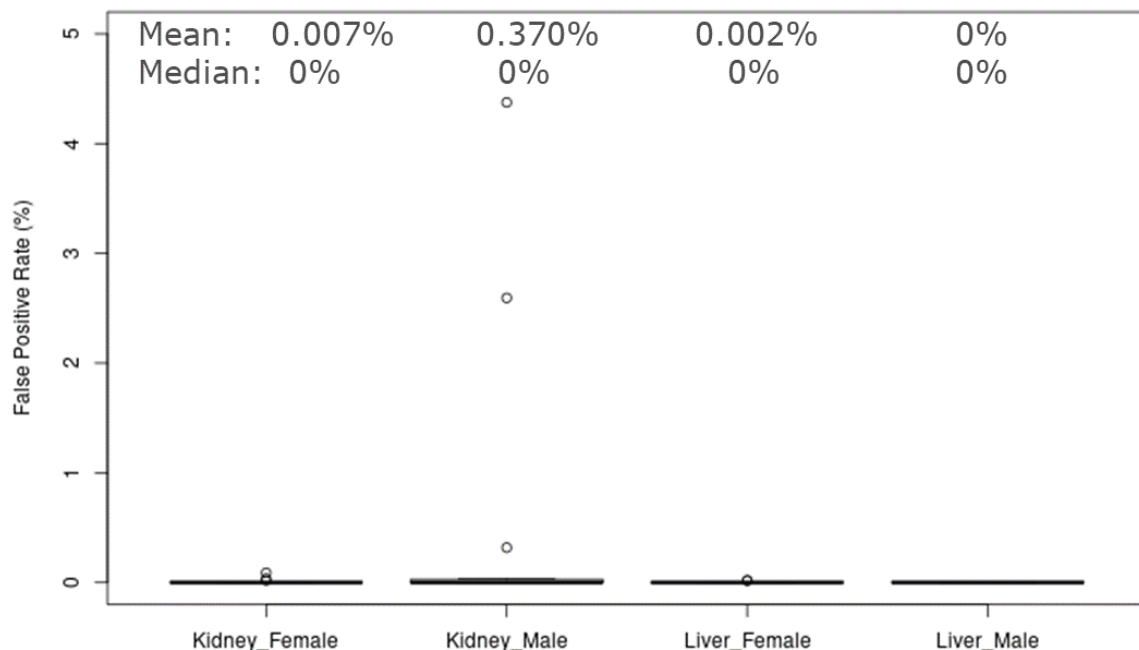6:1 Fluorotelomer Alcohol in Sprague Dawley Rats

Figure C-6. Boxplots of the False Positive Gene Ontology Biological Process Rate for Each Tissue per Sex Combination

Each boxplot displays the distribution of the false positive rates for 20 computationally generated data sets.

Table C-1. Number of False Positives

Generated Data Set	# False Positive Genes				# False Positive GO Biological Process			
	Kidney Female	Kidney Male	Liver Female	Liver Male	Kidney Female	Kidney Male	Liver Female	Liver Male
01	3	0	0	0	0	0	0	0
02	4	0	0	0	2	1	0	0
03	0	2	0	0	0	1	1	0
04	2	1	0	0	0	0	0	0
05	2	3	0	0	0	0	0	0
06	1	0	0	3	0	0	1	0
07	1	6	0	0	0	18	0	0
08	0	0	0	0	0	0	0	0
09	3	0	0	0	0	0	0	0
10	0	0	0	0	0	0	0	0
11	0	1	0	1	0	0	0	0
12	1	4	0	3	1	147	0	0
13	0	2	0	0	0	2	0	0
14	1	0	0	2	0	0	0	0
15	0	3	0	0	0	2	0	0
16	0	1	1	0	0	0	0	0
17	0	0	1	0	0	0	0	0
18	0	2	0	0	0	0	0	0
19	1	0	0	1	0	0	0	0
20	8	7	0	0	5	248	0	0

GO = Gene Ontology.

Appendix D. Benchmark Dose Model Recommendation and Selection Methodologies

Tables

Figures

Table D-1. Benchmark Dose Model Recommendation/Selection Rules for Apical Endpoints

Rule	Criteria for "Viable"	Numerical Threshold	Bin Placement for Rule Failure
BMD Existence	A BMD exists.	NA	Failure
BMD_L Existence	A BMD_L exists.	NA	Failure
AIC Existence	An AIC exists.	NA	Failure
Residual of Interest Existence	The residual at the dose group closest to the BMD (i.e., the residual of interest) exists.	NA	Failure
Variance Model Fit	The variance model used fits the data.	NA	Nonviable
Variance Model Selection	The variance model is appropriate.	NA	Nonviable
Global Goodness of Fit	The mean model fits the data means sufficiently well (BMDS 2.7.0 Test 4 p value >N).	0.1	Nonviable
Degrees of Freedom	There is at least 1 degree of freedom (i.e., more dose groups than model parameters).	NA	Nonviable
BMD-to-BMD_L Ratio	The ratio of BMD to BMD_L is not large (BMD/BMD_L <N).	20	Viable
High BMD_L	The BMD_L is <N times higher than the maximum dose.	1	Viable
High BMD	The BMD is <N times higher than the maximum dose.	1	Viable
Low BMD	The BMD is <N times lower than the minimum nonzero dose.	3	Nonreportable
Control Residual	The residual at control is small (residual <N).	2	Nonviable
Control Standard Deviation	The modeled standard deviation is similar to the actual (<N times different).	1.5	Nonviable
Residual of Interest	The residual at the dose group closest to the BMD (i.e., the residual of interest) is small (residual <N).	2	Nonviable
No Warnings Reported	No warnings in the BMD model system were reported.	NA	Viable

BMD = benchmark dose; NA = not applicable; BMD_L = benchmark dose lower confidence limit; AIC = Akaike information criterion; BMDS = Benchmark Dose Software; N = numerical threshold.
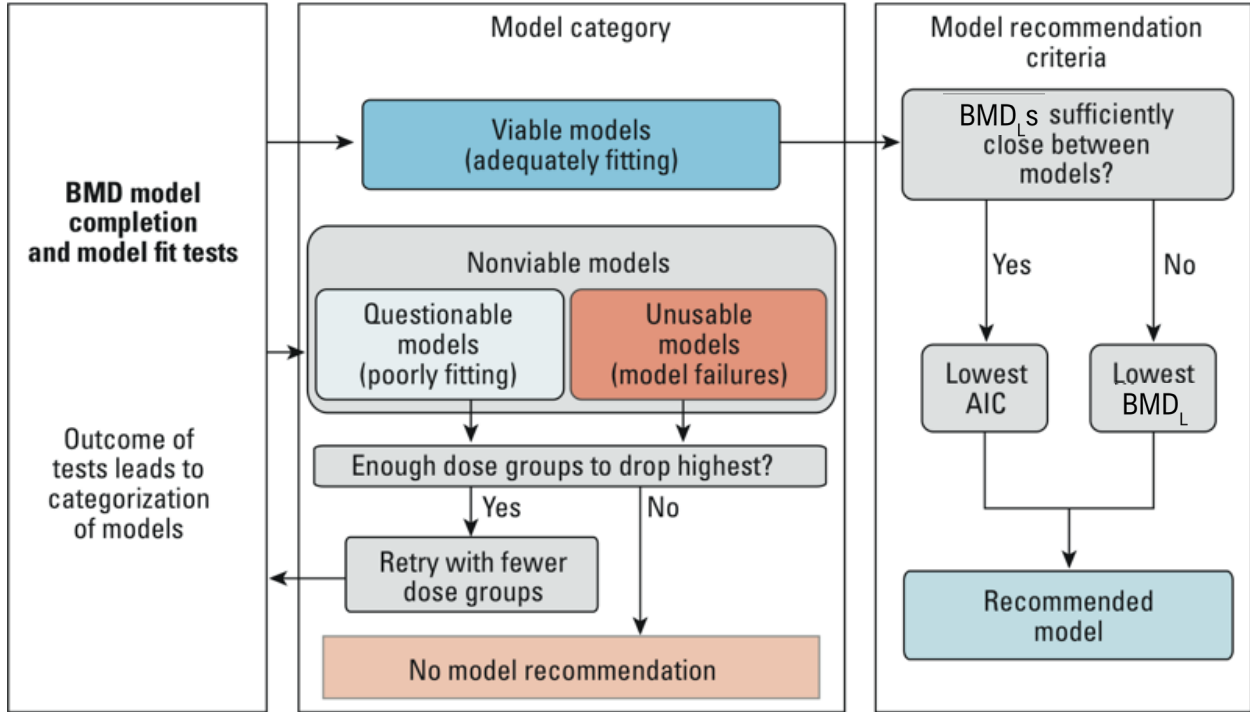
Figure D-1. Benchmark Dose Model Recommendation/Selection Methodology for Automated Benchmark Dose Execution of Apical Endpoints

Source: Figure adapted from Wignall et al. (2014)[23]
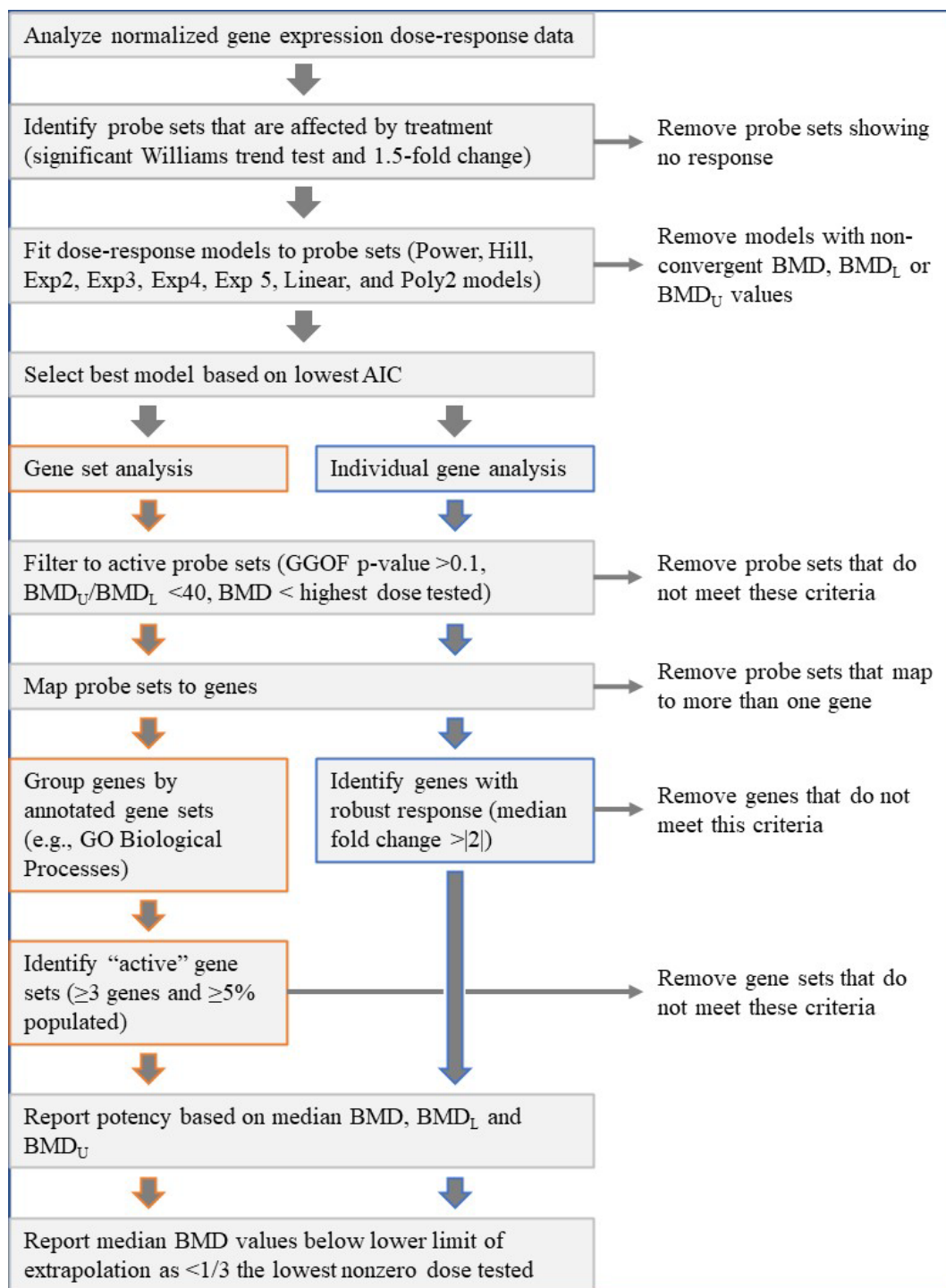BMD = benchmark dose; BMD_L = benchmark dose lower confidence limit; AIC = Akaike information criterion.

Figure D-2. Benchmark Dose Model Recommendation/Selection Methodology for Benchmark Dose Execution of Gene Sets with Expression Changes Enacted by Chemical Exposure

Adapted from Thomas et al. (2007)[34]
Exp = exponential; Poly = polynomial; BMD = benchmark dose; BMD_L = benchmark dose lower confidence limit; BMD_U = benchmark dose upper confidence limit; AIC = Akaike information criterion; GGOF = global goodness of fit; GO = Gene Ontology.

Appendix E. Organ Weight Descriptions

Table of Contents

E.1. Organ Weight Descriptions

Liver: The liver carries out biotransformation and excretion of endogenous and xenobiotic substances, regulation of blood sugar, enzymatic transformation of essential nutrients, generation of blood proteins involved in fluid balance and clotting, and bile production for digestion and absorption of fats. Liver weight changes can be an indication of chemical-induced stress. Specifically, in subacute studies, increases in liver weight in response to low doses of toxicants typically stem from increases in xenobiotic metabolizing enzymes and associated hepatocyte hypertrophy or peroxisome proliferation. Increased liver weight, particularly when accompanied by evidence of leakage of liver-specific enzymes into blood, likely reflects hemodynamic changes related to severe hepatotoxicity. Higher liver weight relative to body weight may also occur at any dose level that causes a slowed rate of body growth and does not necessarily indicate liver toxicity. Decreased liver weight in subacute studies is typically of unknown toxicological significance but in rare cases may be related to glycogen depletion.

Kidney: The kidneys remove waste products and xenobiotics from the body, balance blood electrolytes, regulate blood pressure through the release of hormones, synthesize the active form of vitamin D, and control the production of erythropoiesis. In subacute studies, changes in kidney weight may reflect renal toxicity (particularly if accompanied by increases in other markers of kidney toxicity, e.g., increased Kim-1) and/or tubular hypertrophy. Decreased kidney weights in subacute studies are typically of unknown toxicological significance.

Heart: The heart drives the circulatory system, supplying oxygen and essential macro- and micronutrients to the tissues. Increased heart weight in subacute studies would indicate severe cardiotoxicity, compensatory myocardial hypertrophy, and/or pulmonary injury. Decreased heart weight in subacute studies is often of unknown toxicological significance; however, it may be caused by decreased load on the heart from dehydration or modulation of contractility.

Appendix F. Supplemental Data

The following supplemental files are available at https://doi.org/10.22427/NIEHS-DATA-NIEHS-07.[29]

F.1. Apical Benchmark Dose Analysis

Mean Body Weight Summary
C20027-01_Mean_Body_Weight_Summary.docx

Organ Weights Summary
C20027-01_Organ_Weights_Summary.docx

Clinical Chemistry Summary
C20027-01_Clinical_Chemistry_Summary.docx

Hematology Summary
C20027-01_Hematology_Data_Summary.docx

Hormone and Enzymes Summary
C20027-01_Hormone_Summary.docx

BMD, NOEL and LOEL Summary for Apical Endpoints
C20027-01_BMD_BMDL_LOEL_and_NOEL_Summary_for_Apical_Endpoints_Sorted_by_BMD_LOEL_from_Low_to_High.docx

Male BMD Apical Endpoints Model Fits
C20027-01_Appendix_Male_07282021.docx

Female BMD Apical Endpoints Model Fits
C20027-01_Appendix_Female_07282021.docx

BMD Model Recommendation Selection Rules
C20027-01_Benchmark_Dose_Model_Recommendation_Selection_Rules_for_Apical_Endpoints.docx

Read Me
C20027-01_ReadME.docx

Male Model Parameters
C20027-01_Parameter_Male_07282021.xlsx

Female Model Parameters
C20027-01_Parameter_Female_07282021.xlsx

BMDs code package
C20027-01_bmds.zip

F.2. Genomic Benchmark Dose Analysis

BMDExpress Project File (bm2 format)
C20027-
01_EPA_PFAS_Kidney_Overflow_plate_removed_S1500_Plus_Analysis_Traditional.bm2

Top 10 Genes Ranked by Potency of Perturbation_Kidney
C20027-
01_Kidney_Top_10_Genes_Ranked_by_Potency_of_Perturbation_Sorted_by_BMD_Median.do
cx

Top 10 GO Biological Process Gene Sets_Kidney
C20027-
01_Kidney_Top_10_GO_Biological_Process_Gene_Sets_Ranked_by_Potency_of_Perturbation
_Sorted_by_BMD_Median.docx

Top 10 Genes Ranked by Potency of Perturbation_Liver
C20027-
01_Liver_Top_10_Genes_Ranked_by_Potency_of_Perturbation_Sorted_by_BMD_Median.docx

Top 10 GO Biological Process Gene Sets_Liver
C20027-
01_Liver_Top_10_GO_Biological_Process_Gene_Sets_Ranked_by_Potency_of_Perturbation_S
orted_by_BMD_Median.docx

BMDExpress Expression Data_Kidney_Female
C20027-01_Kidney_6-1_FTOH_Female.txt

BMDExpress Expression Data_Kidney_Male
C20027-01_Kidney_6-1_FTOH_Male.txt

BMDExpress Expression Data_Liver_Female
C20027-01_Liver_6-1_FTOH_Female.txt

BMDExpress Expression Data_Liver_Male
C20027-01_Liver_6-1_FTOH_Male.txt

BMDExpress Individual Gene BMD Results_Kidney_Male
C20027-01_Kidney_6-
1_FTOH_Male_williams_0.05_NOMTC_foldfilter1.5_BMD_S1500_Plus_Rat_GENE_true_true
_pval0.1_ratio40_foldchange2_conf0.5.txt

BMDExpress GO Biological Process Deduplicated BMD Results_Kidney_Male
C20027-01_Kidney_6-
1_FTOH_Male_williams_0.05_NOMTC_foldfilter1.5_BMD_S1500_Plus_Rat_GO_BP_true_tr
ue_pval0.1_ratio40_conf0.5_deduplicate.txt

BMDExpress Individual Gene BMD Results_Kidney_Female
C20027-01_Kidney_6-
1_FTOH_Female_williams_0.05_NOMTC_foldfilter1.5_BMD_S1500_Plus_Rat_GENE_true_true_pval0.1_ratio40_foldchange2_conf0.5.txt

BMDExpress GO Biological Process Deduplicated BMD Results_Kidney_Female
C20027-01_Kidney_6-
1_FTOH_Female_williams_0.05_NOMTC_foldfilter1.5_BMD_S1500_Plus_Rat_GO_BP_true_true_pval0.1_ratio40_conf0.5_deduplicate.txt

BMDExpress Individual Gene BMD Results_Liver_Male
C20027-01_Liver_6-
1_FTOH_Male_williams_0.05_NOMTC_foldfilter1.5_BMD_S1500_Plus_Rat_GENE_true_true_pval0.1_ratio40_foldchange2_conf0.5.txt

BMDExpress GO Biological Process Deduplicated BMD Results_Liver_Male
C20027-01_Liver_6-
1_FTOH_Male_williams_0.05_NOMTC_foldfilter1.5_BMD_S1500_Plus_Rat_GO_BP_true_true_pval0.1_ratio40_conf0.5_deduplicate.txt

BMDExpress Individual Gene BMD Results_Liver_Female
C20027-01_Liver_6-
1_FTOH_Female_williams_0.05_NOMTC_foldfilter1.5_BMD_S1500_Plus_Rat_GENE_true_true_pval0.1_ratio40_foldchange2_conf0.5.txt

BMDExpress GO Biological Process Deduplicated BMD Results_Liver_Female
C20027-01_Liver_6-
1_FTOH_Female_williams_0.05_NOMTC_foldfilter1.5_BMD_S1500_Plus_Rat_GO_BP_true_true_pval0.1_ratio40_conf0.5_deduplicate.txt

BMDExpress Prefilter Results_ Kidney _Female
C20027-01_BMDExpress_Prefilter_Results_Kidney_Female.txt

BMDExpress Prefilter Results_ Kidney _Male
C20027-01_BMDExpress_Prefilter_Results_Kidney_Male.txt

BMDExpress Prefilter Results_ Liver _Female
C20027-01_BMDExpress_Prefilter_Results_Liver_Female.txt

BMDExpress Prefilter Results_ Liver _Male
C20027-01_BMDExpress_Prefilter_Results_Liver_Male.txt

Animal and Fastaq Metadata
C20027-01_Animal_and_FASTQ_Metadata.zip

Kidney Principal Components Analysis Files
C20027-01_Kidney_PCA.zip

Liver Principal Components Analysis Files
C20027-01_Liver_PCA.zip

Individual Gene BMD Analysis Results File
C20027-01_Individual_Gene_Defined_Category_Files_for_Gene_Level_BMD_Analysis_of_Array_Platform_GPL1355.zip

BMDExpress Software
C20027-01_Software.zip

BMDExpress Project File (JSON format)
C20027-01_EPA_PFAS_Kidney_Overflow_plate_removed_S1500_Plus_Analysis_Traditional_JSON.zip

GO Biological Process BMD Analysis Results
C20027-01_Functional_Classification_Annotation_Files_for_GO_Biological_Process_Analysis_of_Array_Platform_GPL1355.zip

F.3. Study Tables

I04 – Mean_Body_Weight_Summary
C20027-01_I04_–_Mean_Body_Weight_Summary.pdf

I05 – Clinical_Observations_Summary
C20027-01_I05_–_Clinical_Observations_Summary.pdf

PA06 – Organ_Weights_Summary
C20027-01_PA06_–_Organ_Weights_Summary.pdf

PA41 – Clinical_Chemistry_Summary
C20027-01_PA41_–_Clinical_Chemistry_Summary.pdf

PA43 – Hematology Summary
C20027-01_-_PA43_–_Hematology_Summary.pdf

PA48 – Summary of Tissue Concentration
C20027-01_-_PA48_-_Summary_of_Tissue_Concentration.pdf

R07 – Hormone_Summary
C20027-01_R07_–_Hormone_Summary.pdf

F.4. Individual Animal Data

Individual Animal Body Weight Data
C20027-01_Individual_Animal_Body_Weight_Data.xlsx

Individual Animal Clinical Chemistry Data
C20027-01_Individual_Animal_Clinical_Chemistry_Data.xlsx

Individual Animal Clinical Observations Data

C20027-01_Individual_Animal_Clinical_Observations_Data.xlsx

Individual Animal Hormone Data

C20027-01_Individual_Animal_Hormone_Data.xlsx

Individual Animal Organ Weight Data

C20027-01_Individual_Animal_Organ_Weight_Data.xlsx

Individual Animal Hematology Data

C20027-01_Individual_Animal_Hematology_Data.xlsx

Individual Animal Tissue Concentration Data

C20027-01_Individual_Animal_Tissue_Concentration_Data.xlsx